# CHARLES UNIVERSITY


**Faculty of Science**

Department of Genetics and Microbiology

PhD study program: Molecular and Cellular Biology, Genetics and Virology




**Sandra Lettlová, MSc**


## Mechanismy rezistence a metabolismus železa u nádorových kmenových buněk

## Mechanisms of resistance and iron metabolism in cancer stem cells

Doctoral thesis


Supervisor: Jaroslav Truksa, PhD

Laboratory of Tumour Resistance

Institute of Biotechnology CAS, v. v. i.



Praha, 2018

## Statement of originality

I declare that I wrote the thesis independently and that I stated all the information sources and literature. This work or a substantial part of it was not presented to obtain another academic degree or equivalent.

In Prague, October 2018

……....…….

Sandra Lettlová, MSc

I further declare that I have truthfully stated my contribution to the works published with the collective authorship in the chapter 5. “Results“.

In Prague, October 2018

……....…….

Sandra Lettlová, MSc

……....…….

Supervisor: Jarolsav Truksa, PhD

## Acknowledgements

Here, I would like to express my gratitude to my supervisor Dr. Jaroslav Truksa for his support, encouragement and kind guidance during my whole PhD studies and preparation of this thesis. My thanks go also to all members of the Laboratory of Tumour Resistance and the Laboratory of Molecular Therapy for their help in experimental work, great support and pleasant working atmosphere.

This work was supported by the Czech Science Foundation grant 13-28830S to J.T., the Ministry of Health of the Czech Republic grant no. AZV 17-28470A to P.S., the Kellner Family Foundation grant to J.T. and the Grant Agency of Charles University Grant no. GAUK112315 to S.L. It was also funded by the Ministry of Education, Youth and Sports of CR within the LQ1604 National Sustainability Program II (Project BIOCEV-FAR) to J.T. and LO1503 to P.S., by the project „BIOCEV“(CZ.1.05/1.1.00/02.0109) and by the Czech Academy of Sciences (RVO:86652036).

## Abstract (EN)

Analogously to normal stem cells within the tissues, cancer stem cells (CSCs) have been proposed to be responsible for maintenance and growth of tumours. CSCs represent a small fraction of cells within the tumour, which is characterised by self-renewal capacity and ability to give rise to a tumour when grafted into immunocompromised mice. Cells with increased stemness properties are believed to be responsible for tumour resistance, metastases formation and relapse after tumour treatment.

The first part of this work concentrates on resistance of the tumours, which is often associated with increased expression of ATP-binding cassete (ABC) transporters pumping chemotherapeutics out of the cells. For the purposes of this study, we utilized an *in vitro* model of CSCs, based on cultivation of cells as 3D "spheres". Expression profiling demonstrates that our model of CSCs derived from breast and prostate cancer cell lines express higher mRNA level of ABC transporters, particularly *ABCA1*, *ABCA3*, *ABCA5*, *ABCA12*, *ABCA13*, *ABCB7*, *ABCB9*, *ABCB10*, *ABCC1*, *ABCC2*, *ABCC3*, *ABCC5, ABCC8*, *ABCC10*, *ABCC11* and *ABCG2* among the cell lines tested. The protein level of ABC transporters tested in breast CSCs showed higher expression of ABCB8, ABCC1, ABCC2, ABCC10 and ABCG2 but downregulation of ABCB10 and ABCF2 proteins. Consistently, T47D and MCF7 spheres show resistance to daunorubicin and doxorubicin and interestingly, higher sensitivity to ABCC1 and ABCG2 inhibitors. These results suggest that ABC transporters may play an important role in maintenance of CSC phenotype unrelated to drug efflux.

The transition from oestrogen dependent to oestrogen independent tumour growth in breast cancer is associated with loss of oestrogen receptor α (ERα) and is connected with worse prognosis. This process might be regulated by microRNAs, 22 nucleotides long, single stranded, non-coding RNAs that negatively regulate gene expression by binding to mRNA, resulting in translation inhibition and mRNA degradation. We found that oncogenic microRNA-301a-3p (miR-301a-3p) is highly elevated in our *in vitro* model of breast CSCs, which show a decrease in ER signalling. We demonstrated that miR-301a-3p negatively regulates ER signalling by direct repression of ERα mRNA translation. High miR-301a-3p expression decreases the sensitivity of oestrogen dependent MCF7 cells to 17-β oestradiol

and similarly inhibits growth of the tumour derived from this cell line in nude mice. Yet, the resulting tumours show significantly increased expression of genes related to CSCs and epithelial to mesenchymal transition suggesting for enrichment of CSCs population. Moreover, miR-301a-3p expression negatively correlates with *ESR1* level in biopsies from breast cancer patients. Thus, miR-301a-3p may serve as a prognostic marker of poor patient prognosis, oestrogen independency and resistance to anti-oestrogenic drugs.

The last part of this work is focused on metabolism of iron in CSCs. Iron is indispensable micronutrient required as a cofactor for normal function of a plethora of proteins involved in cellular respiration, Krebs cycle, redox reactions as well as enzymes necessary for DNA replication and repair. Not surprisingly, deregulation of iron metabolism leads to many pathological situations including cancer. We show that MCF7 spheres exhibit higher labile iron pool, higher iron uptake with predominant mitochondrial iron accumulation and are more susceptible to iron chelation. MCF7 spheres also show activation of IRP/IRE system, explaining higher iron uptake and decrease in iron storage. Activity of iron sulphur cluster (ISC) containing enzymes in MCF7 spheres is lower suggesting for disruption of ISC machinery. Further, MCF7 spheres show higher oxidative environment reflected by higher level of reactive oxygen species and lower level of reduced glutathione. Gene expression profiling of CSCs derived from breast and prostate cell lines identified specific gene signature related to iron metabolism consisting of genes related to iron uptake (*CYBRD1*, *TFRC*), iron sensing and iron regulation (*ACO1*, *IREB1*), mitochondrial haem and ISC synthesis (*ABCB10*, *GLRX5*), hypoxia response (*EPAS1*, *QSOX1*), iron export and iron export regulation (*HEPH*, *HFE*), suggesting for profound changes in iron metabolism. Moreover, principal component analysis based on this signature is able to distinguish CSC from non-CSC population *in vitro*. Our findings show critical changes in iron metabolism related to CSC phenotype.

Altogether, our results point to a critical role of CSCs in tumour biology, highlighting differences between normal cancer cells and CSCs that could be potentially used for cancer diagnostics and therapy.

## Abstract (CZ)

Rakovinné kmenové buňky (RKB), stejně jako normální kmenové buňky v tkáních, zodpovídají za zachování a růst nádorů. RKB představují malou frakci buněk uvnitř nádoru, která je charakteristická vlastní obnovovací kapacitou a schopností vyvolat nádor v myších s nefunkčním imunitním systémem. U buněk se zvýšenými kmenovými vlastnostmi se předpokládá, že jsou odpovědné za rezistenci nádorů k léčbě, tvorbu metastáz a návrat nádorového onemocnění.

První část této práce se zabývá rezistencí nádorů, která je často spojena se zvýšenou expresí „ATP-binding cassete" (ABC) transportérů pumpujících chemoterapeutikum ven z buněk. Pro účely této studie jsme použili *in vitro* model RKB založený na kultivaci buněk jako tzv. 3D "sféry". Expresní profil ukazuje, že náš model RKB odvozený z buněčných linií rakoviny prsu a prostaty exprimuje celkově vyšší hladinu ABC transportérů, zejména *ABCA1*, *ABCA3*, *ABCA5*, *ABCA12*, *ABCA13*, *ABCB7*, *ABCB9*, *ABCB10*, *ABCC1*, *ABCC2*, *ABCC3*, *ABCC5, ABCC8*, *ABCC10*, *ABCC11* a *ABCG2*. Analýza proteinové hladiny ABC transportérů v RKB prsu pak ukázala vyšší expresi transportérů ABCB8, ABCC1, ABCC2, ABCC10 a ABCG2 a naopak snížení hladiny proteinů ABCB10 a ABCF2. V souladu s těmito daty, sféry připravené z buněčných linií T47D a MCF7 vykazují rezistenci k daunorubicinu a doxorubicinu, a zajímavě také vyšší citlivost k inhibitorům transportérů ABCC1 a ABCG2. Tyto výsledky naznačují, že ABC transportéry mohou hrát důležitou roli při udržování fenotypu RKB, jež nesouvisí s transportem léčiv.

Nádory rostoucí nezávisle na přítomnosti estrogenu často ztratí estrogenový receptor α (ERα), což je spojeno s horší prognózou pacientek. Tento proces může být regulován pomocí mikroRNA, 22 nukleotidů dlouhých, jednořetězcových, nekódujících RNA, které negativně regulují genovou expresi vazbou na mRNA, což vede k inhibici translace mRNA a její degradaci. Dále jsme zjistili, že onkogenní microRNA-301a-3p (miR-301a-3p) je vysoce zvýšená v našem modelu prsních RKB, které vykazují pokles ER signalizace. Ukázali jsme, že miR-301a-3p negativně reguluje ER signalizaci přímou represí translace mRNA kódující ERα. Vysoká exprese miR-301a-3p snižuje citlivost estrogen dependentních MCF7 buněk k 17-β estradiolu a podobně vede k inhibici růstu nádoru pocházejícího z této buněčné linie v nahých myších, které mají poškozený imunitní systém. Vzniklé nádory nicméně vykazují

významně zvýšenou expresi genů souvisejících s fenotypem RKB a epiteliálně-mezenchymální tranzicí, naznačující obohacení populace nádoru o RKB. Navíc exprese miR-301a-3p negativně koreluje s hladinou exprese genu *ESR1* u biopsií z pacientů s rakovinou prsu. MiR-301a-3p tak může sloužit jako ukazatel závislosti růstu nádoru na estrogenu a jeho rezistenci vůči anti-estrogenním lékům, ale také jako ukazatel prognózy pacienta.

Poslední část této práce je zaměřena na metabolismus železa v RKB. Železo je nepostradatelným prvkem, který je nutný jako kofaktor pro normální funkci mnoha enzymových proteinů, které se účastní buněčného dýchání, Krebsova cyklu, redoxních reakcí, ale také replikace a opravy DNA. Není divu, že deregulace metabolismu železa vede k mnoha patologickým situacím, včetně nádorového bujení. Naše data ukazují, že sféry odvozené z buněčné linie MCF7 vykazují vyšší množství volného železa, vyšší příjem železa s jeho převažující akumulací v mitochondriích a jsou citlivější k chelaci železa. Sféry z MCF7 buněk také vykazují aktivaci IRP/IRE systému, což potvrzuje vyšší absorpci železa a snížení feritinově vázaných železových zásob. Aktivita enzymů obsahujících železo-sirné klastry je ve sférách snížena, což naznačuje narušení mechanismu jejich biogeneze. Dále MCF7 sféry vykazují vyšší oxidační prostředí, které je odrazem vyšší tvorby reaktivních druhů kyslíku a nižší hladiny redukovaného glutationu. Expresní profil genů spojených s metabolismem železa u RKB odvozených z buněčných linií rakoviny prsu a prostaty odhalil specifický expresní genový profil založený na rozdílné expresi genů souvisejících s vychytáváním železa (*CYBRD1*, *TFRC*), detekcí hladiny železa a její regulací (*ACO1*, *IREB1*), mitochondriální syntézou hemu a železo-sirných klastrů (*ABCB10*, *GLRX5*), hypoxií (*EPAS1*, *QSOX1*), exportem železa a regulací jeho exportu (*HEPH, HFE*), což poukazuje na značné změny v metabolismu železa u RKB. Analýza hlavních komponent založená na tomto genovém profilu je navíc schopna rozlišit RKB od ostatních nádorových buněk *in vitro*. Tato data tak dokumentují důležité změny metabolismu železa v souvislosti s fenotypem RKB.

Závěrem lze konstatovat, že naše výsledky dále prohlubují poznatky o zásadní úloze RKB v biologii nádorů, přičemž vystihují rozdíly mezi normálními rakovinnými buňkami a RKB, které by mohly potenciálně sloužit při diagnostice nádorů a jejich léčbě.

## List of publications

Publications related to the thesis are underlined.

1. **Lettlova S**, Brynychova V, Blecha J, Vrana D, Vondrusova M, Soucek P, Truksa J. MiR-301a-3p Suppresses Estrogen Signaling by Directly Inhibiting ESR1 in ERα Positive Breast Cancer. Cell. Physiol. Biochem, 2018;46:2601-2615.

2. Rychtarcikova Z*, **Lettlova S***, Tomkova V, Korenkova V, Langerova L, Simonova E, Zjablovskaja P, Alberich-Jorda M, Neuzil J, Truksa J. Tumor-initiating cells of breast and prostate origin show alterations in the expression of genes related to iron metabolism. Oncotarget. 2016;8:6376-6398.

   *equal contribution

3. Blecha J, Novais SM, Rohlenova K, Novotna E, **Lettlova S**, Schmitt S, Zischka H, Neuzil J, Rohlena J. Antioxidant defense in quiescent cells determines selectivity of electron transport chain inhibition-induced cell death. Free Radic. Biol. Med. 2017;112:253-266.

4. Kralova J, Kolar M, Kahle M, Truksa J, **Lettlova S**, Balusikova K, Bartunek P. Glycol porphyrin derivatives and temoporfin elicit resistance to photodynamic therapy by different mechanisms. Sci. Rep. 2017;7:44497.

5. Truksa J, Dong LF, Rohlena J, Stursa J, Vondrusova M, Goodwin J, Nguyen M, Kluckova K, Rychtarcikova Z, **Lettlova S**, Spacilova J, Stapelberg M, Zoratti M, Neuzil J. Mitochondrially Targeted Vitamin E Succinate Modulates Expression of Mitochondrial DNA Transcripts and Mitochondrial Biogenesis. Antioxid. Redox Signal. 2015;22:883-900.

6. Tomasetti M, Nocchi L, Staffolani S, Manzella N, Amati M, Goodwin J, Kluckova K, Nguyen M, Strafella E, Bajzikova M, Peterka M, **Lettlova S**, Truksa J, Lee W, Dong LF, Santarelli L, Neuzil J. MicroRNA-126 Suppresses Mesothelioma Malignancy by Targeting IRS1 and Interfering with the Mitochondrial Function. Antioxid. Redox Signal. 2014;21:2109-2125.

# Content

# List of abbreviations

| | |
|---|---|
| ABC | ATP-binding cassette |
| AKT | RAC-alpha serine/threonine-protein kinase |
| ALAS2 | Aminolevulinate synthase 2 |
| ALDH | Aldehyde dehydrogenase |
| APP | Amyloid beta precursor protein |
| ATP | Adenosine triphosphate |
| BCA | Bicinchinonic acid |
| BCL-2 | B-cell lymphoma 2 |
| BIM | BCL2-interacting mediator of cell death |
| BMP | Bone morphogenetic protein |
| BSA | Bovine serum albumin |
| CCK-8 | Cell counting kit-8 |
| CCL2 | Chemokine C-C motiv ligand 2 |
| CDB | Cell dissociation buffer |
| CDC14A | Cell division cycle 14A |
| CDK6 | Cyclin dependent kinase 6 |
| DCF-DA | 2′,7′-dichlorofluorescein diacetate |
| DFO | Deferoxamine |
| DHE | Dihydroethidium |
| DMEM | Dulbecco's Modified Eagle Medium |
| Dp44mT | Di-2-pyridylketone-4,4-dimethyl-3-thiosemicarbazone |
| CI | Complex I |
| CP | Ceruloplasmin |
| CSC | Cancer stem cell |
| CSTD | Cathepsin D |
| CUL1 | Cullin-1 |
| CXCL12 | Chemokines C-X-C motif ligand 12 |
| DCYTB/CYBRD1 | Duodenal cytochrome b reductase |
| DGCR8 | DiGeorge critical region gene 8 protein |
| DMT1/SLC11A2/NRAMP2 | Divalent metal transporter 1/Solute carrier family 11 member 2/Natural resistance-associated macrophage protein 2 |
| $E_2$ | Oestradiol |
| EGF | Epidermal growth factor |
| EMSA | Electrophoretic mobility shift assay |
| EMT | Epithelial to mesenchymal transition |
| ER | Oestrogen receptor |
| ERK | Extracellular signal-regulated kinase |
| EV | Empty vector |
| FBS | Foetal bovine serum |
| FBXL5 | F-box/LRR-repeat protein 5 |
| FDX2 | Ferredoxin |
| FGF | Fibroblast growth factor |
| FPN/SLC40A1 | Ferroportin/Solute carrier family 40 member 1 |
| FTH | Ferritin heavy chain |
| FTL | Ferritin light chain |
| FXN | Frataxin |
| GAPDH | Glyceraldehyde-3-phosphate dehydrogenase |
| GLRX5 | Glutaredoxin 5 |

| | |
|---|---|
| GREB1 | Growth regulation by oestrogen in breast cancer 1 |
| GSH | Reduced form of glutathione |
| GSSG | Oxidised form of glutathione – glutathione disulphide |
| HAMP | Hepcidin |
| HEPH | Hephaestin |
| HEPES | 4-(2-hydroxyethyl)-1-piperazineethanesulfonic acid |
| HER2 | Human epidermal growth factor receptor 2 |
| HFE | Hereditary haemochromatosis protein |
| HFE2/HJV | Haemochromatosis type 2 protein/ Haemojuvelin |
| HIF | Hypoxia-inducible factor |
| HIF-2α/EPAS1 | Hypoxia-inducible transcription factor-2α/Endothelial PAS domain-containing protein 1 |
| HMOX1 | Haem oxygenase 1 |
| HMGA2 | High mobility groups A2 |
| HPF | Hydroxyphenyl fluorescein |
| HSPA9 | Heat shock 70 kDa protein 9 |
| IL | Interleukin |
| IRE | Iron responsive element |
| IRP1/ACO1/IREB1 | Iron-responsive element-binding protein 1/Aconitase 1/Iron regulatory protein 1 |
| IRP2/ACO3/IREB2 | Iron-responsive element-binding protein 2/Aconitase 3/Iron regulatory protein 2 |
| ISC | Iron-sulphur cluster |
| ICSA1 and 2 | Iron-sulfur cluster assembly 1 and 2 |
| ISCU | Iron-sulphur cluster assembly enzyme scaffold protein |
| LIC | Leukemia initiating cell |
| LIP | Labile iron pool |
| LYRM4 | LYR motif-containing protein 4 |
| MAPK | Mitogen-activated protein kinase |
| MDR | Multi-drug resistance |
| MET | Mesenchymal to epithelial transition |
| MFRN1 and 2 | Mitoferrin 1 and 2 |
| miRNA | MicroRNA |
| miR-301a-3p | MicroRNA-301a-3p |
| MRCKα | CDC42-binding protein kinase α |
| MRP | Multi-drug resistance protein |
| NADPH | Nicotinamide adenine dinucleotide phosphate |
| NKRF | NF-κB-repressing factor |
| NBD | Nucleotide binding domain |
| NF-κB | Nuclear factor kappa B |
| NOTCH1 | Neurogenic locus notch homolog protein 1 |
| NTBI | Non-transferrin bind iron |
| OCT-4 | Octamer-binding protein 4 |
| PBS | Phosphate-buffered saline |
| PCA | Principal component analysis |
| PDCD4 | Programmed cell death 4 |
| PDGF | Platelet derived growth factor |
| PCBP | Poly r(C)-binding protein |
| PHD | Prolyl hydroxylase |
| PI3K | Phosphatidylinositol 3-kinase |

| | |
|---|---|
| PR | Progesterone receptor |
| pre-miRNA | Precursor microRNA |
| pri-miRNA | Primary microRNA |
| PTEN | Phosphatase and tensin homologue |
| QSOX1 | Sulfhydryl oxidase 1 |
| RKB | Rakovinné kmenové buňky |
| ROS | Reactive oxygen species |
| RISC | RNA induced silencing complex |
| RPMI | Roswell park memorial institute medium |
| RUNX3 | Runt-related transcription factor 3 |
| RT-qPCR | Reverse transcription-quantitative polymerase chain reaction |
| SC | Stem cell |
| SDS | Sodium dodecyl sulphate |
| SIH | Salicyl isonicotinoyl hydrazine |
| SKA2 | Spindle and kinetochodre associated complex subunit 2 |
| SKP1 | S-phase kinase associated protein 1 |
| SMAD | Sma and mother against decapentaplegic |
| SNAIL | Snail family transcriptional repressor 1 |
| SOX2 | SRY (sex determining region Y)-box 2 |
| STE | Sucrose, Tris, Edta buffer |
| STEAP | 6-transmembrane epithelial antigen of the prostate |
| TAM | Tumour associated macrophages |
| TBE | Tris, Boric acid, Edta buffer |
| TBS-T | Tris-buffered saline with 0,05% Tween 20 |
| Tf | Transferrin |
| TfR1 and 2 | Transferrin receptor 1 and 2 |
| TF | Transcription factor |
| TGF-β | Transforming growth factor β |
| TNF-α | Tumour necrosis factor-α |
| TMD | Transmembrane domain |
| TMRM | Tetramethylrhodamine methyl ester |
| TMPRSS6 | Transmembrane protease serine 6, matriptase-2 |
| TP53 | Tumour protein p 53 |
| TWIST1 | Twist family bHLH transcription factor 1 |
| UBE2N | Ubiquitin-conjugating enzyme E2 N |
| UTR | Untranslated region |
| VDAC | Voltage dependent anoint channel |
| VEGF | Vascular endothelial growth factor |
| VIM | Vimentin |
| ZEB1 and ZEB2 | Zinc finger E-box binding homeobox 1 and 2 |
| ZIP14/SLC39A14 | Zrt/Irt-like protein 14/Solute carrier family 39 member 14 |
| ΔΨm | Mitochondrial membrane potential |

# 1. INTRODUCTION

## 1.1. Objectives and significance of the study

Despite the considerable progress in the knowledge of cancer biology, cancer is still the leading cause of death in economically developed countries. Although we are able to effectively treat the primary disease, cancer recurrence remains a major problem as treated cells evolve mechanisms how to evade treatment and remain resistant to therapy (1). The fast proliferating cancer cells can also spread from the original site to other parts of the body where they form metastases, which are often the cause of cancer death. Thus, although patients overcome primary tumour, they eventually relapse with often harder to treat secondary tumours (1). In this regard, making cancer drug treatment more effective and finding a way of overcoming secondary tumour formation is of high clinical importance.

Tumours are heterogeneous entities and consist of multiple cellular populations. The ongoing cancer research tackle the idea, which is starting to be accepted by scientific community, that cancer stem cells (CSCs) present the main reason for ineffective cancer treatment, leading to metastasis formation and cancer recurrence. Although the biology of these cells within the tumours is extensively studied, the effective treatment targeting the whole tumour population is still not available. This is due to the high plasticity of CSCs enabling them to adjust to unfavourable conditions such as undergoing treatment and continue in tumour growth (2). For these reasons, we decided to study the biology of CSCs from angles of view of resistance to treatment and metabolism of iron, trying to find new therapeutic opportunities or novel diagnostic and prognostic markers.

CSCs are believed to have higher level of adenosine triphosphate (ATP)-binding cassette (ABC) transporters, whose main function is attributed to detoxification, but due to the variety of transporter substrates, these proteins may also have other functions important for stem cell maintenance, which have not been described in the literature yet. Study of these mechanisms could thus elucidate new implications of ABC transporters important for the biology of CSCs.

In breast cancer, the loss of oestrogen receptor α (ERα) is always connected with overall worse prognosis of the treatment but reports connecting ERα loss with CSCs phenotype are

scarce. ERα negative tumours become independent on oestrogenic signalling for their growth and become resistant to treatment by anti-oestrogenic drugs. In most cases, breast CSCs are reported to be ERα negative (3). Although ER signalling promotes proliferation of the ERα positive tumour, it is also reported to inhibit the epithelial to mesenchymal transition (EMT) process (4). Thus, it is important to study the mechanisms, which lead to loss of ERα, as they increase invasiveness of cells, their stem cells characteristics and resistance to treatment.

Next part of this thesis is focused on metabolism of iron in CSCs. Iron is very important element for many cellular processes indispensable for cellular proliferation and also for normal function of human body (5). The role of iron in cancer has been already studied and reports refer to importance of iron for cancer progression (6,7). Although iron chelators have been proved to have therapeutic effect in specific cancer types such as bladder cancer and some haematological malignancies (8,9), they are not widely used as cancer therapeutics. Metabolism of iron in CSCs has not been studied at all, therefore defining the role of iron metabolism in these cells may be the basis for new therapeutic approaches.

# 2. LITERATURE REVIEW

## 2.1. Mechanisms of cancer resistance

Drug resistance is the main reason for failure of cancer treatment. The resistance may be either pre-existent (intrinsic) or induced by therapy (acquired). Intrinsic resistance refers to a failure of a tumour to respond to therapy, while in acquired resistance, an initially responsive tumour subsequently progresses during the course of treatment (10). The mechanisms of cancer resistance are highly complex and not fully understood. Cancer cells may evade the effect of therapy by inactivation of the anticancer drug or changing the drug metabolism. Another way is decreasing the intracellular drug concentration either by reducing the absorption of the drug or by increasing the export of the drug out of the cell, or compartmentalization of the drug within the cell, where it is not effective. Further mode of evasion includes inhibition of the cell death induction, changing the targets of chemotherapeutic agents by mutations or dysregulation the target expression level, enhancing the DNA repair, gene amplification, epigenetic altering or microRNAs (miRNAs) actions. The important contributing factors are also tumour microenvironment and tumour heterogeneity (10,11).

### 2.1.1. Tumour heterogeneity

Tumour heterogeneity is a prominent factor contributing to therapeutic failure. Tumours are not homogeneous mass of cells, instead they are dynamic entities quickly evolving during the disease progression, consisting of heterogeneous population of malignant but also non-malignant cells such as immune cells, endothelial cells or cancer associated fibroblast (12). Tumour heterogeneity can be described as inter-tumoral and intra-tumoral (13). The inter-tumour heterogeneity refers to heterogeneity in tumours of different tissue and cell types, but also to heterogeneity of tumours of the same tissue but in different patients or to heterogeneity of various tumours within the same patient. The inter-tumour heterogeneity provides basis for classifying cancer into types and subtypes according to gene and protein signature and specific markers expression, which may provide clinically relevant prognostic information (13). The intra-tumour heterogeneity is defined as a variation within the same

tissue of the same patient (13). The main reason for tumour heterogeneity is genomic instability, which is caused by various distinct routes, allowing for creation of genetically and phenotypically diverse subclones of cells within the tumour (14,15). Diverse cell populations are subjected to clonal selection by tumour microenvironment and therapeutic context, leaving different genomic background of clones with phenotypic advantage that influence tumour evolution and patient outcome. This branched tumour evolution model (or stochastic model) (Fig. 2.1. A) thus allows for extensive tumour heterogeneity, which has been observed in a range of tumour types (16–18).

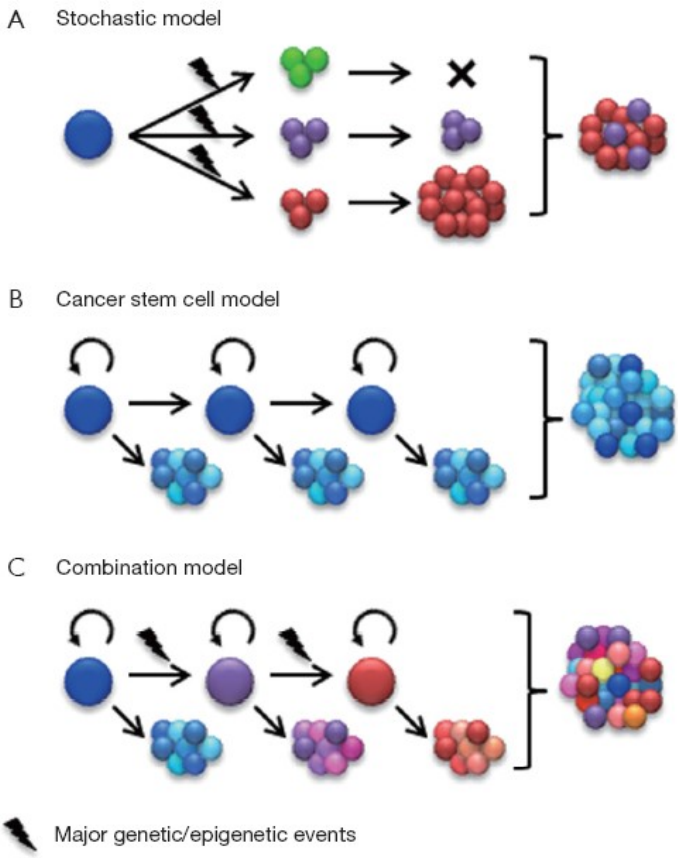


**Fig. 2.1. Modelling of tumour heterogeneity. A**, Stochastic or branched evolution model assumes that tumour heterogeneity is defined by intrinsic factors, **B**, Cancer stem cell model assumes that tumour is organised in a hierarchical structure with cancer stem cell on the top, **C**, Combination or plasticity model suggest that tumour heterogeneity is driven by combination of two above mentioned models. Figure adapted from ref. (19).

Other researchers believe that the intra-tumour heterogeneity is based on CSC model (Fig. 2.1. B) where it is suggested that only a subset of cancer cells defined as CSCs are able to

self-renew and differentiate into a variety of cell types, each with its own abilities and phenotypes. The resulting hierarchical organization includes CSCs that give rise to intermediate progenitors and terminally differentiated progeny (20). However, the clonal evolution model and CSC model are not mutually exclusive. The connection between these two models explains a plasticity model (Fig. 2.1. C) postulating that cancer cells can interconvert between stem cell and differentiated states upon intrinsic or extrinsic stimuli (21). Thus, genomic instability can give rise to a cancer cell with stem cell phenotype, which has specific features influencing tumour outcome.

#### *2.1.1.1. Heterogeneity of breast cancer in relation to oestrogen receptor α*

Breast cancer is the most prevalent type of cancer in women worldwide (22). Breast cancer displays inter- and intra-tumour heterogeneity, which can complicate diagnosis and challenge therapy. The most reproducibly identified molecular subtypes of breast cancer are defined according to ERα, progesterone receptor (PR) and receptor tyrosine-protein kinase ERBB2 (known as human epidermal growth factor receptor 2 (HER2)) status expression. Luminal A type ($ER^+/PR^+/HER2^-$) of breast cancer has better prognosis than luminal B type ($ER^+/PR^+/HER2^+$) characterised by higher expression of proliferation markers such as Ki67. Aggressive and invasive HER2 enriched type ($ER^-/PR^-/HER2^+$) has a poor prognosis and triple negative type, which does not express any of the three receptors, has the worst prognosis (23,24). Within these subtypes, the genomic and transcriptomic profiling of breast tumours revealed new subgroups, providing better view for assessing the prognosis and treatment (25).

Tumours with ERα and PR expression, which are diagnosed in 75 % of breast cancer patients, are mostly well-differentiated, less invasive and are associated with better prognosis than tumours without ERα and PR expression (24,26). ERα is one of the oestradiol ($E_2$)-activated transcription factor, which regulates a wide range of genes connected with cellular proliferation, differentiation and migration (27), and plays a crucial role in normal mammary gland biology and development (28). $E_2$/ERα signalling promotes proliferation of ERα positive breast cancer cells and it is important for the growth of the primary tumour. Nevertheless, the expression of ERα negatively correlates with the progressive grade of

invasive ductal breast cancer (29). Moreover, ERα signalling antagonises pathways leading to EMT and CSC phenotype (30,31). Thus, ERα expression is considered to be a good indicator for breast cancer treatment and tumour growth dependency on oestrogenic receptor signalling is exploited for treatment with selective oestrogen receptor modulators (tamoxifen), selective oestrogen receptor down regulators (fulvestrant) or aromatase inhibitors (letrozole) (32). The main problem in clinical treatment of breast cancer is resistance to hormonal therapies caused by transition of originally hormone-dependent tumour to tumour growth that is hormone-independent and often connected with aggressive metastatic behaviour (33,34). To date, multiple mechanisms have been proposed to explain how breast cancer cells escape dependency on oestrogen control and acquire hormone-independent, invasive and resistant phenotype. Among them, epigenetic modulation (35), transcription regulation (36), gene mutation (37), alternative usage of splice variants (38), posttranslational modifications (39) or microRNA deregulation (40) have been described so far.

### 2.1.2. Cancer stem cells

In many adult tissues, stem cells (SCs) are responsible for tissue homeostasis and regeneration (41). SCs differ from other cells by their capacity for long term self-renewal and an ability to differentiate into one or multiple cell lineages that enables them to create a hierarchical tissue organization that is driven by intrinsic mechanisms (41). Based on this concept, Dick and colleagues (42,43) have shown that in human acute leukemia, only a subset of cells is able to propagate tumour when transplanted into immunodeficient mice. These leukemic cells are expressing the same markers as normal haematopoietic SCs ($CD34^+/CD38^-$) and were called leukemia initiating cells (LICs) or CSCs (43). Subsequently, a small fraction of cells (less than 0,04 % (44)) with self-renewing capacity and ability to reconstitute secondary tumours in immunodeficient mice, was also found in solid tumours. Gradually, CSCs and their specific markers were found in breast cancer ($CD44^+/CD24^{-/low}$ and $ALDH1^{high}$ (45,46)), pancreatic cancer ($CD44^+/CD24^+/ESA^+$)(47), brain tumours ($CD133^+$) (48), colorectal cancer ($CD133^+$) (49), prostate cancer ($CD44^+/\alpha2\beta1^{high}/CD133^+$) (50), melanoma ($CD271^+$) (51), ovarian cancer ($CD44^+/CD117^+$)

(52) and other solid tumours. The principal characteristics of CSCs are self-renewal, tumour initiation and long term tumour repopulation potential that create the heterogeneous lineages of cancer cells comprising the tumour (53). These properties allow CSCs to differentiate into heterogeneous cancer cells with altered phenotypes that influence treatment, propagation and maintenance of the tumour (21). Important processes such as EMT and metastasis formation are also connected with CSCs. EMT is a process in which an epithelial cell loses its adhesion with its neighbours and adopts a mesenchymal morphology allowing the cell to migrate long distances. At specific destination, the cell can reacquire epithelial phenotype again in a process called mesenchymal to epithelial transition (MET) and eventually form a secondary tumour or metastases. EMT is regulated by signalling pathways, microRNAs, transcription factors (TFs) (such as Snail family transcriptional repressor 1 (SNAIL), Zinc finger E-box binding homeobox 1 and 2 (ZEB1 and ZEB2), Twist family bHLH transcription factor 1 (TWIST1)) and other factors that promote transition to migratory phenotype (54,55). EMT phenomenon also promotes cancer cell stemness. Upregulation of TWIST1, ZEB1 or SNAIL TFs confers CSC properties and enhances tumour propagation in immunodeficient mice (56,57). Increasing evidence indicates that metastases are initiated by specific cancer cells with CSC properties and that CSCs are the cause of tumour initiation, self-renewal and metastasis formation (58–60). The plasticity and dormancy of metastases is also a feature of CSCs supporting this idea (61). Another important feature of CSCs is their resistance to therapy leading to tumour relapse. CSCs are either intrinsically or extrinsically resistant which means that either they are already resistant to therapy or they become resistant under the selective pressure of therapy. There is supporting evidence that radio- or chemotherapy often enriches or induces cells with CSC phenotype (62–64). There are several ways how CSCs can avoid effective therapy. First, the selectivity of conventional chemotherapy is often based on killing the fast proliferating cancer cells. But CSCs are rather less proliferative and more quiescent which gives them the capability to survive chemotherapeutic treatment (65–67). Moreover, CSCs are resistant to DNA damage-induced cell death as they possess high DNA repair capability. The quiescent phenotype of CSCs also contributes to resistance by giving the cell more time for DNA repair. CSCs escape radiotherapy and chemotherapy induced DNA damage by preferential activation of DNA damage checkpoints and by faster DNA damage repair compared to differentiated tumour cells (63,68,69). CSCs have also higher expression of free radical scavenging machinery,

giving them the ability to escape reactive oxygen species (ROS) producing agents, which are deleterious to normal cancer cells (70). Moreover, CSCs have elevated level of anti-apoptotic proteins, thus their threshold level for inducing apoptosis is higher than in non-CSC counterparts (71,72). Undergoing the EMT process confers resistance to therapy as cells that underwent EMT have lower level of ROS and TFs controlling EMT have important role in resistance to therapy (73). Resistance and an accelerated repopulation potential of CSCs is also ascribed to persistent activation of pathways important for embryonic development and tissue homeostasis such as Notch, Wnt/β-catenin and Hedgehog (74,75). The microenvironment of the tumour plays another important role in CSCs resistance. Cell-to-cell interactions and tumour stroma derived growth factors and cytokines play a role in mediating the connections between CSCs, their niche and non-CSCs, and are involved in maintaining CSCs self-renewal and sensitivity to radiation and cytotoxic drugs (76,77). Among these molecules we can name interleukins (IL-6, 8), chemokines (C-X-C motif ligand 12, CXCL12; C-C motif ligand 2, CCL2), platelet derived growth factor (PDGF), epidermal growth factor (EGF), tumour necrosis growth factor-alpha (TNF-α), vascular endothelial growth factor (VEGF), fibroblast growth factor (FGF) and transforming growth factor-beta (TGF-β) (76,77). The low oxygen tension within CSCs niches has also positive influence on cancer resistance and CSCs maintenance. Hypoxia activates hypoxia-inducible factors (HIFs) HIF-1α and HIF-1β and EMT phenotype (78,79). HIF transcription factors not only regulate cellular response to hypoxia but also activate developmental pathways Notch, Wnt/β-catenin and Hedgehog (80–82). Similarly to normal SCs, CSCs express high level of so called multidrug resistance (MDR) proteins or ABC transporters that mediate drug efflux and thus decrease the intracellular drug concentration to inefficient level, leading to resistance (83). Consistently with this notion, CSCs can be isolated based on higher efflux of Hoechst 33342 dye by the ABCG2 transporter (84,85). Aldehyde dehydrogenase (ALDH), a marker of CSCs, catalyses the oxidation of aldehydes to carboxylic acids and its activity is important for CSCs maintenance (86). ALDH confers resistance against chemo- and radiotherapy by abrogating oxidative stress by producing reduced nicotinamide adenine dinucleotide phosphate (NAD(P)H) (87) and by activation of pro-survival pathways as phosphatidylinositol 3-kinase/RAC-alpha serine/threonine-protein kinase (PI3K/AKT) and mitogen-activated protein kinase/extracellular signal-regulated kinase (MAPK/ERK) (88).

All of these above mentioned properties of CSCs show their important role during tumour growth and relapse. The goal of cancer therapy should thus be the elimination or terminal differentiation of CSCs by combination of therapeutic agents. Although many features of the CSCs biology are already known, properties defining their role in cancer development require further investigation.

### 2.1.3. MicroRNAs

MiRNAs are single stranded, 22 nucleotides long, non-coding RNAs that negatively regulate the post-transcriptional expression of genes (89). Genes coding miRNAs are transcribed by RNA polymerase II as a primary miRNAs (pri-miRNAs) (90). Pri-miRNAs are first processed in the nucleus by enzyme complex called Drosha-DiGeorge critical region gene 8 protein (Drosha-DGCR8) into precursor miRNAs (pre-miRNAs) (Fig. 2.2.) (91). After processing, pre-miRNAs are transported to cytoplasm (92) for final cleavage by ribonuclease Dicer into 22 nucleotides long mature miRNAs (Fig. 2.2.) (93). Mature miRNAs are then assembled into multiprotein RNA induced silencing complex (RISC) and guided to complementary bind the target mRNA to suppress gene expression by translation inhibition and/or mRNA degradation (Fig. 2.2.) (94). The functional strand of miRNA can bind into 3’ untranslated region (UTR), coding region, 5’ UTR or promoter region of different target mRNA. Thus, one miRNA might modulate expression of hundreds of mRNA transcripts (95). On the other hand, expression of certain mRNA might be regulated by different miRNAs in an orchestrated manner (96). One miRNA might regulate expression of mRNA molecules coding for proteins in one signalling pathways or interconnected nodes in the regulatory networks and thereby amplify the regulatory effect (97). Last but not least, miRNAs are also used in a feedback regulation (97).

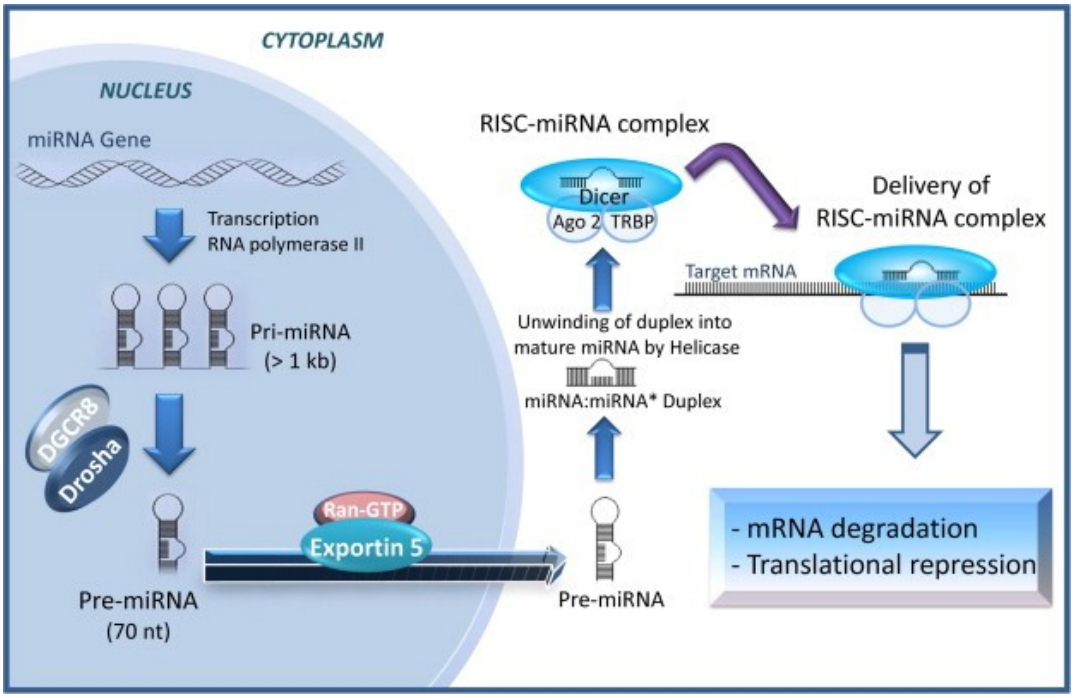


**Fig. 2.2. Schema of biosynthesis, processing and function of miRNAs.** MiRNAs are transcribed by RNA polymerase II into primary miRNAs (pri-miRNAs) which are processed by Drosha-DGCR8 (DiGeorge critical region gene 8 protein) enzyme complex into precursor-miRNAs (pre-miRNAs). The pre-miRNAs are exported into cytoplasm by exportin-5 and Ran-GTP, where they are cleaved by ribonuclease Dicer into 22 nucleotides long mature miRNAs. Helicase unwinds duplex miRNA:miRNA*, miRNA* fragment is degraded and miRNA molecule binds to an Argonaute (Ago) protein and forms a RNA induced silencing complex (RISC) that target complementary mRNA leading to translational repression and mRNA degradation. Figure adapted from ref. (98).

### *2.1.3.1. MicroRNAs in tumorigenesis*

MiRNAs are evolutionary conserved, expressed in all kind of tissues and cell types and are involved in many biological processes including regulation of cell cycle, differentiation, proliferation, apoptosis, and response to stress stimuli. Due to their wide spectrum of functions, deregulation of miRNA expression is a sign of many pathological conditions, including cancer (99). In tumorigenesis, miRNAs can act as tumour suppressors whose downregulation by deletion or methylation of the miRNA locus leads to activation of oncogenes. Contrary, upregulation of oncogenic miRNAs by amplifying the miRNA encoding locus in DNA may inhibit action of the tumour suppressors (98). MiRNAs regulate various aspects of carcinogenesis from tumour initiation to tumour growth and progression into metastasis, tumour resistance to therapy and CSCs maintenance (100). Usually,

the overall downregulation of miRNAs is present in many cancers compared to their normal tissue counterparts as they are connected with regulation of differentiation. Let-7, the most studied tumour suppressor miRNA, has been shown to regulate EMT and CSCs (101). Let-7 is downregulated in many cancers, especially in CSCs and its knockdown increases self-renewal and sphere formation (102). Targets of let-7 represent oncogenes coding for RAS, MYC, high mobility groups A2 (HMGA2), cell cycle regulators cyclin D, cyclin dependent kinase 6 (CDK6), M-phase inducer phosphatase 1 (CDC25a), proliferation signalling pathways PI3K/AKT by targeting insulin growth factor 1 receptor, mRNA of ribosomal proteins, metabolic enzymes etc. (103) Let-7 suppression also leads to enhanced expression of octamer-binding protein 4 (OCT-4) and SRY (sex determining region Y)-box 2 (SOX2) TFs and enhanced CSCs properties (104). Other tumour suppressor miRNAs are miR-34, -200 and -205. MiR-34 inhibits CSCs and metastasis by direct repression of CD44, B-cell lymphoma 2 (BCL-2) and neurogenic locus notch homolog protein 1 (NOTCH1) proteins expression (105,106). Moreover, miR-34 represses pluripotent SCs reprograming by targeting pluripotency genes *NANOG*, *SOX2* and *N-MYC* (107). MiR-200 attenuates EMT directly by targeting EMT-related TFs ZEB1 and ZEB2 (108) and reduces CSC properties by repressing the stem self-renewal factor polycomb complex protein BMI-1 (109). ZEB1 in feed-forward loop directly inhibits transcription of miR-200 to stabilise EMT phenotype (110). Several additional studies show that upregulation of miR-200 enhances the chemo-sensitivity to several anti-cancer agents (111). MiR-205 acts as a radio-sensitizing miRNA by inhibiting DNA damage repair through direct repression of *ZEB1* and *ubiquitin-conjugating enzyme E2 N* (*UBE2N*) mRNA expression (112). Interestingly, expression of miR-34, -200 and -205 is induced by frequently inactivated tumour protein 53 (TP53), connecting TP53 with regulation of EMT (113). Contrary, the expression of oncomiR miR-21 is associated with poor prognosis in many types of cancer where it targets tumour suppressors genes such as *phosphatase and tensin homolog* (*PTEN*) or *programmed cell death 4* (*PDCD4*) (114).

These several examples show potential of miRNAs for anticancer therapy, as they may regulate genes in both CSCs and non-CSCs and regulate progression of the disease and resistance to therapy. For this reason, miRNAs may also serve as good evaluating and prognostic factors in treatment of malignancies.

#### *2.1.3.2. Oncogenic microRNA-301a*

MiR-301a has been recently discovered as an oncogenic miRNA whose expression is connected with tumour progression and poor prognosis of patient with pancreatic (115), breast (116), gastric (117), colorectal (118) and hepatocellular cancer (119). MiR-301a is positioned in the intron of *spindle and kinetochodre associated complex subunit 2* (*SKA2*) gene, which is a part of Ska complex important for proper chromosomal segregation during mitotic division (120). High SKA2 protein expression correlates with miR-301a expression, which is regulated by SKA2 in a positive feedback loop (121), contributing to worse phenotype (116). In breast cancer, miR-301a directly inhibits tumour suppressor gene *PTEN*, which leads to constitutively active Wnt/β-catenin signalling, supporting invasive phenotype (122). MiR-301a positively regulates nuclear factor kappa B (NF-κB) signalling in pancreatic cancer by direct repression of translation of *NF-κB-repressing factor* (*NKRF*) mRNA. Moreover, NF-κB in a positive feedback loop increases expression of miR-301a, which leads to persistent activation of NF-κB signalling. Inhibition of miR-301a causes reduction in tumour growth derived from pancreatic cancer cells *in vivo* (123). In pancreatic cancer cells, miR-301a also supports cellular proliferation by inhibition of pro-apoptotic gene *BCL2-interacting mediator of cell death* (*BIM*) (115). High expression of miR-301a was also described in gastric cancer where it inversely correlates with cell differentiation and supports cell proliferation and invasion by inhibition of tumour suppressor gene *runt-related transcription factor 3* (*RUNX3*) (117). These and several more studies show that miR-301a is an oncogenic miRNA influencing several signalling pathways important for tumour development and could be used as a biomarker of cancer progression.

### 2.1.4. ABC transporters

As mentioned above, failure of conventional or targeted chemotherapy can be attributed to increased efflux of therapeutic agents out of the cells, leading to a decrease of intracellular drug concentration to inefficient level. This phenomenon usually leads to resistance to multiple agents and it is caused by increased expression of ABC transporter superfamily (124). ABC transporters have important physiological role as they transport hormones, lipids, peptides, ions, signalling molecules and xenobiotics across the plasma membrane or

intracellular membranes of the endoplasmic reticulum (125), nucleus (126), Golgi (127), peroxisomes, mitochondria (128) and lysosomes (129). Some ABC transporters have a very narrow substrate specificity, whereas others can transport very broad spectrum of compounds and these transporters have usually high potential to transport anticancer drugs.

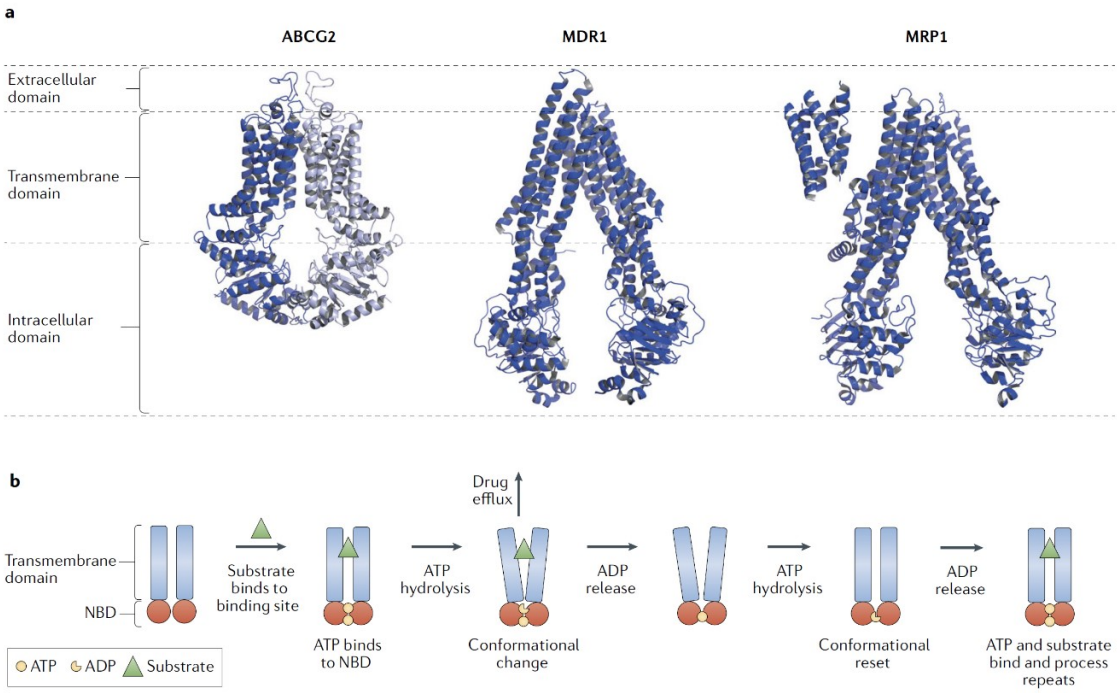


**Fig. 2.3. Structure and mechanism of ABC transporters. A**, Structures of the three best known transporters ABCG2, ABCB1 (MDR1), ABCC1 (MRP1). **B**, Scheme of ABC transporter pumping action. Substrate binds to its binding pocket and 2 ATP molecules bind to nucleotide binding domains (NBDs). Hydrolysis of ATP causes conformational change of the transporter which allows the substrate to be released on the other side of the membrane. The hydrolysis of the second ATP molecule allows for conformational reset of ABC transporter and process may be repeated. Figure adapted from ref. (130).

The polypeptide chain of functional transporter typically contains four domains, two ATP-binding domains, known as nucleotide binding domains (NBDs), and two transmembrane domains (TMDs) (Fig. 2.3. A). All four domains may be located in one polypeptide chain constituting full transporter or within two polypeptides creating half transporter with one TMD and one NBD. Half transporters must form homo- or heterodimers to assemble a functional transporter (131). TMDs contain 6-11 membrane spanning α-helices and are responsible for substrate recognition and binding. NBDs bind ATP and energy from its

hydrolysis is used to induce conformational change in TMDs to move substrate across membrane, irrespective of concentration gradient (131) (Fig. 2.3. B).

### *2.1.4.1. ABC transporters subfamilies and their physiological functions*

The 48 members of the ABC transporter family are divided into seven subfamilies A-G, according to their sequence similarity, structure and character of transported compounds (131). To date, 12 members of the ABCA subfamily have been identified. The A subfamily encompasses the largest ABC transporters, having more than 200 kDa of predicted molecular weight. They are expressed in diverse organs and tissues where they play an important role in trafficking of cellular cholesterol and other lipids. Subcellularly, these transporters are localised in plasma and lysosomal membranes (132). Mutations in genes from this group are connected with genetic diseases related to lipid transport such as Harlequin ichthyosis (*ABCA12*), neonatal surfactant deficiency (*ABCA3*) or neurodegenerative diseases such as Alzheimer's disease (132).

The group B of the ABC transporters includes 11 members with different functions and subcellular localization. ABCB1 is expressed in the intestinal epithelium, liver, kidney and in blood-brain barrier epithelial cells where it pumps xenobiotics to detoxify organism (133). ABCB2 and ABCB3 (also called TAP1 and TAP2) are half-transporters forming heterodimers in membranes of endoplasmic reticulum where they pump peptides from cytosol for presentation on the major histocompatibility complexes of class I, which is important for immune response against infected or malignant cells (125). Another half-transporter is ABCB9, which forms homodimers in lysosomes, pumping peptides into lysosomal lumen (134). Full transporters ABCB4 and ABCB11 are expressed in liver where they regulate secretion of bile acids (135). The last members of B group are mitochondrial transporters localised in outer (ABCB6) and inner (ABCB7, ABCB8 and ABCB10) mitochondrial membranes. They have important role in iron-sulphur cluster (ISC) and haem biosynthesis (128).

The C group of ABC transporters includes 12 full transporters with diverse functions. ABCC7 (also known as cystic fibrosis transmembrane conductance regulator CFTR)

functions as chloride ion channel in epithelial cell membranes. Mutation in *ABCC7* gene leads to dysregulation of epithelial fluid transport resulting in cystic fibrosis (136). ABCC8 and ABCC9 (also known as SUR1 and SUR2) are sulfonylurea receptors which together with potassium channels regulate insulin secretion (137). Remaining members ABCC1, ABCC2, ABCC3, ABCC4, ABCC5, ABCC6, ABCC10, ABCC11 and ABCC12 (also called MRP1-9) belong to the multidrug resistance proteins (MRPs). They are able to transport a wide range of xenobiotics and endogenous compounds such as glutathione conjugates, glucuronide conjugates, sulfate conjugates, purine and pyrimidine nucleotide analogues, antracyclines, vinca alcaloids etc. Some substrates of MRPs also serve as an important signalling molecules altering signalling pathways in tumours, enabling them to survive and proliferate (124).

ABC transporters belonging to the group D are localised in peroxisomal (ABCD1-3) and lysosomal (ABCD4) membranes. Peroxisomal ABC transporters are involved in transport of long chain and branched chain fatty acids or their CoA-derivatives into peroxisomes whereas ABCD4 transport vitamin B12 from lysosome to cytosol. Dysfunction of ABCD1 leads to X-linked adrenoleukodystrophy, a severe neurodegenerative disease (138). Groups E (ABCE1) and F (ABCF1-3) consist of ABC transporters that have only NBDs and do not contain any TMDs. ABCE1 contains two ISCs that have important role for translation initiation and ribosomal biogenesis (139). ABCF transporters are thought to be involved in inflammation process and regulation of translation (140). The last group of the ABC transporter family includes five members ABCG1, ABCG2, ABCG3, ABCG5 and ABCG8, which are all half transporters. ABCG1 is important for intracellular sterol and lipid homeostasis (141). ABCG2 may exist as a higher order homooligomer in plasma membranes of epithelial cells in gastrointestinal tract, blood brain barrier, liver, placenta and stem cells where it fulfils its function by protecting the cells from xenobiotics. Various compounds have been shown to be substrates of ABCG2 including anticancer drugs, sulfate and glucuronide conjugates of sterols and xenobiotics, natural compounds and toxins, fluorescent dyes, photo-sensitisers and antibiotics (142). ABCG5 and ABCG8 form heterodimers that pump sterols out of enterocytes and hepatocytes. Mutations in *ABCG5* and *ABCG8* genes cause sitosterolemia; a metabolic disorder characterised by hyper-absorption and decreased biliary excretion of dietary sterols (143).

### *2.1.4.2. ABC transporters in cancer biology*

Several members of ABC transporters are known as MDR proteins due to their ability to efflux cytotoxic chemotherapeutics. MDR phenomenon is a term for resistance to several anti-cancer drugs that are structurally and functionally unrelated. More than half of the members of ABC transporters have been shown to confer drug resistance, from which the most crucial are ABCB1, ABCC1 and ABCG2 (144). The most common chemotherapeutic substrates of selected ABC transporters are listed in Table 2.1. Numerous studies showed a correlation between expression of ABCB1, ABCC1 and ABCG2 transporters and malignant progression, aggressive phenotype and poor overall survival in various types of cancers (reviewed in (145)). The overall patient survival also decreases with increasing number of simultaneously expressed ABC transporter genes (146). ABCB1 (also known as P-glycoprotein or MDR1) was the first ABC transporter identified and connected with resistance to anticancer drugs (147). P-glycoprotein transports neutral or positively charged hydrophobic compounds and has been shown to transport a wide range of cancer chemotherapeutics (Table 2.1.), which seem to induce its expression (148). ABCG2 (also known as breast cancer resistant protein) is a half transporter that was firstly identified as a mediator of doxorubicin resistance in breast cancer (149). ABCG2 is able to transport a particularly wide range of chemotherapeutics (Table 2.1.). ABCC1 (also known as MRP1) was identified in small cell lung cancer cell line as a mediator of acquired resistance to doxorubicin (150). Substrates of ABCC1 represent unmodified hydrophobic molecules and a broad range of xenobiotics and endogenous substrates (Table 2.1.), mostly glutathione and glucuronide conjugates. ABCC1 transports reduced as well as oxidised glutathione and thus might also have a role in maintaining and modulating responses to oxidative stress (151).

Some ABC transporters are highly expressed in CSCs to protect them against xenobiotics. ABCG2 is considered a CSC marker and its expression is important for maintenance of stem cell phenotype and proliferation (152). In line with this concept, some reports also indicate that ABCG2 has a role in resistance that is independent of drug efflux (153). Inhibition of ABCB1 was also reported to reduce CSC phenotype (154,155) and ABCB5 was reported as a marker of malignant-melanoma-initiating cells (156). Concordantly, signalling pathways and TFs involved in CSC maintenance were reported to regulate expression of ABC transporters. Hedgehog signalling regulates ABCB1 and ABCG2 expression (157). ABCG2

is also a target of Notch signalling (158). OCT-4, a pluripotent transcription factor, can regulate genes coding for ABC transporters (159). ABCC1 and ABCC4 expression is a highly predictive factor in neuroblastoma, because of its transcriptional regulation by *N-MYC* oncogene, a driver of neuroblastoma tumorigenesis (160,161). The presence of ABC transporters in CSCs from tumours of different tissues, where they are involved in the transport of various substrates, indicates that they are also involved in basic cellular processes. In addition to drug efflux, ABC transporters also contribute to tumorigenesis by transporting signalling molecules such as prostaglandins, leukotrienes, sphingosine-1-phosphate, platelet activating factor, cholesterol and cyclic nucleotides (Table 2.1.). These molecules act in an autocrine or paracrine manner, they bind to their receptors and activate pathways involved in cell proliferation, migration, angiogenesis, cell survival and inflammation (162).

**Table 2.1. Chemotherapeutics and endogenous substrates of ABC transporters (162,163).**

| ABC transporter | Chemotherapeutic substrates | Endogenous (cellular) subtrates |
|---|---|---|
| **ABCB1** | Doxorubicin, daunorubicin, vinblastine, docetaxel, irinotecan, topotecan, paclitaxel, chloroquine, glucocorticoids | PAF |
| **ABCC1** | Doxorubicin, daunorubicin, methotrexate, vincristine, etoposide, chloroquine | $LTC_4$, $PGA_2$, 15d-$PGJ_2$, $PGE_2$ and S1P |
| **ABCC2** | Methotrexate, vinblastine, etoposide, vincristine, cisplatin, epirubicin, taxanes, doxorubicin | $LTC_4$, $PGD_2$, $PGA_1$ and $PGE_2$ |
| **ABCC3** | Etoposide, methotrexate | $LTC_4$ and 15d-$PGJ_2$ |
| **ABCC4** | Mercaptopurine, thioguanine, campotothecins, azidothymidine, azathioprine, topotecan, methotrexate | $LTB_4$, $LTC_4$, $PGA_1$, $PGE_1$, $PGE_2$, $PGF_{1\alpha}$, $PGF_{2\alpha}$, $TXB_2$, cAMP and cGMP |
| **ABCC5** | Fluorouracil, mercaptopurine, thioguanine, azathioprine, methotrexate | cAMP and cGMP |
| **ABCC6** | Antracyclines, etoposide | $LTC_4$ |
| **ABCC10** | Docetaxel, paclitaxel, vincristine, vinblastine, nucleoside analogues and epothilone B | $LTC_4$ |
| **ABCC11** | Methotrexate, fluorouracil | $LTC_4$, cAMP and cGMP |
| **ABCG2** | Mitoxantrone, topotecan, doxorubicin, daunorubicin, irinotecan, imatinib, methotrexate | cGMP |

cAMP, cyclic AMP; cGMP, cyclic GMP; LT, leukotriene; PAF, platelet activation factor; PG, prostaglandin; S1P, sphingosine- 1-phosphate; TX, thromboxane

The strategy to overcome resistance by generating inhibitors of ABCB1, ABCC1 or ABCG2 has advanced into production of the third generation inhibitors. Despite significant improvement in specificity, there are still extensive side effects and inhibitors failed to show any benefits (164). The main reasons for ABC transporter inhibitors failure are redundancy of ABC transporters and also interference of inhibitors with the normal ABC transporter physiology (165).

Thus, new strategies and understanding molecular mechanisms that modulate the expression and post-transcriptional regulation of ABC transporters, will be necessary to overcome cancer resistance.

## 2.2. Metabolism of iron

### 2.2.1. Importance of iron

Elemental iron is a fundamental micronutrient which has an indispensable role in mammalian cells. The human body utilises iron for synthesis of iron-containing proteins where iron is incorporated in form of haem or ISCs. These proteins are then involved in basic cellular processes, such as cell replication, metabolism and growth. The iron-containing proteins include oxygen transporting proteins, haemoglobin and myoglobin, enzymes important for function of mitochondrial respiratory chain, Krebs cycle and redox reactions as well as enzymes necessary for DNA replication and repair. Cellular iron level must thus be tightly regulated as improperly sequestered free iron catalyses production of ROS through the Fenton and Haber-Weiss reactions (166,167). Balanced iron metabolism is achieved by strict coupling of iron uptake with iron demands connected with distribution of iron into cellular compartments, which are involved in iron utilization and storage. Defects in proteins involved in iron metabolism are associated with chronic degenerative disorders having neurodegenerative, haematological or metabolic phenotype (5). Besides this, defects in mitochondrial and cytoplasmic ISC biogenesis and its insertion into particular proteins may also cause DNA damage and genome instability; a condition which leads to many pathological situations including cancer (168).

## 2.2.2. Iron trafficking

The human body absorbs 1-3 mg of iron every day to replenish the losses in sweat, urine, blood and desquamated cells. The systemic iron level is maintained by controlled intestinal absorption of dietary non-haem ferric iron by enterocytes *via* divalent metal transporter 1 (DMT1, also known as SLC11A2 or NRAMP2) (169). Prior to the absorption, the ferric ($Fe^{3+}$) iron is reduced to ferrous ($Fe^{2+}$) iron by ferric reductases such as duodenal cytochrome b (DCYTB, also known as CYBRD1), which is together with DMT1 expressed on the apical side of the membrane of enterocytes (170). Haem iron is also taken up by enterocytes as an intact metalloporphyrin, and after entering the cells, it is broken down into $Fe^{2+}$, bilirubin and carbon monooxide by haem oxygenase (HMOX1) (Fig. 2.4.) (171). Intracellular transport of iron from apical to the basolateral side of enterocytes is still not fully described (172). Export of iron from enterocytes into bloodstream is facilitated by basolateral divalent iron exporter ferroportin (FPN, also known as SLC40A1) (173) with the help of ferroxidase hephaestin (HEPH), which oxidises $Fe^{2+}$ to $Fe^{3+}$. HEPH is anchored into basolateral membrane of enterocytes together with FPN to enhance the iron export in these cells (Fig. 2.4.). In other cells of the body, this role is taken by circulating HEPH homolog, known as ceruloplasmin (CP) (174).

Upon release from enterocytes, oxidised iron rapidly binds to serum transferrin (Tf), which can bind two $Fe^{3+}$ ions. Under normal conditions, only 30 % of serum Tf is occupied by iron, providing a sufficient buffering capacity in case of sudden increase in free iron level called non-Tf-bound iron (NTBI), which may be toxic (175). The complex Tf-diferric iron binds to transferrin receptor 1 and 2 (TfR1 and 2, encoded by *TFRC* and *TFR2* genes) on all cells, followed by clathrin-mediated endocytosis of TfR with bound Tf (Fig. 2.4.) (176). Upon endosome acidification, $Fe^{3+}$ is released from Tf, and reduced by endosomal 6-transmembrane epithelial antigen of the prostate (STEAP) family of ferriductases (in case of immature erythroid cells STEAP3) to $Fe^{2+}$ (177) and exported to the cytosol by DMT1 (178) or directly to mitochondria by a “kiss and run” mechanism (179). While iron ions may pass freely through the outer mitochondrial membrane into intermembrane space through voltage dependent anoint channel (VDAC), crossing the inner membrane is an active process dependent on membrane potential. Transport of iron to mitochondria through the inner membrane is facilitated by mitoferrins, MFRN1 and MFRN2 (180).

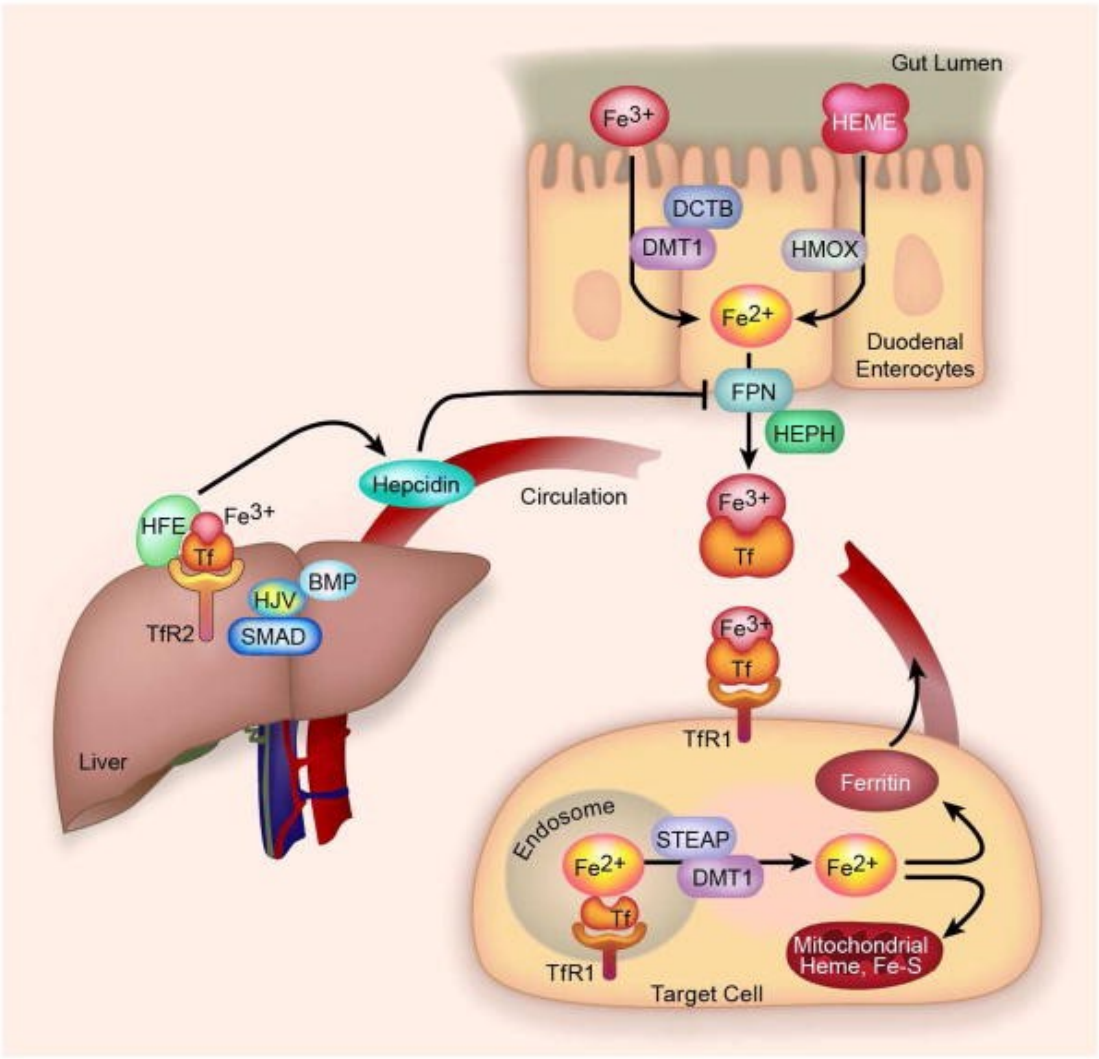


**Fig. 2.4. Overview of iron trafficking.** $Fe^{3+}$ is reduced to $Fe^{2+}$ by Duodenal cytochrome b reductase (DCTB) and enters intestinal cells through divalent metal transporter 1 (DMT1). Haem is also taken up by enterocytes and $Fe^{2+}$ is released by haem oxygenase (HMOX). $Fe^{2+}$ is exported from cells by ferroportin (FPN) and after oxidization by hephaestin (HEPH), iron binds to transferrin (Tf) in the bloodstream. Tf binds to transferrin receptor 1 and 2 (TfR1 and TfR2) on target cells. TfR1 is endocytosed and after acidification of the endosome, Fe3+ is released from TfR1, reduced by 6-transmembrane epithelial antigen of the prostate (STEAP) reductase and transported from endosome to cytosol by DMT1. From cytosol, iron is transported to sites of its utilization (e.g. mitochondrion for haem and Fe-S cluster synthesis) or stored within ferritin. In the liver, Tf binds to TfR2 and protein HFE and together with GPI-anchored protein haemojuvelin (HJV), bone morphogenetic protein (BMP) and SMAD signal transduction pathways, controlling the production of Hepcidin. Hepcidin controls the release of iron from cells by internalization and degradation of FPN. Figure adapted from ref. (181).

TfR with bound Tf is then recycled on the cell surface where Tf without bound iron dissociates from TfR at neutral pH (182). TfR2 has 30 times lower affinity for Tf and differs

from TfR1 in such a way that its expression is not regulated by the intracellular level of iron (183). Upon higher iron demand, iron depleted cells express and secrete glyceraldehyde-3-phosphate dehydrogenase (GAPDH) which acts as transferrin receptor and enhance cellular uptake of Tf and iron (184). In addition to Tf bound iron, NTBI can also be very efficiently taken up by many cell types using the NTBI transporters of the Zrt/Irt-like protein family, especially by the ZIP14 (also known as SLC39A14) (185).

Free intracellular iron is toxic to the cell and it is therefore obvious that it is sequestered by association with iron-binding proteins or chaperones, which either store iron or transport it within the cell. In cytosol, we can find members of poly r(C)-binding proteins (PCBPs), PCBP1 and PCBP2, functioning as an iron ion chaperones. They bind iron in cytosol and deliver it to cytosolic acceptors such as iron storage protein ferritin (186), iron exporter protein FPN1 (187) or to the iron cofactor requiring enzymes like iron-dependent prolyl hydroxylases (PHDs) and asparaginyl hydroxylases that modify HIF1α (188).

Iron storage is a crucial part of intracellular iron homeostasis. The cytosolic iron is stored within ferritin, the major intracellular iron storage protein. Ferritin is composed of 24 protein subunits, the ferritin light (FTL) and the feritin heavy chains (FTH), which form a nanocage or a spherical shell. This subunits are coded by *FTL* and *FTH* genes. One ferritin molecule can store around 4500 of iron ions, which entry and exit ferritin through pores in the ferritin shell (189). The ferritin expression increases with rising cellular iron concentration. High concentration of iron loaded ferritin leads to ferritin aggregation. These aggregates then fuse with lysosomes, where ferritin is degraded into mixture of $Fe^{3+}$ and a protein component called haemosiderin (190). Ferritin is also secreted from the cells in amounts that strongly correlate with intracellular iron concentration (190).

### 2.2.3. Systemic iron homeostasis

Systemic iron homeostasis is maintained by regulation of duodenal iron absorption, iron recycling of senescent erythrocytes and mobilization of iron from the storage sites (liver, spleen). Hepcidin (HAMP) is a small circulating peptide that is upregulated in hepatocytes in response to high iron stores and inflammation and it is downregulated during hypoxia and

iron deficiency. Hepcidin acts as an important regulator of iron stores by binding to iron exporter FPN on its target cells (hepatocytes, macrophages and enterocytes), causing FPN internalization and degradation, which leads to retention of iron within the cell (191,192). The central role in regulating hepcidin level in response to iron level plays the bone morphogenetic protein/sma and mother against decapentaplegic (BMP/SMAD) pathway (Fig. 2.4.) (193). BMPs belong to the TGF-β superfamily of cytokines. Several members of BMPs have been demonstrated to increase hepcidin levels with BMP6 being the key hepcidin modulator (194). BMP6 is produced by liver cells in response to hepatic iron stores (195). The binding of BMP to its receptor BMPR on the cell surface requires binding of BMP with its cell surface co-receptor haemochromatosis type 2 protein (HFE2, also known as haemojuvelin (HJV)) for full activation of hepcidin expression (Fig. 2.4.) (196). The amount of HFE2 is regulated by cell surface serine protease matriptase-2 (TMPRSS6) expressed primarily in the liver. When activated, TMPRSS6 inhibits *HAMP* gene transcription by cleaving HFE2 and thus abrogating its function as a BMP co-receptor (197). Importantly, molecules that can sense circulating level of iron such as TfR2, TfR1 and hereditary haemochromatosis protein (HFE) are required for BMP pathway activity (Fig. 2.4.) TfR2 has been recently found to be involved in upregulation of BMP6 in response to high iron level and HFE is probably involved in efficient downstream transmission of the regulatory signal from BMP6 (198). Mutations/dysfunction of HFE, TFR2 and HFE2 leads to inappropriately low levels of hepcidin, causing a disease termed hereditary haemochromatosis, characterized by iron overload and tissue damage in skin, heart, liver, pancreas, joints and gonads (199). TfR1, HFE and TfR2 have been proposed to form a complex that senses serum iron saturation and regulates hepcidin expression (200).

### 2.2.4. Cellular iron homeostasis

Since iron is important in biological redox reactions and cells have no mechanism how to eliminate iron excess, the maintenance of cellular iron is coordinated by tight regulation of iron uptake, storage and export. The commonly described mechanism of regulation is *via* iron-dependent binding of iron regulatory proteins (IRPs) to the iron-responsive elements (IREs). IREs are stem-loop structures of RNA located in 5‘ or 3‘ UTRs of mRNAs coding

for iron metabolism-related proteins. Binding of IRPs to IREs located at the 5‘ end of UTRs of certain mRNAs leads to translational repression of such genes. On the other hand, binding of IRPs to IRE situated at the 3’ end of UTR causes mRNA stabilization and its enhanced translation (Fig. 2.5.) (201). When the iron concentration in the cell is low, IRPs bind to the 5’ IREs of ferritin and FPN mRNA, thereby inhibiting translation of these genes, and to the 3’IREs of TfR1 and DMT1 mRNA leading to increase in their stability and expression. It leads to higher iron acquisition from plasma Tf and a decrease in ferritin synthesis as iron storage becomes futile under iron deficiency. Inversely, a high cellular iron concentration causes dissociation of IRPs from IREs, leading to an increase in translation of ferritin and FPN mRNAs and degradation of TfR1 and DMT1 mRNAs (Fig. 2.5.). The superfluous amount of iron is then stored within ferritin and the intracellular flux of iron through TfR1 is suppressed (202–206). The functional 5’ IRE motif has been identified in other mRNAs coding for proteins involved in haem synthesis (erythroid aminolevulinate synthase, ALAS2) (207), hypoxia adaptation (hypoxia-inducible transcription factor-2α, HIF-2α also known as EPAS1) (208), tricarboxylic acid cycle (mitochondrial aconitase, ACO2) (209) or in Alzheimer’s disease (amyloid beta precursor protein, APP) (210). The 3’ IRE motif has been also found in mRNAs for proteins participating in cytoskeletal reorganization (CDC42-binding protein kinase α, also known as MRCKα) (211) and cell cycle control (cell division cycle 14A, CDC14A) (212). These examples show that IRP/IRE regulation extends to other processes besides iron homeostasis (213).

The main IRPs are IRP1 (also known as ACO1 or IREB1) and IRP2 (also known as ACO3 or IREB2) belonging to the aconitase family of proteins (214). This family also encompasses ACO2, the mitochondrial enzyme containing a cubic [4Fe-4S] cluster in its active site, which catalyses the conversion of citrate to isocitrate *via cis*-aconitate intermediate during Krebs cycle (215). IRP1 and IRP2 both bind IRE containing mRNA but they differ in several ways. IRP1 also contains the [4Fe-4S] cluster in its active site and works as a bifunctional enzyme. Under normal conditions, with the ISC inserted into its active site, IRP1 resembles the cytosolic function of ACO2, but in iron depleted cells, holo-IRP1 is converted into apo-IRP1 possessing the IREs binding activity (216). Unlike IRP1, IRP2 does not contain ISC and thus exhibits only IREs binding function (217).

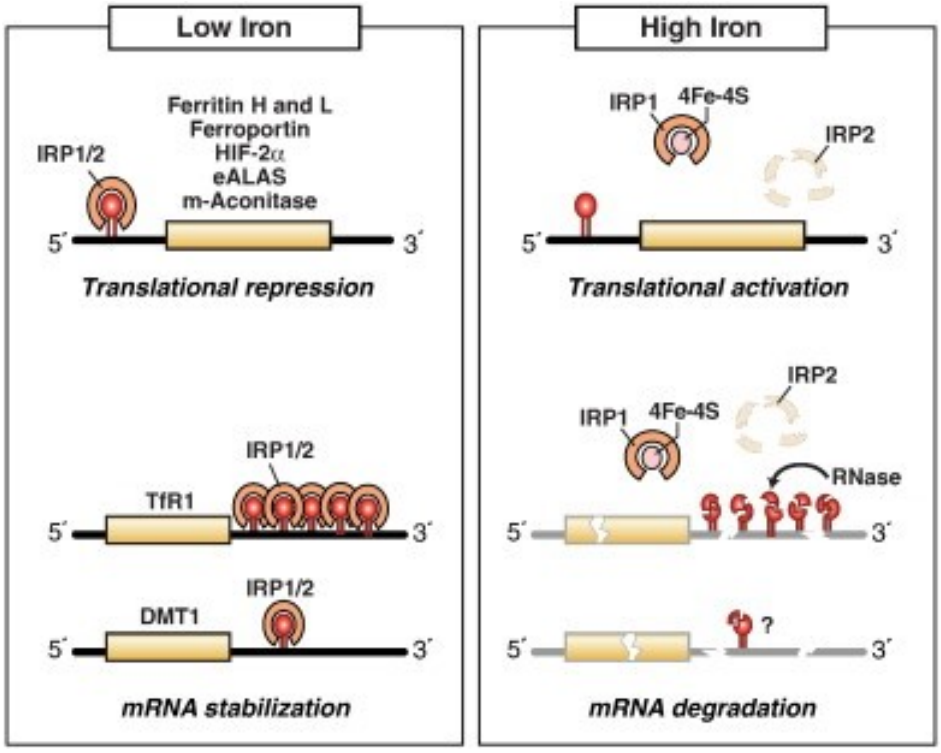


**Fig. 2.5. Regulation of translation of mRNAs containing iron-responsive elements by iron responsive proteins (IRP1/2).** When iron is limited, IRPs1/2 are activated and bind to 5' ends of mRNAs coding for ferritin, ferroportin, hypoxia inducible factor-2α (HIF-2α), 5-aminolevulinate synthase (ALAS) or m-aconitase, which leads to translation repression, and to 3' end of mRNAs coding for transferrin receptor 1 (TfR1) and divalent metal transporter 1 (DMT1) leading to mRNA stabilization. In iron replete cells, IRPs1/2 dissociate from target mRNAs. Figure adapted from ref. (218).

IRP1 is regulated by multiple mechanisms. A key role in IRP1 regulation plays the [4Fe-4S] cluster, which provides a direct sensor of the level of cellular iron as formation of the ISC cofactors is iron dependent. Several enzymes, as described in the chapter 2.2.5., are necessary for the biogenesis of ISCs and thus conversion of apo-IRP1 to holo-IRP1. Silencing of components of mitochondrial and cytosolic ISC biogenesis and/or iron deprivation leads to disruption of ISC formation and thus to activation of the IRP1 (218). IRP1 is also regulated by ROS and reactive nitrogen species. The [4Fe-4S] cluster is solvent accessible and reactive species such as superoxide anion ($O_2^{\cdot -}$) or peroxynitrite ($NOO^{\cdot}$) can initiate cluster conversion to the [3Fe-4S], leading to formation of the IRP1 containing the [3Fe-4S] cluster that does not possess IRE binding activity. However, the responses to NO and $H_2O_2$ are more complex, probably involving other signalling pathways, and lead to cluster disassembly and activation of the IRP1/IRE binding on mRNA molecules (219,220).

Excess of iron causes inactivation of the IRP1 by two ways. First is so called iron-sulfur switch that is insertion of the [4Fe-4S] cluster into active site of IRP1, converting it into ACO1. The second mechanism is iron-mediated degradation of the IRP1 (221). IRP1 can be phosphorylated by protein kinase C at the conserved $Ser^{138}$ and $Ser^{711}$ residues. Phosphorylation of $Ser^{138}$ sensitises IRP1 to non-oxidative demetallation of the [4Fe-4S] to the [3Fe-4S] cluster (222) and marks the IRP1 to iron-dependent degradation (221). IRP1 phosphorylated at $Ser^{711}$ displays negligible IREs binding and aconitase activity (223).

IRP2 is regulated merely by iron mediated degradation. In iron replete cells, the IRP2 is targeted for proteasomal degradation by S-phase kinase associated protein 1-cullin-1-F-box/LRR-repeat protein 5 (SKP1-CUL1-FBXL5) E3 ubiquitin ligase complex. FBXL5 is a member of the F-box family adaptor proteins that has substrate specificity to SCF (SKP1-CUL1-F-box) E3 ubiquitin ligases. FBXL5 itself is regulated by intracellular iron level as it is degraded in cells upon iron and oxygen depletion and stabilised in iron-replete cells. This process requires iron-binding haemerythrin-like domain in FBXL5 N-terminus, which in the presence of iron and oxygen, binds iron and stabilises FBXL5 E3 ligase that ubiquitinates IRP2 and targets it to proteasomal degradation (224,225).

### 2.2.5. Iron-sulphur cluster biogenesis

ISCs are inorganic cofactors that typically bind to cysteinyl ligands in ISC binding proteins. Most commonly, the ISC requiring proteins contain rhomboid [2Fe-2S], cuboidal [3Fe-4S] or cubane [4Fe-4S] clusters (226). The biogenesis of mammalian ISCs is a multistep process located in both mitochondria and cytosol.

The first step in ISC formation is assembling of [2Fe-2S] cluster on an iron-sulphur cluster assembly enzyme scaffold protein (ISCU). This is accomplished by desulphuration of soluble cysteine by cysteine desulfurase complex NFS1-ISD11 serving as a sulphur donor (227). NFS1 is a pyridoxal phosphate-dependent transaminase that converts free cysteine to alanine and creates an enzyme-bound persulphide(-SSH) group serving as a source of sulphur (228). ISD11 (also known as LYR motif-containing protein 4 (LYRM4)) acts as a stabilizing partner of NFS1 heterodimer (229) that binds two diametrically opposed ISCU

scaffold proteins. ISCU provides the cysteine ligands to coordinate the nascent cluster. *De novo* [2Fe-2S] cluster synthesis requires the function of reduced ferredoxin (FDX2) (230), which reduces the persulphide sulphur ($S^0$) to sulphide ($S^{2-}$), and frataxin (FXN) for stimulation of sulphur transfer from NFS1 to ISCU (231) and/or possibly providing iron (Fig. 2.6.) (232).

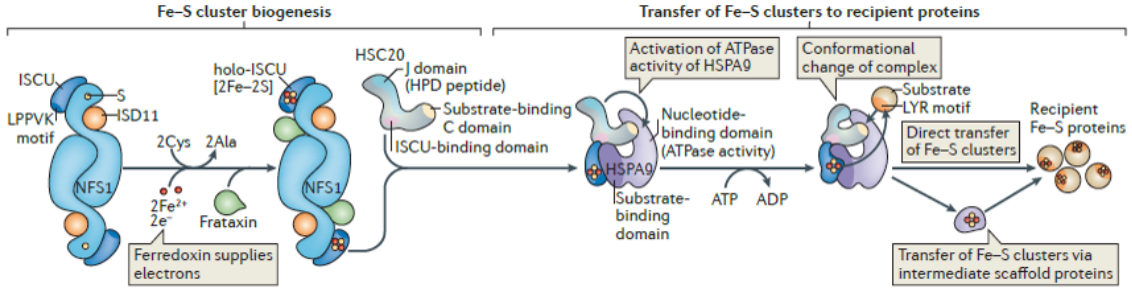


**Fig. 2.6. The Fe-S cluster biogenesis and transfer to recipient proteins.** The cysteine desulphurase NFS1 binds to its stabilizing partner protein ISD11 and two iron-sulphur cluster assembly enzyme scaffold proteins (ISCU). Desulphurase activity of NFS1 generates a persulphide (S, shown as a yellow circle) and cysteinyl ligand provided by ISCU stabilises the nascent cluster. Ferredoxin reduces the persulphide sulphur ($S^0$) to sulphide ($S^{2-}$) (230), and frataxin stimulates transfer of sulphur from NFS1 to ISCU (231) and/or possibly provides iron (232). The co-chaperon HSC20 binds to ISCU and facilitates ISCU release from NFS1-ISD11. The Leu-Pro-Pro-Val-Lys (LPPVK) motif of ISCU is recognised by substrate binding domain of HSPA9. The C domain of HSC20 binds to Leu-Tyr-Arg (LYR) motif of recipient proteins to tether them close to Fe-S cluster. The J domain of HSC20 protein activates ATPase activity of the nucleotide-binding domain of HSPA9. ATP hydrolysis drives conformational change for direct transfer of the Fe-S cluster from ISCU to target protein. The indirect transfer of Fe-S clusters requires other intermediate scaffold proteins. Figure adapted from ref. (233).

After the formation of a nascent cluster, it has to be transferred to target proteins. This is carried out by help of a co-chaperone HSC20, which binds ISCU, and forms a complex with its chaperone partner heat shock 70 kDa protein 9 (HSPA9), a member of the HSP70 heat shock protein family. HSPA9 uses energy from hydrolysis of ATP to drive conformational changes required for transfer of ISC to target proteins (Fig. 2.6.) (234). ISC is transferred directly or indirectly to recipient proteins. Direct transfer is *via* guiding function of HSC20, which binds to leucine-tyrosine-arginine (LYR) motif in acceptor proteins (234). The indirect ISC transfer includes intermediate carriers such as glutaredoxin 5 (GLRX5), which transiently accept [2Fe-2S] cluster and engage chaperone-co-chaperone complex to facilitate cluster insertion into target apoproteins (235). [2Fe-2S] cluster is also used for biosynthesis of the [4Fe-4S] clusters in a process requiring mitochondrial complex of

proteins iron-sulfur cluster assembly 1 and 2 (ISCA1, ISCA2) and putative transferase CAF17 (known as IBA57) (236). Additional factors then facilitate trafficking of newly synthesised [4Fe-4S] clusters to target apoproteins (237).

The biogenesis of cytosolic and nuclear ISC containing proteins is dependent on mitochondrial ISC assembly apparatus for generation of sulphur-containing compounds, which are exported to cytosol by the mitochondrial ABC transporter ABCB7. In the cytosol, these sulphur-containing compounds are then utilised by the cytosolic iron-sulphur protein assembly machinery for ISC formation, followed by ISC insertion into extra-mitochondrial target proteins (reviewed (238,239)).

### 2.2.6. Iron in cancer progression

As mentioned above, iron is an important micronutrient essential for cell replication, DNA synthesis, cellular metabolism and growth, and thus necessary for cancer cell proliferation. Ability to gain and lose electrons, makes iron indispensable in a broad range of enzymatic reactions but also enables iron to generate potentially deleterious ROS. Low levels of ROS may contribute to proliferation but high levels of ROS lead to oxidative damage to lipids, proteins and DNA, which may be mutagenic and/or lethal (166).

Over the years, it has been discovered that iron excess correlates with an increased cancer risk, mutagenesis and enhanced tumour growth. Several studies describe altered iron metabolism in cancer cells to maintain their demand for high iron requirements due to their proliferative nature and metabolic needs (6). Thus, components of machinery maintaining iron acquisition (TfR1, TfR2, DMT1, DCYTB, STEAP), storage (Ferritin), efflux (FPN) and regulation (IRP1 and IRP2) are all perturbed in cancer in a way to provide cells with sufficient amount of iron (reviewed in (6,7)). The higher demand for iron has also been already used in development of anti-cancer therapies. In view of important function of iron in cancer cells, iron chelators provide a way for cancer treatment. Some of them such as deferoxamine (DFO) or di-2-pyridylketone-4,4-dimethyl-3-thiosemicarbazone (Dp44mT) have been shown to inhibit cancer growth *in vitro* and *in vivo* by depletion of cellular iron and formation of ROS (8,240–243). Targeting of TfR1 also showed potential in cancer

treatment for direct targeting by antibodies or development of Tf conjugates for tumour specific TfR1 targeted delivery systems (244). Iron mediated generation of ROS to induce ferroptosis, a form of non-apoptotic cell death, was also utilised in treatment of cancer (245). Interestingly, a combination of iron chelator with antibodies against TfR1 showed an anticancer effect *in vitro* (246), yet this finding has not been translated into cancer treatment so far .

There are seldom reports describing the iron metabolism and importance of iron for biology of CSCs. Recently, it was shown by us (247) that CSCs of prostate and breast origin exhibit altered iron metabolism. Higher iron uptake, TfR1 and ferritin expression was reported in glioblastoma CSCs compared to non-CSCs (248). Contrary, silencing of *FTH* gene expression increased CSCs and EMT markers in ovarian and breast cancer cells (249,250). Another study shows that iron induces CSC phenotype in non-small cell lung cancer cells (251). Further, overexpression of FPN reduced EMT markers in breast cancer (252).

Importantly, data presented in these studies are in agreement with results that we obtained in our *in vitro* model of breast CSCs [245], suggesting that iron metabolism plays an important role in cancer progression and in the maintenance and self-renewal of CSCs. It is thus likely that reprogramming of iron/ROS metabolism is an important aspect of tumour cell survival. Targeting iron metabolism may thus provide new tools for cancer therapy which would not only affect proliferation of cancer cells but it would also target CSCs.

# 3. AIMS OF THE STUDY

Since the main objectives and significance of this work for study of cancer biology with relation to cancer treatment are already discussed in the first chapter of this thesis, in this part, the specific experimental aims of this study are given:

1) Generation of cells in form of floating spheres as an *in vitro* model of CSCs from different breast and prostate cancer cell lines by two different approaches, their comparison and validation of the phenotype of the resulting CSCs

2) Elucidation of the mechanisms of resistance in CSCs

    a. Measurement of the response of CSCs to chemotherapeutic drugs together with usage of specific ABC transporters inhibitors.

    b. Expression profiling of genes coding for 48 ABC transporters in generated spheres by using the high-throughput platform BioMark HD System (Fluidigm).

    c. Confirmation of the most differentialy expressed genes on the protein level for further experimental work.

    d. Elucidating of the role of miR-301a-3p in the *in vitro* model of CSCs.

    e. Defining the molecular mechanisms of miR-301a-3p action.

    f. Determine the role of miR-301a-3p in tumor growth and its relevance as a prognostic factor.

3) Elucidation of iron metabolism in CSCs

    a. Defining the role of iron in CSC biology by using iron chelators and measurement of iron flux in the cells.

    b. Expression profiling of selected iron metabolism-related genes in generated spheres by using the high-throughput platform BioMark HD System (Fluidigm).

c. Confirmation of the most differentialy expressed genes on the protein level for further experimental work.

d. Measurement of oxidative environment, activity of IRP/IRE system and activity of ISC containing enzymes in spheres.

# 4. MATERIALS AND METHODS

## 4.1. Tissue culture and sphere generation

All cell lines used in this work were obtained either directly from American Type Culture Collection or from prof. Lopez (Griffith University, Australia). Cells were routinely cultivated in Dulbecco's modified eagle medium (DMEM, Sigma) (BT474, DU-145, MCF7, T47D, ZR-75–30, ZR-751, MDA-MB-231 cells) or Roswell park memorial institute medium (RPMI, Sigma) (LNCaP cells) supplemented with 10% foetal bovine serum (FBS, Thermo Scientific), 100 U/ml penicillin, 100 μg/ml streptomycin; in 5% $CO_2$ and 37 °C. MCF10A cells were cultivated in DMEM/F12 (Lonza) with 5% horse serum, 100 U/ml penicillin, 100 μg/ml streptomycin, supplemented with 0.1 ng/ml cholera toxin, 20 ng/ml EGF (Thermo Scientific), 0.5 μg/ml hydrocortisone and 1 mg/ml insulin.

For generation of spheres, we used advanced DMEM/F12 or advanced RPMI1640 (for LNCaP cells) (Thermo Scientific) supplemented with 5% proliferation supplement (Stem Cell Technologies), 100 U/ml penicillin, 100 μg/ml streptomycin, 10 mM 4-(2-hydroxyethyl)-1-piperazineethanesulfonic acid (HEPES), 2 mM glutamine, 20 ng/ml EGF, 5 ng/ml FGF (Thermo Scientific), 4 μg/ml heparin (Sigma). The control medium contained 5% FBS, 100 U/ml penicillin, 100 μg/ml streptomycin, 10 mM HEPES and 2 mM glutamine.

MCF7 cells with inducible expression of miR-301a were generated by stable transfection with two vectors from Clontech; trans-activator coded by pEF1-TET3G vector and doxycycline-inducible pTREG-IRES vector containing miR-301a gene or no insert (empty vector, EV),

## 4.2. DNA constructs

### 4.2.1. MiR-301a inducible vector

The sequence of pri-miRNA-301a was amplified by PCR from cDNA obtained from MCF7 cell line using Q5 hot start high-fidelity DNA polymerase (New England BioLabs) with the following primers:

Forward 5' CCCTCGTAAAGTCGACTGCATGTTTCTGTTCGAATG;

Reverse 5' CAGTTACATTAGATCTGGGCAAGTAACTGCAGGAAA.

The amplified sequence was then cloned into the SalI/BglII sites of pTRE3G-IRES vector (Clontech).

### 4.2.2. Luciferase vectors

The whole 4 kbp long 3'UTR sequence of *ESR1* gene was amplified by PCR from cDNA originating from MCF7 cell line using the following primers containing the NotI restriction sites:

Forward 5' TGCAAGTGAGCGGCCGCGAGCTCCCTGGCTCCCACA;

Reverse 3' TGCAAGTGAGCGGCCGCTTAGTTTAATTCTTTATTTGAACATC.

The amplified product was then cloned into NotI site of pTK-Cypridina vector (Thermo Scientific). Vectors with deleted the first, the second and both sites of predicted miR-301a-3p binding were created by site directed mutagenesis by using Q5 Hot start high-fidelity DNA polymerase (New England BioLabs) according to manufacturer´s protocol with the following primers:

Site 1 Forward 5' TTGTTTTCTAAGTAATTGCTGCCTCTGTCTTTTGAGATTCAAGA AAAATTTC;

Site 1 Reverse 5' GAAATTTTTCTTGAATCTCAAAAGACAGAGGCAGCAATTACTT AGAAAACAA;

Site 2 Forward 5' CATCCCGCTGGATTCTTTTTCAATGTTTCATTAAACAAAGCAA AGC;

Site 2 Reverse 5' GCTTTGCTTTGTTTAATGAAACATTGAAAAAGAATCCAGCGGG ATG.

The thermal conditions for PCR were: 98 °C for 5min; 5 cycles of 98 °C for 15 s, 80 °C for 10 s, 70 °C for 30 s and final extension at 72 °C for 8 min then 15 cycles of 98 °C for 10 s, 80 °C for 10 s and 72 °C for 8 min followed by final extension at 72 °C for 10 min. Product of PCR reaction was then incubated with DpnI Fast digest enzyme (Thermo Scientific) at 37 °C for 30 min and transformed into TOP10 ultracompetent cells. All constructs were verified by Sanger sequencing (GATC Biotech).

## 4.3. Luciferase assay

MCF7, T47D and BT474 cells were seeded at a concentration of 40 000 cells per well of a 24-well plate. Next day, cells were transfected with miR-301a-3p mimic (Sigma HMI0442), miR-301a-3p anti-miR (Ambion AM17000) and corresponding controls (Sigma HMC0003, Ambion AM17010) using INTERFERin transfection reagent according to manufacturer's protocol (Polyplus). After 24h, the medium was changed and the second transfection with reporter luciferase vectors (250 ng/well) and normalization pTK-Gaussia-Dura Luc vector (50 ng/well) (Thermo Scientific) was performed using Lipofectamine LTX and Plus Reagent (Thermo Scientific) according to manufacturer's instructions. After 24 h of incubation, medium was harvested to detect the activities of luciferases using the Pierce Gaussia/Cypridina Glow Assay Kit (Thermo Scientific) using infinity M200 reader (TECAN).

## 4.4. MiR-301a-3p mimic and miR-301a-3p anti-miR transfection

MCF7, T47D and BT474 cells were seeded at concentration of 200 000 cells per well of a 6-well plate. Next day, cells were transfected with 40 nM miR-301a-3p mimic (Sigma HMI0442) or 80 nM miR-301a-3p anti-miR (Ambion AM17000) and corresponding controls (Sigma HMC0003, Ambion AM17010) using INTERFERin (Polyplus) according to manufacturer's instruction. After 72h of incubation cells were used for subsequent protein and RNA analysis or for measurement of response of cells to 17-β-$E_2$ (see chapter 4.5.).

## 4.5. Response of MCF7 cells to 17-β-oestradiol

Trypsinised cells were collected, washed several times with phosphate-buffered saline (PBS) and seeded at a concentration of 2 500 cells per well of a 96-well plate in 100 µl of DMEM media without phenol red (Sigma) supplemented with 10% charcoal stripped FBS (Thermo Scientific) and 100 U/ml penicillin, 100 µg/ml streptomycin. Cells were incubated with the increasing concentration of 17-β-$E_2$ for 5 days. Cells were then fixed with 4% paraformaldehyde in PBS, washed with PBS and stained with 0.05% crystal violet dye (Sigma). The unbound dye was washed away with PBS and the bound dye was dissolved in 1% sodium dodecyl sulphate (SDS). The absorbance was measured at 595 nm using infinity M200 reader (TECAN).

## 4.6. Cellular viability assays

Experiments showing sensitivity of cells to iron chelator were performed by using Cell Titer Glow (Promega, G7570) and Cell Titer Fluor assays (Promega, G6080) according to manufacturer's instruction. 5 000 cells per well were seeded into a white 96-well luminescence plate (Cell Titer-Glow) or a 96-well black fluorescent plate (Cell Titer-Fluor) and incubated with increasing concentration of iron chelator salicyl isonicotinoyl hydrazone (SIH) for 72 h. Cells were then incubated with equal amount of Cell Titer-Glow reagent and

luminescence was measured by Infinity M200 reader (TECAN). Similarly, cells were incubated with a fluorogenic peptide glycylphenylalanyl-aminofluorocoumarin and its fluorescence recorded at the excitation wavelength of 400 nm and emission wavelength of 505 nm using infinity M200 reader (TECAN).

Experiments showing sensitivity to daunorubicin and doxorubicin were performed by using cell counting kit-8 (CCK-8; Dojindo, CK04-20). 10 000 cells was seeded into 96-well plate and next day incubated with increasing concentration of doxorubicin or daunorubicin for 48 h. CCK-8 solution was then added into cell suspension and the mixture was incubated for 2 h. Absorbance was measured at 450 nm using infinity M200 reader (TECAN).

## 4.7. RNA isolation and quality determination

The isolation of total RNA was performed by means of RNAzol (Molecular Research Center) and RNA from mice tumours was isolated by RNA Blue (Top-Bio), both according to manufacturer's instructions. RNA quantity was measured by using Nanodrop spectrophotometer (ND-1000, Thermo Scientific), and RNA integrity was measured with the Agilent 2100 Bionalyser (Agilent Technologies).

## 4.8. cDNA synthesis

RNA samples of RNA quality with RNA integrity number 8-10 were used. For fluidigm reverse transcription-quantitative polymerase chain reaction (RT-qPCR), RNA was reverse-transcribed into cDNA by the Maxima H minus reverse transcriptase kit according to manufacturer's instructions (Thermo Scientific), using 400 ng of total RNA as a template and oligo-dT as primers.

For other application in this work, cDNA was synthesised using RevertAid First Strand cDNA Synthesis Kit (Fermentas) following manufacturer's instructions, using 700 ng of total RNA as a template and oligo-dT as primers.

## 4.9. Fluidigm RT-qPCR

Primer BLAST was used to design all primers in this work. The assays were designed to span intron and to have at least one primer covering an exon/exon boundary. The sequences of assays are listed in Supplementary table 1. Each sample for a fluidigm RT-qPCR was pre-amplified with mix of all primer pairs for 18 cycles. One reaction contained: 5 µl of iQ Supermix (Bio-Rad), 2 µl of diluted cDNA, 1.25 µl of pre-amplification primer mix in a final concentration of 25 nM and 1.25 µl of water. The pre-amplification thermal profile was: 95 °C for 60 s, 18 cycles of 95 °C for 15 s and 4 min at 60 °C. RT-qPCR was performed using the high-throughput platform BioMark HD System (Fluidigm) with 96.96 Dynamic Array IFC for gene expression. 5 µl of sample pre-mix contained: 1 µl of 20 x diluted pre-amplified cDNA, 2.5 µl of SsoFast EvaGreen Supermix (Bio-Rad), 0.25 µl of 20 x SG sample loading reagent (Fluidigm) and 1.25 µl of water. 5 µl of assay pre-mix contained: 2 µl of 10 µM primer assays, 2.5 µl of 2 x assay loading reagent (Fluidigm) and 0.5 µl of water. Thermal conditions for fluidigm RT-qPCR were: 98 °C for 3 min, 35 cycles of 98 °C for 5 s and 60 °C for 5 s. Raw data were subtracted from the gDNA control and efficiencies of individual assays were calculated from the serial dilutions of a mixed cDNA sample. Assays with insufficient efficacy or very high Cq values (> 25) were excluded from the analysis. The actual analysis was performed *via* the GenEx software version 6 and the missing values were replaced by the mean of average value calculated from the whole group. Reference genes for normalization were identified by Normfinder; data were normalised to several reference genes (*GAPDH, POLR2A*, *RPLP0*, *HPRT1* and *TBP*). The acquired data were subjected to statistical analysis by using the unpaired t-test *via* the GenEx software version 6; p-value $< 0.05$ was considered statistically significant and results statistically significant with the Dun-Bonferroni correction are marked with #.

## 4.10. RT-qPCR using Eva Green DNA-binding dye

Primers for measurement of RT-qPCR were designed as described in the chapter 4.9. The sequences of used primers are listed in Supplementary table 1. One reaction for normal RT-qPCR contained: 2.5 µL of cDNA (containing 10 ng of template RNA), 1.5 µl of 5 x

HOT FIREpol Eva Green RT-qPCR mix (Solis Biodyne), 0.197 µl of 10 µM primer assays and 3.3 µl of H2O). The thermal profile for RT-qPCR was: 95 °C for 12 min, 38 cycles of 95 °C for 10 s, 60 °C for 20 s and 72 °C for 20 s. The data were analysed *via* GenEx software version 6, reference genes for normalization of the data were selected by Normfinder.

## 4.11. RT-qPCR using TaqMan probe

The expression of hsa-miR-301a-3p was measured by using the TagMan MicroRNA Assay (Applied Biosystems, TM000528); snU6 was used for normalization (Applied Biosystems, TM001973). Hsa-miR-301a-3p and snU6 were transcribed by RevertAid First Strand cDNA Synthesis Kit (Fermentas) using specific RT primers. One reaction for reverse transcription contained: 3.5 µl of RT master mix (1.5 µl of 5 x reaction buffer, 0.095 µl of RNAse inhibitor, 0.75 µl of 10 mM dNTPs, 0.5 µl of reverse transcriptase, 0.655 µl of $H_2O$), 2.5 µl of RNA (2 ng/µl) and 1.5 µl of oligo-dT primers. Thermal profile for reverse transcription was: 16 °C for 30 min, 42 °C for 30 min, and 85 °C for 5 min. The subsequent RT-qPCR was carried out by using HOT FIREpol universal probe mastermix (Solis Biodyne). 1.5 µl of 5 x mastermix, 0.375 µl of TaqMan assay (20 x), 3.125 µl of H2O and 2.5 µl of 5 x diluted cDNA was mixed and run for 95 °C 10 min and 40 cycles of 95 °C for 15 s and 60 °C for 60 s. The data were analysed *via* GenEx software version 6.

## 4.12. Western blotting

The amount of a specific protein was measured by standard western blot assay. Harvested cells were washed with PBS and lysed in RIPA buffer (50 mM Tris, 150 mM NaCl, 0.1% SDS, 0.5% sodium deoxycholate, 1% NP-40) supplemented with protease and phosphatase inhibitors. Protein concentration was measured *via* the bicinchinonic acid (BCA, Thermo Scientific). Samples were mixed with 4 x sample loading buffer and incubated for 5 min at 95 °C (exception was made for ABC transporters, where the samples were not boiled). 50 µg of total protein was resolved on SDS polyacrylamide gels according to standard procedure at 20 mA per gel and blotted onto a nitrocellulose membrane (BioRad) *via* Xcell blotting module (Invitrogen) at a constant voltage (35 V) for 2 h. After blocking with 5%

non-fat milk (Serva)/Tris-buffered saline with 0.05% Tween 20 (TBS-T) for 1 h, the membrane was incubated overnight in 5% bovine serum albumin (Sigma)/TBS-T with primary antibody against ACO1 (PA5-27824, Thermo Scientific), CYBRD1 (bs-8297R, Bioss), EPAS1 (PA116510, Thermo Scientific), GLRX5 (bs-13395R, Bioss), HEPH (bs-15458R, Bioss), HFE (bs-12335R, Bioss), IREB2 (PA116544, Thermo Scientific), QSOX1 (SAB2700031, Sigma), TfR1 (13-6800, Thermo Scientific), SLC39A14 (ab191199, Abcam), SLC40A1 (bs-4906R, Bioss), SLC11A2 (15083, Cell Signalling), Ferritin (ab75973, Abcam), ERα (sc-544, Santa Cruz), PR (8757S, Cell Signaling), GREB1 (HPA024616, Sigma), Cathepsin D (2284S, Cell Signaling), CXCL12 (3740S, Cell Signaling), BMP7 (ab129156, Abcam), ABCA1 (mAB10005, Merck Millipore), ABCA3 (LS-C313351, LSBio), ABCA5 (HPA022032, Sigma), ABCA7 (sc-377335, Santa Cruz), ABCA12 (ab98976, Abcam), ABCB1 (ab170904, Abcam), ABCB6 (ab194409, Abcam), ABCB7 (PA530219, Thermo Scientific), ABCB8 (HPA045187, Sigma), ABCB9 (sc-393412, Santa Cruz), ABCB10 (PA5-30468, Thermo Scientific), ABCC1 (14685S, Cell Signaling), ABCC2 (sc-5770, Santa Cruz), ABCC3 (14182S, Cell Signaling), ABCC4 (12705S, Cell Signaling), ABCC5 (bs-1437R, Bioss), ABCC6 (ab134913, Abcam), ABCC7 (sc-376683, Santa Cruz), ABCC8 (SAB1404430, Sigma), ABCC10 (bs-5761R, Bioss), ABCC11 (sc-249895, Santa Cruz), ABCC12 (sc-249900, Santa Cruz), ABCD3 (sc-20973, Santa Cruz), ABCD4 (sc-31878, Santa Cruz), ABCF1 (sc-377185, Santa Cruz), ABCF2 (sc-390496, Santa Cruz), ABCF3 (HPA036332, Sigma), ABCG1 (ab52617, Abcam), ABCG2 (4477S, Cell Signaling), ABCG4 (PA5-50289, Thermo Scientific), Actin (MA5-15739-HRP, Thermo Scientific), Tubulin (ab4742, Abcam). Next day, the membrane was washed with TBS-T and incubated with corresponding horseradish peroxidase- conjugated antibody in 1% non-fat milk/TBS-T for 1 h. The membrane was then washed again with TBS-T and incubated with either Clarity ECL (Biorad) or Sirius ECL substrate (Advansta) and chemiluminescence was assessed with ImageQuant LAS 4000 (GE Healthcare).

## 4.13. Measurement of labile iron pool

Labile iron pool (LIP) was measured by using fluorescence probe calcein, which binds $Fe^{2+}$ rapidly, stoichio- metrically, and reversibly while forming fluorescence quenched Ca–Fe

complexes (253). Cells were incubated with 250 nM calcein acetoxymethylester-(calcein-AM) for 30 min in medium without serum and sodium bicarbonate supplemented with 1% bovine serum albumin (BSA; Sigma). Cells were then washed twice with Hanks Balanced Salt Solution and seeded at concentration of 10,000 cells per well of 96-well plate. Fluorescence measurement started at the excitation wavelength of 468 nm, emission wavelength of 517 nm, after initial 5 min measurement by using infinity M200 reader (TECAN). Then 100 μM of iron chelator SIH was added and the fluorescence was recorded after 2 min.

## 4.14. Measurement of $^{55}$Fe uptake

Cells were dissociated with cell dissociation buffer (CDB; 1% BSA, 1 mM EDTA, 1 mM EGTA in PBS, pH 7.4), washed twice with the reaction buffer (50 mM HEPES (pH 7.4), 94 mM NaCl, 7.4 mM KCl, 0.74 mM MgCl2, 5 mM D-Glucose) and 200 μl of reaction buffer containing 1 million of cells was put into tube. 1 μl of 1 μCi of $^{55}$Fe in complex with citrate (1:10) was added into tube with cell solution. Tube was then incubated at 37 °C for 90 min with occasional mixing and cooled on ice. Background binding was determined by addition of 1 μCi of $^{55}$Fe to the cells followed by immediate cooling. Samples were then washed 5 x with the reaction buffer, re-suspended in 100 μl of water and added to 5 ml of scintillation fluid. Radioactivity was measured on a scintillation counter and background was corrected.

## 4.15. Measurement of $^{55}$Fe subcellular localization

Cells were incubated with 50 nM $^{55}$Fe complexed with citrate 1:10 for 72 h. Cells were dissociated in CDB and washed with reaction buffer used in the chapter 4.14. Cells were counted and diluted in STE buffer (250 mM sucrose, 10 mM TRIS, 1 mM EDTA) to a concentration of 4 million of cells per 1 ml of STE buffer. Cells were homogenised according to Smitt et al. (254) to retain intact mitochondria. Cellular homogenate was spun at 800 × g for 5 min to collect nuclei then spun at 3000 × g for 5 min and resulting supernatant was spun at 9,000 × g for 10 min to gain mitochondrial fraction and cytosolic fraction. Protein content in each fraction was determined by the BCA assay (Thermo Scientific) and 20 μg of

protein was used for radioactivity measurement by a scintillation counter and background was corrected.

## 4.16. Aconitase activity assay

Activity of aconitase enzyme was measured by using the aconitase activity assay (MAK051, Sigma) according to manufacturer's instructions. Absorbance was measured at 450 nm using infinity M200 reader (TECAN). Background was subtracted by using activity of lysates without substrate and values were normalised to protein content measured by BCA method (Thermo Scientific).

## 4.17. Activity of mitochondrial complex I

Activity of mitochondrial complex I (CI) was detected by mitochondrial respiratory CI assay (ab109721, Abcam) according to manufacturer's instructions. Assay is based on immune-capturing of CI followed by colorimetric reaction measuring its activity. Absorbance was measured at 450 nm using infinity M200 reader (TECAN).

## 4.18. Assessment of the iron responsive protein/iron responsive element binding activity

Harvested cells were spun at 300 × g for 5 min, washed with PBS and lysed in buffer containing 10 mM HEPES (pH 7.4), 3 mM MgCl2, 40 mM KCl, 1 mM DTT and 0.2% NP-40. Proteins were quantified by the BCA method (Thermo Scientific). 60 µg of protein lysate was incubated with 4 µM of Cy5 labelled IRE probe containing the IRE sequence from the human *FTH* gene (Cy5-UCGUCGGGGUUUCCUGCUUCAACAGUGCUUGG-ACGGAACCGGCGCU) in 24 mM HEPES, 60 mM KCl, 5% Glycerol, 0.004 U/µl RNAsin, with or without 2% β-mercaptoethanol in a total volume of 20 µl for 20 min. Then 2 µl of heparin (255,256) was added and mixture was incubated for another 10 minutes.

Consequently, 2.4 µl of 10 x loading dye was added and the reaction mixture was loaded onto 3–20% acrylamide gel in TBE buffer (89 mM Tris (pH 7.6), 89 mM boric acid, 2 mM EDTA). Electrophoresis run at 70 V for 30 minutes, followed by 120 V until the blue dye reached the bottom of the gel. The gel was then visualised by the Typhoon instrument.

## 4.19. Detection of reduced glutathione and reduced/oxidised glutathione ratio level

The level of reduced glutathione (GSH) and ratio between GSH and oxidised glutathione - glutathione disulphide (GSSG) was detected by using fluorescence based kit (BioVision) according to manufacturer's instructions. Briefly, cells were spun, washed with PBS and lysed in cell lysis buffer. Protein concentration was measured by the BCA method (Thermo Scientific). 1 µg of total protein lysate was mixed with 25 µl of assay buffer in black 96-well plate. 25 µl of the glutathione assay mixture or total glutathione assay mixture was added to samples. Fluorescence was measured at the excitation wavelength of 480 nm and emission wavelength at 520 nm using infinity M200 reader (TECAN).

## 4.20. Measurement of the level of mitochondrial membrane potential and reactive oxygen species

Spheres and control cells were dissociated by CDB used in the chapter 4.14 to obtain single cell suspension and incubated with fluorescent probes for 15 min. ROS were assessed by using 5 µM 2′,7′-dichlorofluorescein diacetate (DCF-DA), 2.5 µM dihydroethidium (DHE), 5 µM hydroxyphenyl fluorescein (HPF) or 2.5 µM MitoSOX and mitochondrial membrane potential ($\Delta\Psi m$) was measured by 50 nM tetramethylrhodamine methyl ester (TMRM). After incubation, cells were spun 300 x g for 5 min and re-suspended in PBS. Fluorescence was measured by flow cytometer (BD FACS Calibur) and expressed as a mean fluorescence intensity *via* FlowJo 9.6.2. software.

## 4.21. *In vivo* experiments

All animal studies were approved by Czech Academy of Sciences and conducted in accordance with Czech Council guidelines for the Care and Use of Animals in Research and Teaching.

Female Balb/c nude athymic mice (CAnN.Cg-Foxn1nu/Crl, Charles River) were implanted subcutaneously with 0.72 mg/90-day-release 17β-$E_2$ pellet (Innovative Research of America, NE-121). Next day, mice were injected subcutaneously with MCF7 cells inducibly expressing miR-301a or with an EV in amount of 2 x $10^6$ cells per animal (4 mice per group and experiment was repeated twice). Mice were given doxycycline diet (200 mg/kg, Bio-Serv). The tumour growth was monitored twice a week by ultrasound imaging instrument Vevo770 (Visual Sonics) and quantified by Vevo software version 3. Mice were then sacrificed and tumours taken for further analysis (measurement of gene and protein expression by RT-qPCR and western blot).

## 4.22. Patient samples

Fresh frozen tumour tissue samples were obtained from 111 patients with primary breast carcinoma diagnosed at the Motol University Hospital (Prague, Czech Republic), the Hospital Atlas (Zlin, Czech Republic), and the Faculty Hospital Kralovske Vinohrady (Prague, Czech Republic) between years 2003 and 2014. Processing of the tissue samples was described in detail previously (257). Histological classification of carcinomas was performed according to standard diagnostic procedures (258). Expression of ER and PR was assessed immunohistochemically with the 1% cut-off value for classification of tumours as hormone receptor positive. ERBB2 (OMIM:164870) status was defined as positive in samples with immunohistochemical score 2+ or 3+ confirmed by fluorescence in situ hybridization or silver in situ hybridization analysis. Clinical characteristics of studied breast carcinoma patients are described in Table 4.1.

The expression level of the hsa-miR-301a-3p and snU6 was assessed in patient samples by RT-qPCR as described in the chapter 4.11. All patients were informed about the study and

those who agreed and signed an informed consent participated in the study. The study was approved by the Ethical Commission of the National Institute of Public Health in Prague. The methods were carried out in accordance with guidelines approved by the above Ethical Commission.

**Table 4.1. Clinical characteristics of studied breast carcinoma patients**

| **Characteristics** | **Number of patients (%)** |
|---|---|
| *Menopausal status* | |
| premenopausal | 12 (10.8) |
| postmenopausal | 93 (83.8) |
| not available | 6 (5.4) |
| *Histological type* | |
| invasive ductal carcinoma | 111 (100) |
| *Tumor size, median ± S.D., mm* | 18.5 ± 9.8 |
| *Lymph node metastasis* | |
| positive (pN1-3) | 40 (36.0) |
| negative (pN0) | 60 (54.1) |
| not determined (pNx) | 11 (9.9) |
| *Pathological stage* | |
| I | 39 (35.2) |
| II | 50 (45.0) |
| III | 11 (9.9) |
| not available | 11 (9.9) |
| *Histological grade* | |
| G1 | 17 (15.3) |
| G2 | 54 (48.6) |
| G3 | 40 (36.0) |
| *Oestrogen receptor expression* | |
| positive | 55 (49.5) |
| negative | 56 (50.5) |
| *Progesterone receptor expression* | |
| positive | 55 (49.5) |
| negative | 56 (50.5) |
| *HER2 expression* | |
| positive | 46 (41.4) |
| negative | 65 (58.6) |
| *Pathological subgroup* | |
| $ER^+$, $PR^+$, $ERBB2^+$ | 22 (19.8) |
| $ER^+$, $PR^+$, $ERBB2^-$ | 33 (29.7) |
| $ER^-$, $PR^-$, $ERBB2^+$ | 24 (21.6) |
| $ER^-$, $PR^-$, $ERBB2^-$ | 32 (28.8) |

## 4.23. Statistics

Results are represented as mean values ± SEM from at least three independent experiments. Statistics to calculate the difference between groups was carried out using the Student t-test, where $p < 0.05$ was considered statistically significant.

# 5. RESULTS

The majority of results presented in this thesis were done by me personally. However, in the last part of this thesis dedicated to iron metabolism in CSCs, I also present data which were obtained mainly by Z. Rychtarčíková and other co-workers from the Laboratory of tumour resistance. My main contribution to the iron metabolism project was preparation and cultivation of cell samples for subsequent analysis and expression profiling of the iron metabolism related genes on the mRNA level. Yet, I present all data that are necessary to illustrate the main scientific findings and their relevance to CSC biology as otherwise it would show incomplete picture of our findings and would present only fragmental knowledge of the topic. The data panels that are not the result of my personal work are thus labelled as "adapted from (247)" in all corresponding figure legends.

## 5.1. Spheres as an *in vitro* model of CSCs

To study the properties of CSCs *in vitro*, we used previously published methods of generating CSCs based on formation of non-adherent spheres (Fig. 5.1. A) *via* two alternative approaches. First method utilises cultivation of cancer cells on non-adherent plastic (259) and spheres generated by this approach are further referred as "agar". The second method is based on cultivation of cancer cells on normal plastic but in serum free medium containing proliferation supplement, EGF, FGF and heparin, which was already tested for CSCs generation in our lab (260). We were able to produce spheres from several breast (MCF7, BT474, T47D, ZR-75-30, MDA-MB-231) and prostate (DU-145, LNCaP) cancer cell lines but in some cell lines (DU-145) only the "agar" approach produced spheres. We also used non-malignant cell line of breast origin (MCF10A), from which we were not able to generate spheres by neither of the mentioned approach. Thus, we showed that only malignant cells, but not immortalised ones, have the propensity to generate spheres. However, the second approach generated spheres with more profound expression of CSC and EMT markers (Fig. 5.1. B), and this approach was used for further experiments.

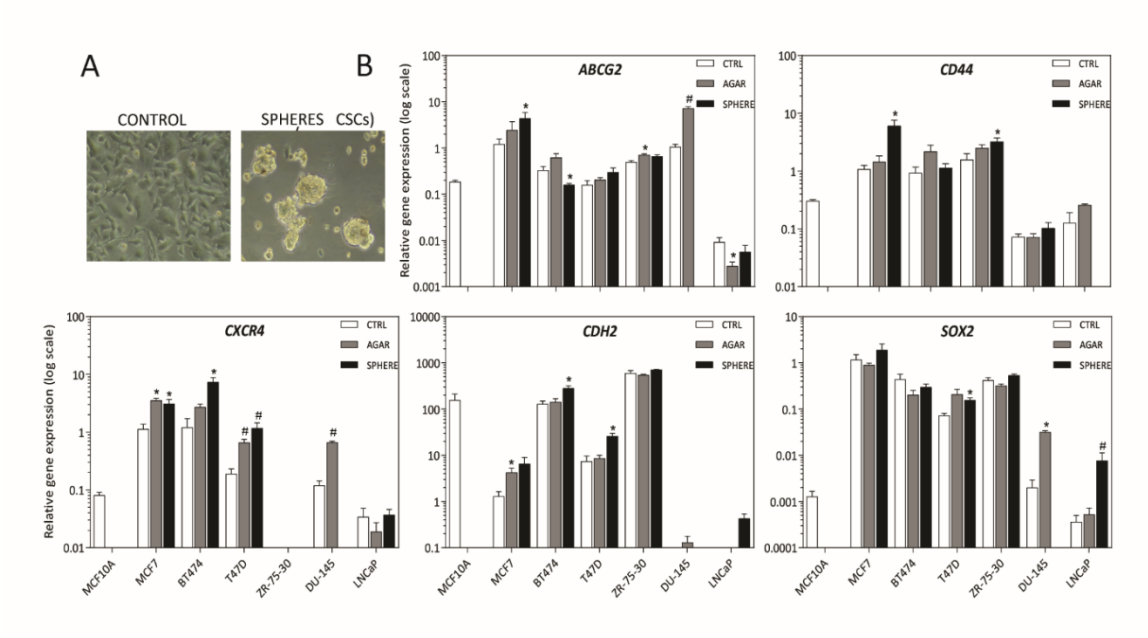


**Fig. 5.1. Expression of cancer stem cell (CSC) and epithelio-mesenchymal transition (EMT) markers in various cell lines and their corresponding spheres representing CSCs. A**, Appearance of MCF7 cells growing under control and sphere forming conditions **B**, Fluidigm RT-qPCR of stem cell and EMT markers in control and sphere cells derived from breast (MCF7, T47D, BT474, ZR-75-30) and prostate (DU-145, LNCaP) cancer cell lines. Experiments were performed at least in triplicate, standard error is SEM. Statistical significance was calculated by GenEx software using the unpaired t-test; * $p < 0.05$, # denotes statistical significance involving Dun-Bonferroni correction.

## 5.2. Mechanisms of resistance in CSCs

### 5.2.1. Spheres derived from MCF7 and T47D cell lines show resistance to anthracyclines doxorubicin and daunorubicin

The presence of CSCs in tumours is reported to be one of the reasons for resistance of tumours to cancer treatment. Therefore, we examined the response of our *in vitro* model of CSCs to commonly used drugs doxorubicin and daunorubicin. We treated control adherent and sphere cells derived from MCF7 and T47D cell lines with increasing concentrations of doxorubicin and daunorubicin for 48 h and measured their viability. We detected significantly higher amount of living cells in spheres derived from both cell lines than in corresponding control adherent cells, both in case of doxorubicin and daunorubicin (Fig. 5.2. A, B, C, D).

In conclusion, our *in vitro* model of CSCs exhibits resistance to commonly used anti-cancer drugs doxorubicin and daunorubicin and confirms the hypothesis that CSCs play a role in resistance.

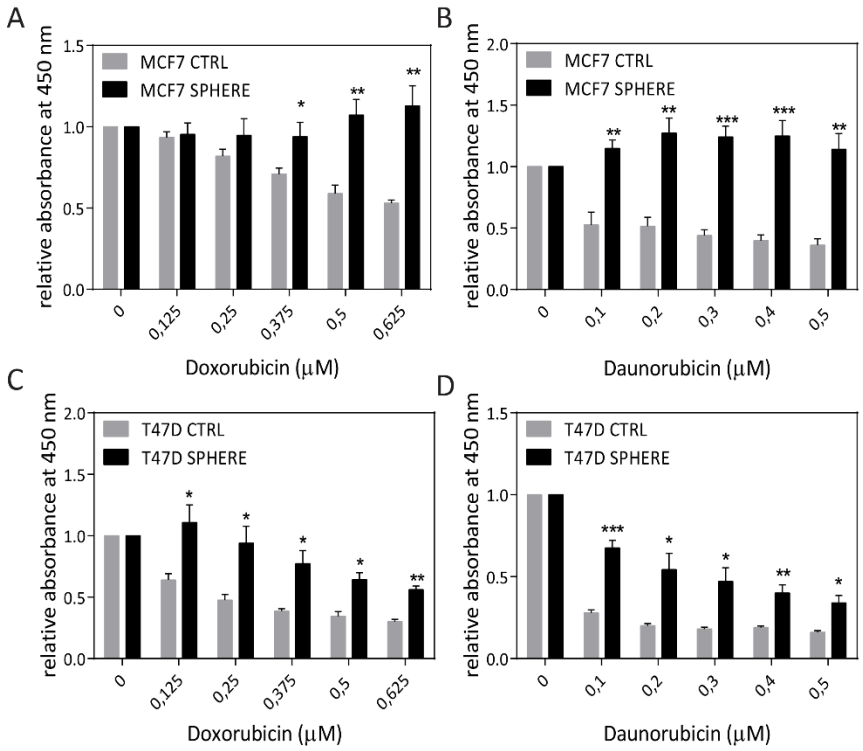


**Fig. 5.2. Spheres derived from MCF7 and T47D cell lines are more viable than control adherent cells in response to doxorubicin and daunorubicin**. **A**, **B**, **C**, **D**, Absorbance of reduced WST-8 formazan dye showing effect of doxorubicin and daunorubicin after 48 h on spheres derived from MCF7 and T47D cell lines and control cells. Experiments were performed in triplicate, standard error is SEM. Statistical significance was calculated using the t-test; * $p < 0.05$, ** $p < 0.01$, *** $p < 0.001$.

## 5.2.2. Inhibitors of ABC transporters decrease viability of CSCs

To see whether the inhibitors of ABC transporters may reverse the effect of chemotherapeutics, we treated cells for 24 h with inhibitors of ABCB1 (verapamil), ABCC1 (MK-571) and ABCG2 (novobiocin) transporters, which are known to transport doxorubicin and daunorubicin. As an assesment of cellular cytotoxicity, we used Cell Titer Glow assay, which detects cellular ATP level and it is used as a measure of cellular viability. Interestingly, we realised that spheres derived from MCF7, T47D and BT474 cell lines were

less viable than control adherent cells in the presence of the inhibitors. We detected a significant reduction in ATP level in MCF7, T47D and BT474 spheres when using MK-571 and novobiocin inhibitors and also a significant decrease in ATP level in BT474 spheres when using verapamil inhibitor in comparison to control adherent cells (Fig. 5.3.).

In summary, ABC transporter inhibitors MK-571, novobiocin and partly verapamil cause a decrease in viability of our *in vitro* model of CSCs, suggesting that ABC transporters play an important role in the biology of these cells.

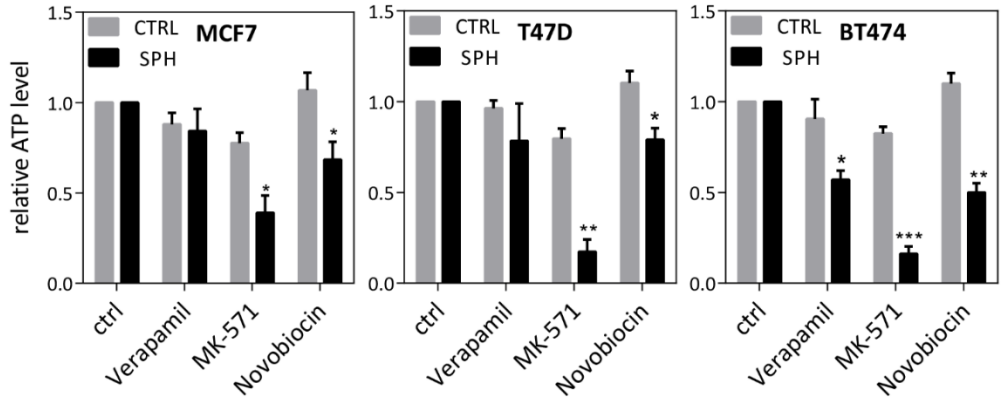


**Fig. 5.3. Inhibitors of ABCB1 (verapamil), ABCC1 (MK-571) and ABCG2 (novobiocin) reduce viability of spheres derived from MCF7, T47D and BT474 cell lines.** Spheres and control MCF7, T47D and BT474 cells were incubated with verapamil (20 μM), MK-571 (80 μM) or novobiocin (100 μM) for 24 h and ATP level was measured by Cell Titer Glow assay. Experiments were performed in triplicate, standard error is SEM. Statistical significance was calculated using the t-test; * $p < 0.05$, ** $p < 0.01$, *** $p < 0.001$.

## 5.2.3. CSCs generated from several cancer cell lines show alterations in expression of genes belonging to the ABC transporter superfamily

The specificity of verapamil, MK-571 and novobiocin against given transporter might be questionable as they also exerts other mechanisms of action. To better understand the role of ABC transporters in biology of CSCs, we decided to perform expression profiling of 48 members of ABC transporter family. Using fluidigm RT-qPCR from Biomark, we performed expression profiling of these genes in control adherent and sphere cells derived from various breast (MCF7, T47D, BT474, ZR-75-30) and prostate (DU-145, LNCaP)

cancer cell lines and non-malignant (MCF10A) cell line of breast origin. We obtained expression profile of 39 genes belonging to ABC transporters that were detectable in our cell lines and showed reliable RT-qPCR standard curves (Table 5.1.). We detected significant changes in gene expression in almost all groups of ABC transporters, the most significant mRNA upregulation across cell lines was detected in *ABCA1*, *ABCA3*, *ABCA5*, *ABCA12*, *ABCA13*, *ABCB7*, *ABCB9*, *ABCB10*, *ABCC1*, *ABCC2*, *ABCC3*, *ABCC5, ABCC8*, *ABCC10*, *ABCC11* and A*BCG2* (Table 5.1.). Interestingly, although there were some downregulated ABC transporters in individual cell lines, there was not a single one that would be significantly downregulated in all cell lines tested.

Next, we decided to assess the expression of ABC transporters also on the protein level by western blot analysis in breast cancer cell lines. Firstly, we wanted to check only the most upregulated genes, but we eventually discovered that the protein level of most ABC transporters did not significantly correlate with their mRNA level. Thus, we decided to measure the protein level of additional ABC transporters in MCF7, T47D and BT474 cell lines. We detected significant changes between control and sphere cells in almost all groups of ABC transporters with exception of the ABCD and ABCE groups (Fig. 5.4.). From western blot analysis, we selected the most differentially expressed ABC transporters, which were significantly altered in all three cell lines. Among these are ABCB8, ABCC1, ABCC2, ABCC10 and ABCG2 upregulated while ABCB10 and ABCF2 transporters are downregulated in spheres, and their role in biology of CSCs will be further studied.

In summary, we performed an expression profile of all 48 ABC transporters on mRNA and majority of them on protein level. We selected several ABC transporters which showed highest difference in expression between sphere and control cells for further study of their role in the biology of CSCs.

**Table 5.1. Expression profiling of ABC transporters in CSCs derived from breast and prostate cancer cell lines.**

| | | (MCF7 SPH) vs (MCF7 CTRL) | | (T47D SPH) vs (T47D CTRL) | | (BT474 SPH) vs (BT474 CTRL) | | (ZR-75-30 SPH) vs (ZR-75-30 | | (DU-145 AGAR) vs (DU-145 CTRL) | | (LNCaP SPH) vs (LNCaP CTRL) | |
|---|---|---|---|---|---|---|---|---|---|---|---|---|---|
| | Gene | Fold change | *P-Value* | Fold change | *P-Value* | Fold change | *P-Value* | Fold change | *P-Value* | Fold change | *P-Value* | Fold change | *P-Value* |
| 1 | *ABCA1* | | *0.7446* | 3.78 | *0.0009* | 8.14 | *0.0135* | 1.17 | *0.6380* | 1.45 | *0.5310* | 2.32 | *0.0453* |
| 2 | *ABCA2* | 1.02 | *0.8976* | -1.19 | *0.2064* | -1.14 | *0.4335* | 1.15 | *0.6777* | 1.20 | *0.3730* | 1.56 | *0.0312* |
| 3 | *ABCA3* | 1.96 | *0.0119* | 1.60 | *0.3375* | 3.96 | *0.0068* | 1.60 | *0.7153* | 11.88 | *0.0385* | 1.62 | *0.0300* |
| 4 | *ABCA4* | -1.23 | *0.5424* | 1.54 | *0.3890* | -5.51 | *0.0115* | 1.10 | *0.8703* | -1.68 | *0.0545* | 2.71 | *0.1559* |
| 5 | *ABCA5* | 1.23 | *0.5406* | 3.29 | *0.0032* | 6.28 | *0.0061* | 2.51 | *0.0251* | 3.40 | *0.0135* | 2.22 | *0.0598* |
| 6 | *ABCA7* | 1.54 | *0.0331* | 1.33 | *0.3484* | 1.09 | *0.6745* | -1.32 | *0.5971* | 3.65 | *0.0267* | 1.29 | *0.1911* |
| 7 | *ABCA10* | -1.41 | *0.0523* | 1.09 | *0.4930* | 1.07 | *0.4853* | -4.45 | *0.2672* | -1.35 | *0.1932* | 1.11 | *0.5479* |
| 8 | *ABCA12* | 2.43 | *0.0912* | 3.72 | *0.0039* | 2.19 | *0.0368* | -1.01 | | 2.20 | *0.0859* | 1.32 | *0.4692* |
| 9 | *ABCA13* | 2.14 | *0.2248* | 3.97 | *0.0003* | -1.16 | *0.8219* | 1.77 | *0.3722* | 3.73 | *0.0005* | 2.48 | *0.0509* |
| 10 | *ABCB1* | 1.43 | *0.2607* | | | -1.23 | *0.7141* | | | 7.30 | *0.1812* | | |
| 11 | *ABCB4* | 2.20 | *0.0022* | | | | | | | | | | |
| 12 | *ABCB6* | 1.86 | *0.0437* | 1.34 | *0.0001* | 1.45 | *0.0545* | -2.20 | *0.4241* | 1.82 | *0.0091* | 1.19 | *0.1194* |
| 13 | *ABCB7* | 1.36 | *0.0166* | 1.85 | *0.0255* | 1.52 | *0.0131* | 2.18 | *0.1724* | 2.05 | *0.0782* | 1.16 | *0.3627* |
| 14 | *ABCB8* | 1.39 | *0.1300* | 1.46 | *0.0760* | 1.31 | *0.0261* | 1.25 | *0.4125* | 1.94 | *0.0214* | 1.04 | *0.7424* |
| 15 | *ABCB9* | 1.59 | *0.0620* | 1.65 | *0.0538* | 2.25 | *0.0335* | -1.02 | *0.8416* | 3.05 | *0.0978* | 2.17 | *0.0025* |
| 16 | *ABCB10* | 1.93 | *0.0167* | 1.72 | *0.1498* | 1.71 | *0.1549* | 2.73 | *0.0670* | 2.40 | *0.0454* | 1.34 | *0.0851* |
| 17 | *ABCB11* | | | | | 1.69 | *0.3496* | | | | | -3.86 | *0.0010* |
| 18 | *ABCC1* | 1.62 | *0.0673* | 2.92 | *0.0228* | 1.88 | *0.0406* | 2.51 | *0.0713* | 7.84 | *0.0505* | 1.34 | *0.0481* |
| 19 | *ABCC2* | 7.13 | *0.0008* | 5.64 | *0.0085* | 3.42 | *0.0214* | 3.60 | *0.0537* | 11.37 | *0.0014* | 1.49 | *0.2588* |
| 20 | *ABCC3* | 1.52 | *0.4250* | 4.29 | *0.0016* | 15.73 | *0.0000* | | | 5.45 | *0.0108* | | |
| 21 | *ABCC4* | 1.34 | *0.3057* | | | 3.27 | *0.1727* | 1.28 | *0.4261* | 1.51 | *0.3116* | -1.04 | *0.9284* |
| 22 | *ABCC5* | 2.20 | *0.0122* | 4.04 | *0.0036* | 1.48 | *0.2568* | -1.04 | *0.9606* | 4.91 | *0.0260* | 1.26 | *0.3320* |
| 23 | *ABCC6* | 4.20 | *0.0803* | -1.11 | *0.6528* | | | | | 2.81 | *0.3394* | -1.47 | *0.3892* |
| 24 | *ABCC7 (CFTR)* | | | 2.29 | *0.0000* | -2.03 | *0.3997* | | | | | 2.28 | *0.0089* |
| 25 | *ABCC8* | 2.02 | *0.0123* | 1.96 | *0.0754* | 3.94 | *0.0009* | | | | | 1.58 | *0.0799* |
| 26 | *ABCC10* | 1.64 | *0.0809* | 1.82 | *0.2097* | 1.58 | *0.0029* | 1.53 | *0.0022* | 2.47 | *0.0489* | 2.58 | *0.0052* |
| 27 | *ABCC11* | 17.00 | *0.0012* | 4.10 | *0.0046* | 5.06 | *0.0103* | | | | | | |
| 28 | *ABCC12* | | | 21.31 | *0.0002* | 10.52 | *0.0144* | | | | | | |
| 29 | *ABCD1* | 1.46 | *0.2771* | -1.45 | *0.2096* | 1.74 | *0.1282* | -1.33 | *0.0393* | 1.11 | *0.8475* | -1.42 | *0.0680* |
| 30 | *ABCD2* | -1.10 | *0.7000* | | | | | 2.72 | *0.2072* | -1.72 | *0.1879* | 1.29 | *0.6938* |
| 31 | *ABCD3* | 1.64 | *0.0490* | 1.04 | *0.8695* | 1.76 | *0.0274* | -2.59 | *0.4817* | 1.54 | *0.2811* | 1.06 | *0.7386* |
| 32 | *ABCD4* | 1.09 | *0.4228* | 1.07 | *0.7292* | 1.06 | *0.6164* | 1.45 | *0.2833* | 1.26 | *0.0407* | 1.09 | *0.5529* |
| 33 | *ABCE1* | 1.03 | *0.8798* | -1.08 | *0.8438* | -1.23 | *0.3721* | 1.30 | *0.6154* | 1.58 | *0.5806* | 1.80 | *0.0567* |
| 34 | *ABCF1* | 1.28 | *0.0773* | 1.36 | *0.1496* | 1.43 | *0.0049* | -2.39 | *0.4739* | 1.31 | *0.1170* | 1.42 | *0.0020* |
| 35 | *ABCF2* | 1.21 | *0.1116* | 1.16 | *0.2832* | -1.02 | *0.8878* | 1.29 | *0.1748* | 1.08 | *0.5564* | 1.38 | *0.0048* |
| 36 | *ABCF3* | 1.31 | *0.0636* | 1.20 | *0.0264* | 1.43 | *0.0076* | 1.48 | *0.3320* | 1.42 | *0.0843* | 1.22 | *0.0045* |
| 37 | *ABCG1* | 2.39 | *0.0644* | 1.66 | *0.0825* | 5.09 | *0.0003* | | | 3.36 | *0.0595* | -1.91 | *0.1341* |
| 38 | *ABCG2* | 2.77 | *0.1416* | 1.85 | *0.1586* | -2.01 | *0.0411* | 1.36 | *0.0424* | 6.84 | *0.0003* | -1.21 | *0.6552* |
| 39 | *ABCG4* | 1.17 | *0.7282* | 2.19 | *0.0105* | 1.39 | *0.6257* | -1.00 | | 2.19 | *0.1464* | 1.42 | *0.3851* |

Table shows fold changes in expression of given genes (downregulation is expressed as negative fold change, red field show fold change > 1.5, yellow field show fold change < -1.5), statistical significance was calculated by t-test, green field show $p < 0.05$. The analysis was performed by GenEx software. Genes *ABCA6*, *ABCA8*, *ABCA9*, *ABCB2*, *ABCB3*, *ABCB5*, *ABCC13*, *ABCG5*, *ABCG8* were excluded from the analysis due to assay inefficiency or their low detection.

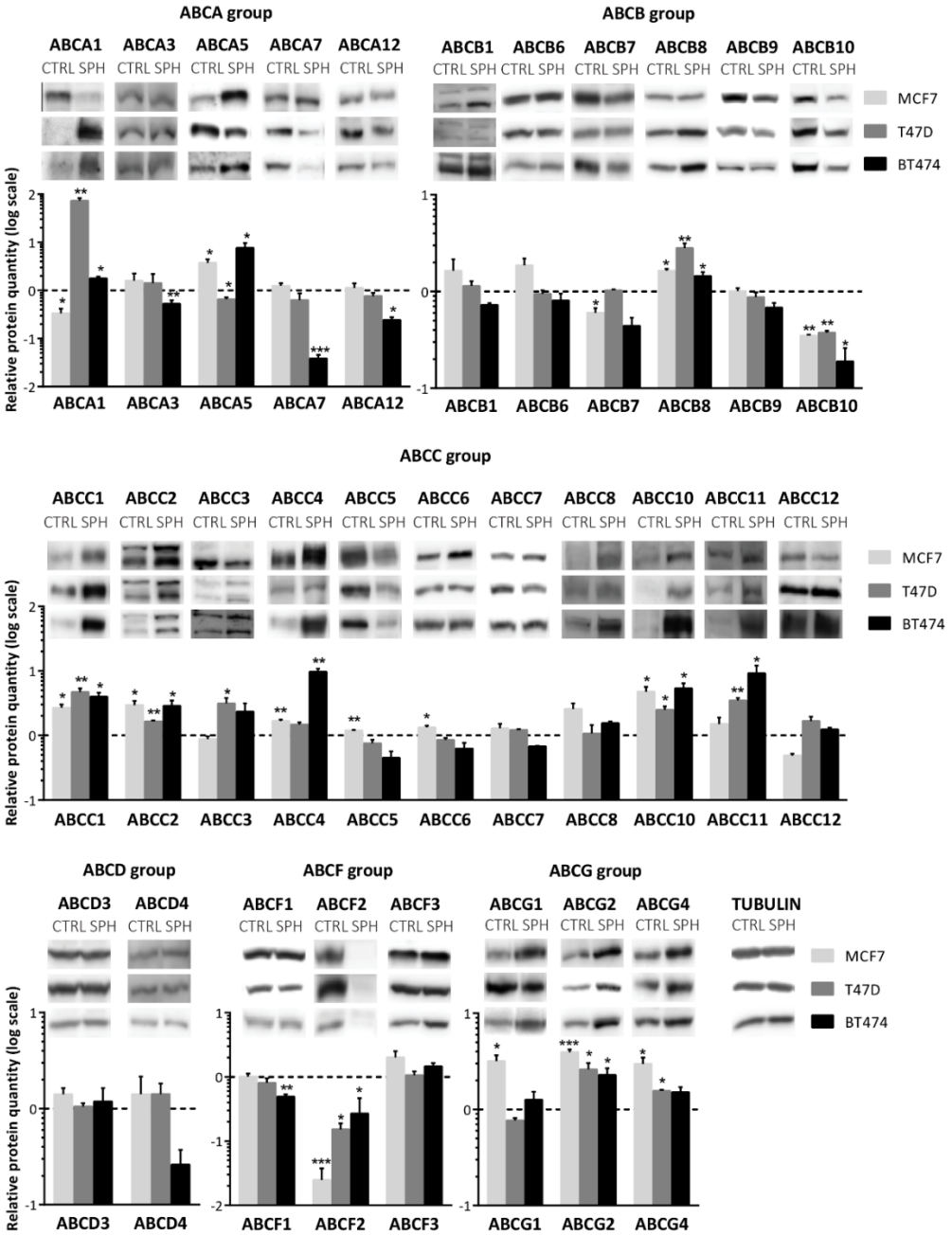


**Fig. 5.4. Expression of ABC transporters in spheres derived from MCF7, T47D and BT474 cell lines.** Representative western blots showing expression of given ABC transporters in control and sphere cells derived from MCF7, T47D and BT474 cancer cell lines. Bellow each set of western blot pictures is the densitometry evaluation of a given ABC transporter in each cell line expressed relatively to control adherent cells which were given value 0 (logarithm of 0 equals 1). Bars over the line intersecting value 0 show upregulation of ABC transporters, bars below 0 value show down-regulation of ABC transporters in sphere samples. Densitometry was performed by image J software, each western blot was related to corresponding tubulin protein (representative western blots shown), which was used as a loading control. Experiments were performed in triplicate, standard error is SEM. Statistical significance was calculated using the t-test, where the values obtained from the spheres were compared to the control values; * $p < 0.05$, ** $p < 0.01$, *** $p < 0.001$.

### 5.2.4. CSCs generated from breast cancer cells lines show increased expression of miR-301a-3p

Increasing evidence suggests that invasive properties of breast cancer cells are related to their reprogramming into CSCs (59,261). It has been recently discovered that expression of miR-301a-3p correlates with invasive properties of breast cancer cells and also other tumour types (116,123,262). Moreover, it was also reported that expression of miR-301a-3p supports EMT (263). Therefore, we assessed the expression level of miR-301a-3p in our *in vitro* model of CSCs by using a specific Taqman assay. We generated spheres from several ERα positive breast cancer cell lines (MCF7, T47D, BT474 and ZR-751) and compared the expression level of miR-301a-3p between spheres and control counterparts. MCF10A were included as a control representing normal breast epithelial cells. We detected significantly increased expression level of miR-301a-3p in spheres when compared to control cells in MCF7, T47D and ZR-751 cell lines (Fig. 5.5. A). However, we did not detected any difference in miR-301a-3p expression level between sphere and control cells in the BT474 cell line, which might be explained by already very high miR-301a-3p expression level in BT474 control cells when compared to other tested adherent cells.

Importantly, we analysed the ER signalling in the spheres derived from MCF7 cell line and corresponding control cells as oestrogen signalling has been proposed to play an important role in maintenance and self-renewal capacity of CSCs (3,264). We detected inhibition of ER signalling in spheres as documented by western blot analysis showing a decrease in ERα protein expression followed by decreased protein expression of ERα regulated genes such as growth regulation by oestrogen in breast cancer 1 (GREB1) and PR (Fig. 5.5. B).

Together, our data show increased expression of miR-301a-3p in CSCs which exhibit inhibition of ER signalling.

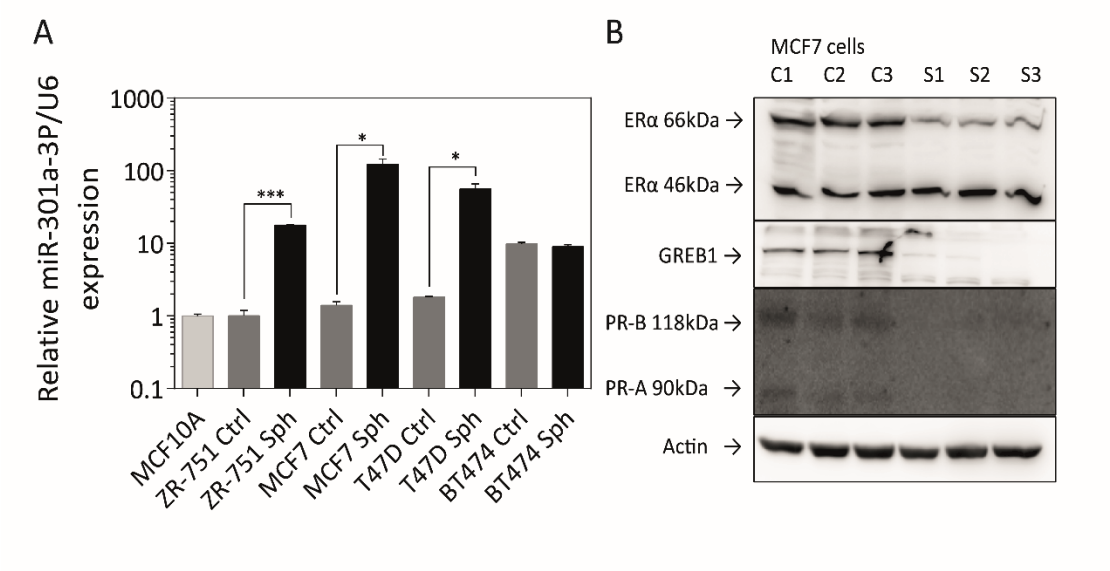


**Fig. 5.5. Mir-301a-3p is highly upregulated in CSCs with downregulated ER signalling.** **A**, RT-qPCR was used to measure expression of miR-301a-3p in different cell lines cultivated as spheres and normal adherent cells. **B**, Western blots showing decreased expression of ERα, GREB1 and PR proteins in MCF7 control and sphere cells. Experiments were performed in triplicate, standard error is SEM. Statistical significance was calculated using the t-test, where the values obtained from the spheres were compared to the control values; * $p < 0.05$, *** $p < 0.001$.

## 5.2.5. *ESR1* mRNA is a direct target of miR-301a-3p

In order to gain further insight into whether miR-301a-3p plays a role in regulation of ER signalling, we searched for miR-301a-3p binding sequences within the *ESR1* mRNA encoding ERα protein. For this purposes, we used three different publicly available miRNA databases (MiRanda, TargetScan, miRBase) where we found that within 3' UTR of *ESR1* mRNA are two miR-301a-3p seed sequences (Fig. 5.6. A).

To validate the prediction that miR-301a-3p negatively regulates expression of *ESR1* mRNA through binding into its 3' UTR, we cloned a 4 kbp long 3' UTR of *ESR1* mRNA (containing two miR-301a-3p binding sites) downstream of the *Cypridina* luciferase gene in a reporter plasmid system. MCF7 cells transfected with miR-301a-3p mimic and miR-301a-3p anti-miR and corresponding controls were then transfected with reporter plasmid. We detected a significant decrease in luciferase activity in cells transfected with miR-301a-3p mimic and conversely significant increase in luciferase activity in cells transfected with miR-301a anti-miR (Fig. 5.6. B). We did not detect any change in luciferase activity, when reporter plasmid

with deleted miR-301a-3p binding sites was used (Fig. 5.6. B). To identify, which miR-301a-3p binding site is more crucial in regulation of *ESR1* mRNA translation, we also constructed the same reporter system with deleted first, second or both miR-301a-3p binding sites and transfected them into MCF7, T47D and BT474 cells. We detected significant increase in luciferase activity in cells transfected with these reporter plasmids, meaning both binding sites are important in regulation of *ESR1* mRNA translation (Fig. 5.6. C). However, removal of the first site resulted in an increase in luciferase activity comparable to luciferase activity of the plasmid carrying both deleted miR-301a-3p binding sites while deletion of the second binding site led to only partial increase (Fig. 5.6. C), meaning that the first site has a prominent role in regulation of *ESR1* mRNA translation by miR-301a-3p.

To confirm the biological relevance of miR-301a-3p in regulation of *ESR1* mRNA translation, we assessed the effect of the ectopic miR-301a-3p expression on the level of *ESR1* mRNA and its protein product ERα. We detected that high level of miR-301a-3p resulted in a significant decrease in *ESR1* mRNA level in MCF7, T47D and BT474 cells (Fig. 5.6. D), as well as in a decrease in ERα protein level in these cells, however protein decrease was significant only in MCF7 and T47D cells (Fig. 5.6. E). Our data also show that downregulation of miR-301a-3p by using miR-301a-3p anti-miR had only marginal effect on *ESR1* mRNA and protein expression which was significant only in BT474 cells (Fig. 5.6. D, E). It is in line with the fact, that BT474 cell line has the highest endogenous miR-301a-3p level and thus, its downregulation was the most effective (Fig. 5.6. D).

Altogether, our results demonstrate that miR-301a-3p recognises and binds to 3' UTR of *ESR1* mRNA to supress its translation, resulting in a decrease in ERα protein level.

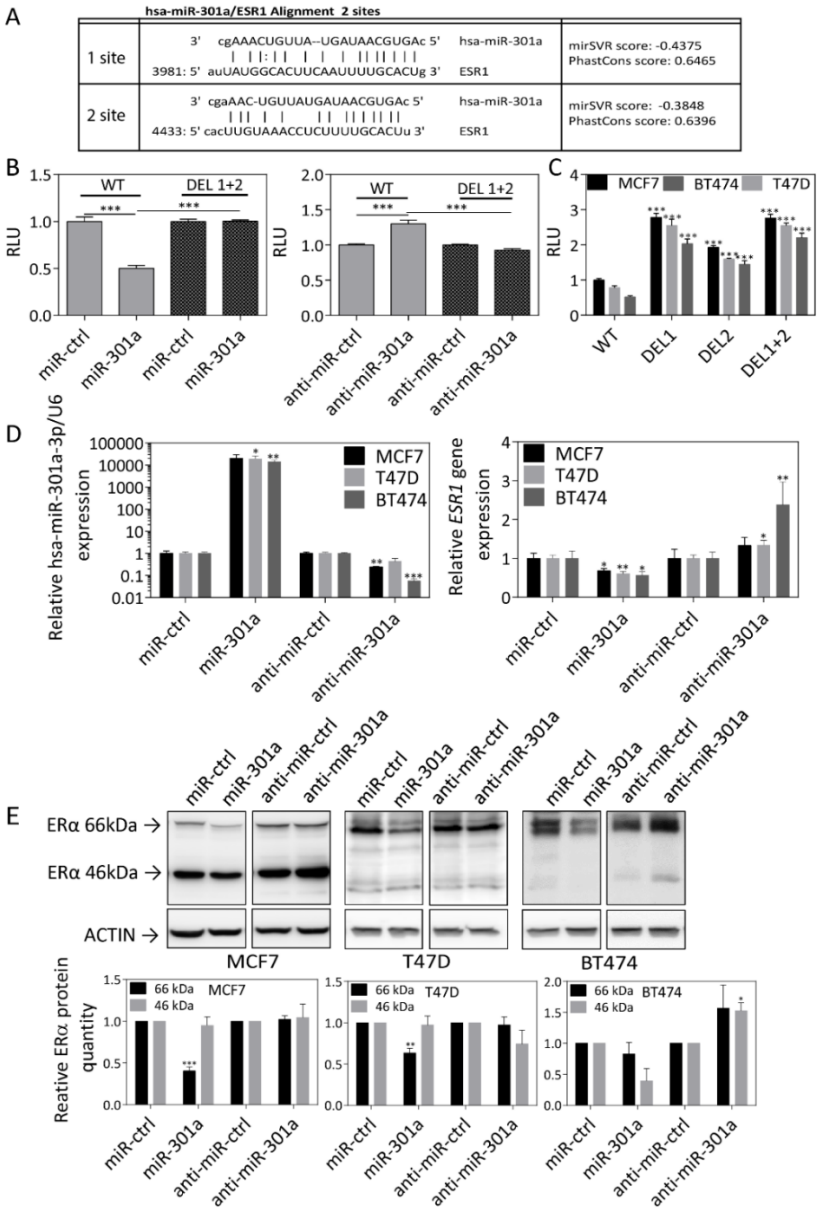


**Fig. 5.6. *ESR1* mRNA is a direct target of miR-301a-3p**. **A**, Schematic diagram of miR-301a-3p binding sites in the *ESR1* 3'UTR mRNA. Cypridina luciferase reporter vectors containing the wild type *ESR1* 3'UTR mRNA (WT) or deleted first, second or both (DEL1, DEL2, DEL1+2) putative miR-301a binding sites were generated. **B**, Relative luciferase activity of WT and DEL1+2 vectors in MCF7 cells transfected with miR-301a-3p and control mimic and miR-301a-3p and control anti-miR. **C**, Relative luciferase activity of WT, DEL1, DEL2 and DEL1+2 vectors in MCF7, BT474 and T47D cell lines. **D**, RT-qPCR showing miR-301a-3p and *ESR1* mRNA expression level in MCF7, BT474 and T47D cell lines after transfection with miR-301a-3p mimic and miR-301a-3p anti-miR. **E**, Representative western blots showing expression of ERα protein in MCF7, BT474 and T47D cell lines after transfection with miR-301a-3p mimic and miR-301a-3p anti-miR and densitometry evaluation by image J software shown at the bottom panel **E**. Experiments were performed in triplicate, standard error is SEM. Statistical significance was calculated using the t-test; * $p < 0.05$, ** $p < 0.01$, *** $p < 0.001$.

### 5.2.6. MiR-301a-3p mimic downregulate canonical oestrogen receptor signalling pathway

ERα is a ligand activated transcription factor that regulates expression of many target genes and is one of the crucial marker for cancer diagnosis and treatment (265). For this reason, we assessed the influence of miR-301a-3p on expression of genes that are positively or negatively regulated by ERα. As an experimental system, we used MCF7, T47D and BT474 cell lines transfected with miR-301a-3p mimic, miR-301a-3p anti-miR and corresponding control RNAs. Increased ectopic expression of miR-301a-3p leads to a significant decrease in mRNA expression of genes that are positively regulated by ERα such as *progesterone receptor α* (*PGRA*), *GREB1*, *CXCL12* or *cathepsin D* (*CSTD*) and to a significant increase in mRNA expression of *bone morphogenetic protein 7* (*BMP7*), a gene which is negatively regulated by ERα (Fig. 5.7.). Changes in the expression of these genes were also replicated on protein level (Fig. 5.8.). The effect of downregulation of miR-301a-3p by miR-301a-3p anti-miR on ERα signalling pathway was significant only in BT474 cell line (Fig. 5.7., 5.8.). In MCF7 and T47D cell lines, the effect of miR-301a-3p anti-miR was only marginal (Fig. 5.7., 5.8.). As mentioned in the previous chapter, BT474 cell line has already high endogenous level of miR-301a-3p, thus the effect of miR-301a-3p anti-miR is the most evident here and resulted in a significant upregulation of *ESR1* mRNA and ERα protein, which was accompanied by statistically significant increase in mRNA level of ERα regulated genes *GREB1*, *PGRA* and *CXCL12* (Fig. 5.7.).

In conclusion, our findings demonstrate that miR-301a-3p negatively regulates the activity of the ER signalling pathway.

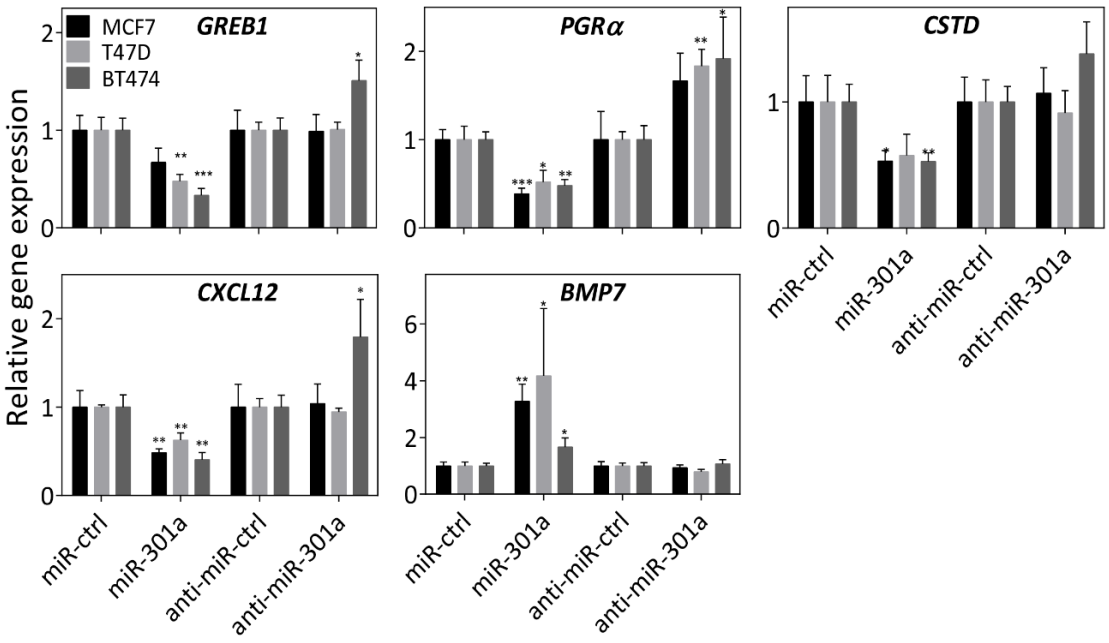


**Fig. 5.7. Mir-301a-3p affects expression of genes regulated by ERα positively (*GREB1*, *PGRA*, *CSTD*, *CXCL12*) and negatively (*BMP7*) in MCF7, T47D and BT474 cells.** RT-qPCR showing mRNA expression of *GREB1*, *PGRA*, *CSTD*, *CXCL12* and *BMP7* genes in MCF7, BT474 and T47D cells transfected with miR-301a-3p mimic and miR-301a-3p anti-miR. Experiments were performed in triplicate, standard error is SEM. Statistical significance was calculated using the t-test; * $p < 0.05$, **$p < 0.01$, *** $p < 0.001$.

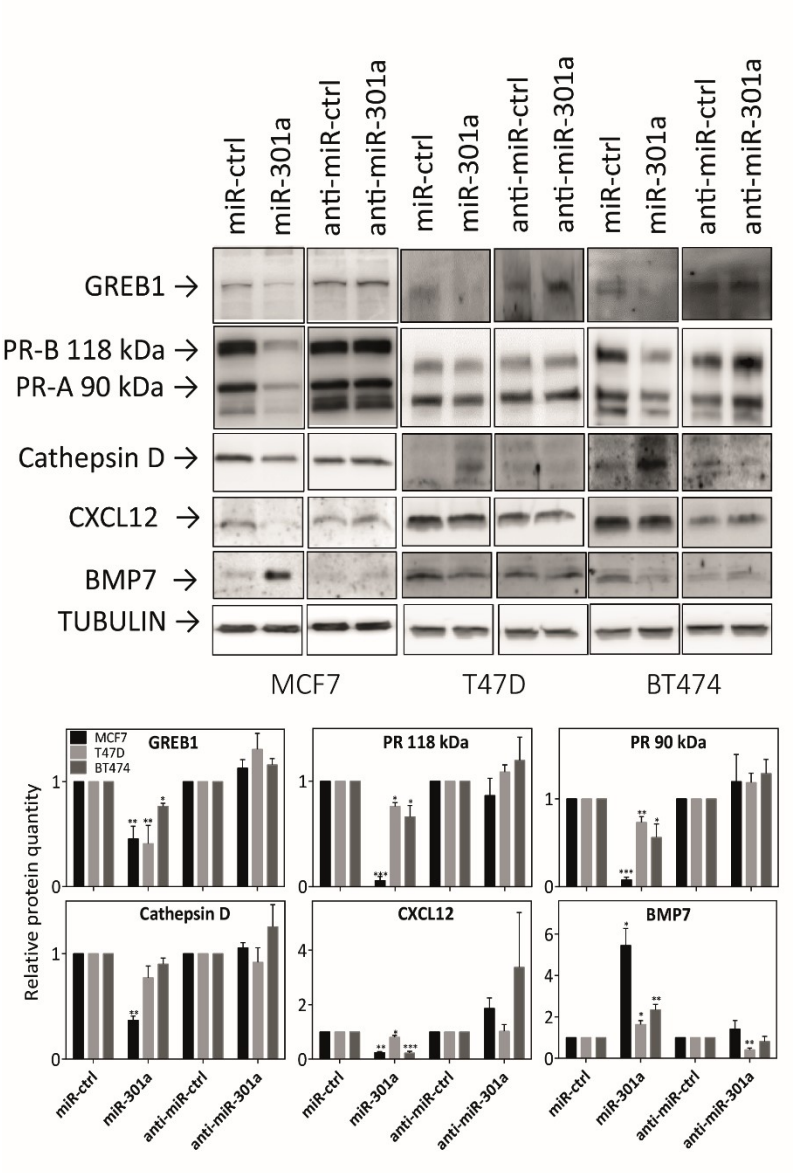


**Fig. 5.8. MiR-301a-3p affects expression of proteins regulated by the ERα signalling in MCF7, T47D and BT474 cells**. Active ERα signalling induces certain proteins (GREB1, PR, CSTD, CXCL12) while others are downregulated (BMP7). Representative western blots showing expression of GREB1, PR, Cathepsin D, CXCL12 and BMP7 proteins in MCF7, T47D and BT474 cells transfected with miR-301a-3p mimic and miR-301a-3p anti-miR and densitometry evaluation by image J software (bottom panel). Experiments were performed in triplicate, standard error is SEM. Statistical significance was calculated using the t-test; * $p < 0.05$, ** $p < 0.01$, *** $p < 0.001$.

### 5.2.7. Upregulation of miR-301a-3p level in MCF7 cell line leads to blunted response to 17-β oestradiol

Because ERα is an $E_2$-activated transcription factor which stimulates proliferation of ERα positive breast cancer cells, we assessed the effect of miR-301a-3p overexpression on the response of MCF7 cell line to 17-β $E_2$. MCF7 cells transfected with miR-301a-3p mimic and anti-miR and corresponding controls were seeded in a 96-well plate and cell number in oestrogen-free medium as well as in the presence of increasing concentrations of 17-β E2 was measured by crystal violet assay (266). We detected significantly less cells in cells transfected with miR-301a-3p mimic in response to 17-β $E_2$ in comparison with cells transfected with control mimic (Fig. 5.9. A). We did not see any statistically significant difference in response to 17-β $E_2$ in cells transfected with miR-301a-3p anti-miR and control anti-miR (Fig. 5.9. B), probably due to already low basal level of miR-301a-3p in these cells.

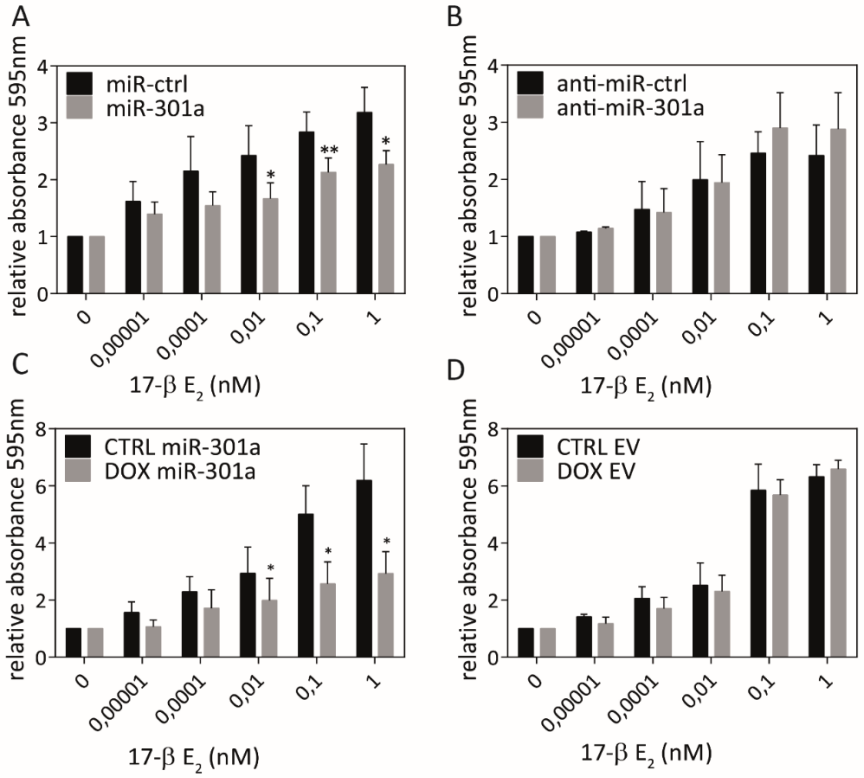


**Fig. 5.9. MiR-301a-3p modulates growth of MCF7 cells in response to 17-β oestradiol (17-β $E_2$)**. **A**, **B**, **C**, **D** Absorbance at 595 nm obtained by the crystal violet staining, demonstrating the effect of 17-β $E_2$ on growth of MCF7 cells transfected with miR-301a-3p mimic and miR-301a-3p anti-miR and MCF7 cell line inducibly expressing miR-301a or EV after induction by doxycycline. Experiments were performed in triplicate, standard error is SEM. Statistical significance was calculated using the t-test; * $p < 0.05$, **$p < 0.01$.

The effect of miR-301a-3p upregulation was also replicated in MCF7 cell line with doxycycline inducible expression of miR-301a (Fig. 5.9. C). Increased level of miR-301a by doxycycline resulted in decreased number of cells in response to 17-β $E_2$. No such effect was seen when using MCF7 cell line stably transfected with EV (Fig. 5.9. D).

In summary, the decrease of ERα expression by miR-301a-3p leads to decreased response of MCF7 cells to 17-β $E_2$.

### 5.2.8. Overexpression of miR-301a leads to decreased growth of MCF7 cell line *in vivo*, inhibition of oestrogen receptor signalling and enrichment of CSCs

In order to determine the role of miR-301a in tumour growth, Balb/c nude athymic mice were implanted with a slow-release $E_2$ pellet and injected subcutaneously with MCF7 cell line expressing either miR-301a or EV after induction by doxycycline. Both MCF7 cell lines with inducible expression of miR-301a or EV (Fig. 5.10. A) exhibited similar growth *in vitro* as shown *via* confluency measurement by JuLI™ FL cell analyser (Fig. 5.10. B), and the changes in proliferation rates are thus not due to inherent properties of selected clones of MCF7 cells. The mice were given a doxycycline diet (200 mg/kg) and the tumour growth was monitored twice a week with ultrasound imaging (Vevo770). We detected profound inhibition of tumour growth in group of mice injected with miR-301a overexpressing cells in comparison with group of mice injected with cells carrying EV (Fig. 5.11. A). Tumour volume and tumour mass were significantly reduced in group overexpressing miR-301a versus control group (Fig. 5.11. A, B, C).

Furthermore, the miR-301a overexpression led to a decrease in expression of ERα and PR proteins in tumours as shown by western blot analysis (Fig. 5.11. D), and also to inhibition of the ER signalling, measured by RT-qPCR (Fig. 5.11. E). These *in vivo* data are in line with previously measured *in vitro* results and confirm the fact that MCF7 cells are dependent on oestrogen for their growth and once the ER signalization is restricted, they stop proliferation. Moreover, we have detected significantly increased expression of genes such

as *CD44*, *ALDH1*, *ABCG2*, *Vimentin* (*VIM*), *ZEB1*, *ZEB2*, *HER2* and *VEGFA* related to CSC, EMT and metastasis phenotype (Fig. 5.11. F)

In conclusion, miR-301a overexpression inhibits ERα expression and thus ER signalling, which results in inhibition of tumour growth of the oestrogen-dependent MCF7 cell line *in vivo*, but also to enrichment of CSCs population within the tumour.

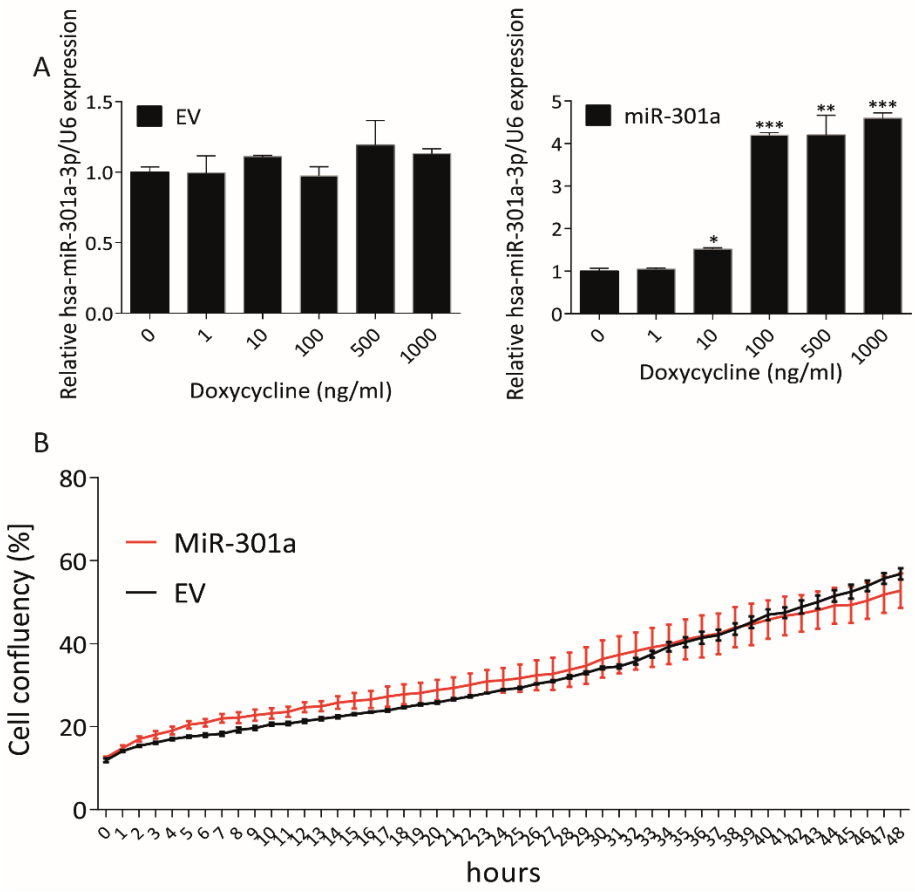


**Fig. 5.10. Characteristics of the miR-301a or EV doxycycline inducible MCF7 cell lines.** **A**, RT-qPCR showing expression of miR-301a-3p after doxycycline addition in miR-301a doxycycline-inducible MCF7 cell line and in MCF7 cell line carrying EV. **B**, Graph showing confluency curve of MCF7 cell lines carrying doxycycline inducible miR-301a or EV measured without addition of doxycycline by JuLI™ cell analyzer. Experiments were performed in triplicate, standard error is SEM. Statistical significance was calculated using the t-test; * $p < 0.05$, **$p < 0.01$, *** $p < 0.001$.

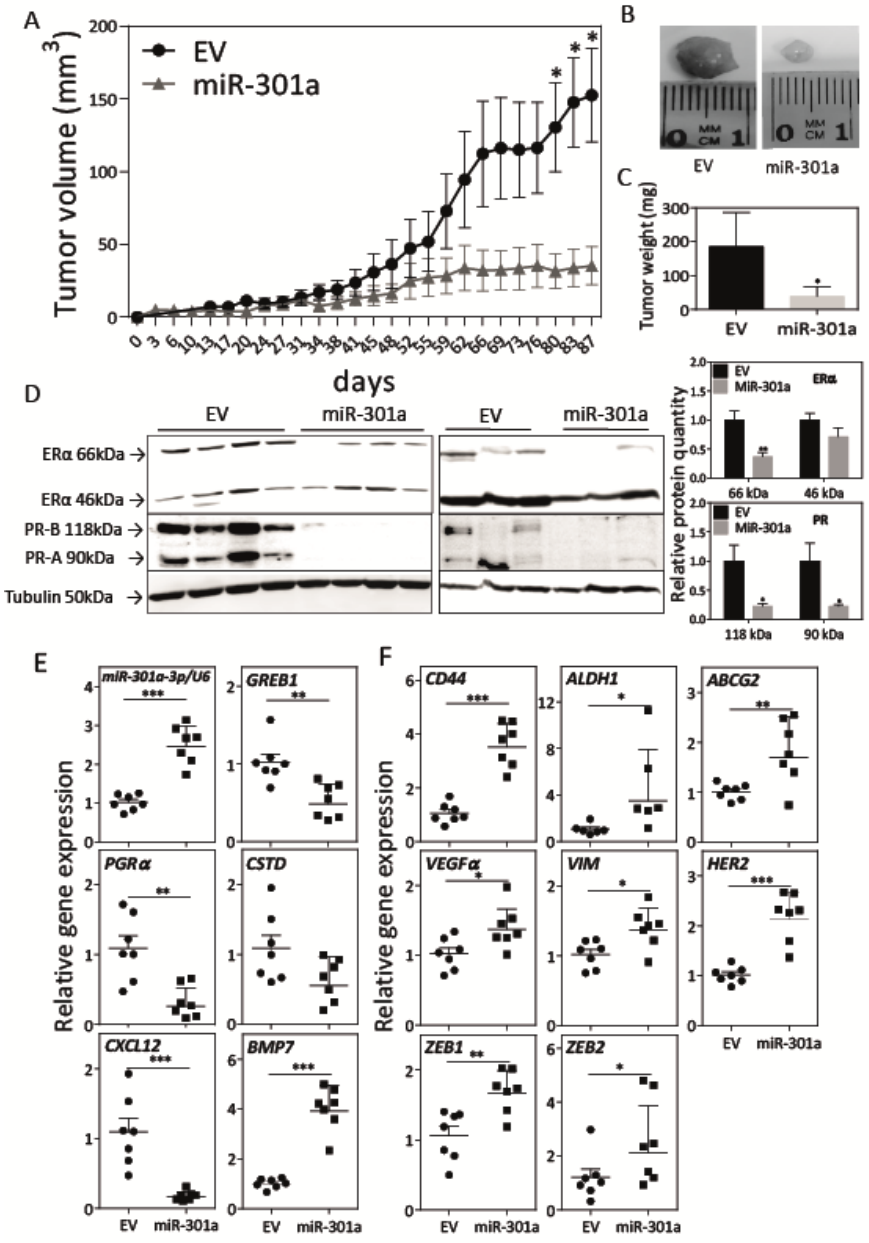


**Fig. 5.11. Mir-301a-3p reduce tumour growth and inhibit ER signalling *in vivo*. A**, Growth of MCF7 cell line inducibly expressing miR-301a or EV after doxycycline addition in Balb/c nude mice (injected $2x10^6$ cells per animal), which were implanted with slow-release oestradiol pellet and given a doxycycline diet. Tumour volume was monitored twice a week and evaluated by ultrasound imaging instrument Vevo 770. **B**, Photographs showing representative tumours formed. **C**, Weight of the tumours at the end of the experiment. **D**, Western blots showing expression of ERα and PR proteins in tumour samples in control or miR-301a overexpressing tumours and corresponding densitometry evaluation by image J **E**, **F**, RT-qPCR showing mRNA expression of miR-301a-3p and *GREB1*, *PGRA*, *CSTD*, *CXCL12*, *BMP7*, *CD44*, *ALDH1*, *ABCG2*, *VEGFA*, *VIM, ZEB1, ZEB2* and *HER2* genes in control and miR-301a overexpressing tumours. Animal experiment was performed twice, 4 animals in each group, standard error is SEM (n=7). Statistical significance was calculated using the t-test; * $p < 0.05$, ** $p < 0.01$, *** $p < 0.001$.

### 5.2.9. Expression of miR-301a-3p negatively correlates with *ESR1* level in breast cancer patient samples

To determine the role of miR-301a-3p in breast cancer, we assessed its expression level in 111 tumour tissue samples obtained from patients with primary breast carcinoma, divided into four groups according to ER, PR and HER2 expression status. ER status was further confirmed by TaqMan RT-qPCR (Fig. 5.12. A). We detected that expression of miR-301a-3p is gradually increased in groups in following order $ER^+/PR^+/HER2^- < ER^+/PR^+/HER2^+ < ER^-/PR^-/HER2^+ < ER^-/PR^-/HER2^-$ (Fig. 5.12. B), and it is significantly increased in groups with $ER^-/PR^-$ phenotype when compared to groups with $ER^+/PR^+$ phenotype. Moreover, there is a statistically significant negative correlation between *ESR1* mRNA and miR-301a-3p levels in the primary tumour samples (Fig. 5.12. C). Unlike ER and PR, the expression of *HER2* had no significant correlation with miR-301a-3p expression in studied samples (Fig. 5.12. B).

In summary, these data show that expression of miR-301a-3p negatively correlates with ER/PR status, suggesting that higher level of miR-301a-3p is connected with lower *ESR1* expression.

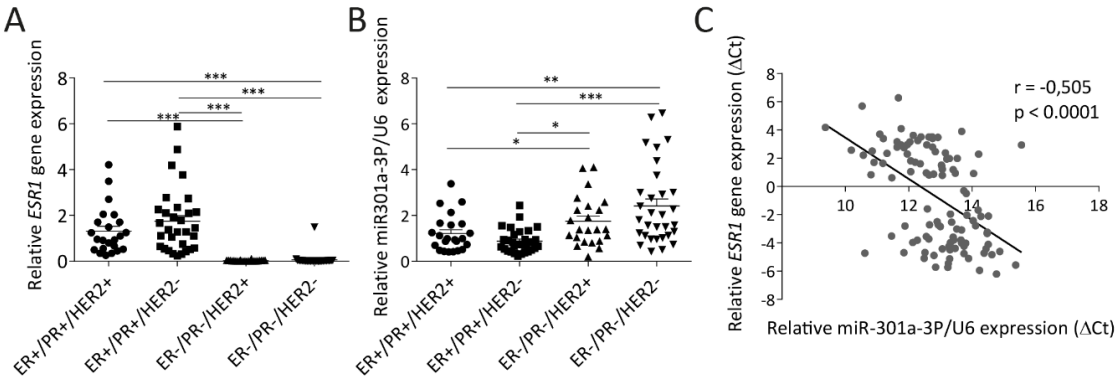


**Fig. 5.12. MiR-301a-3p and *ESR1* levels inversely correlate in human breast cancer. A**, RT-qPCR using Taqman probe showing level of *ESR1* mRNA in breast cancer tissues divided according to their ER, PR and HER2 status into 4 groups. **B**, RT-qPCR using Taqman probe showing level of miR-301a-3p in breast cancer tissues divided according to their ER, PR and HER2 status into 4 groups. **C**, Pearson's correlation scatter plot of the correlation between *ESR1* gene and miR-301a-3p in breast cancer tissues. Results are represented as mean values ± S.E.M. Statistical significance was calculated using the t-test; * $p < 0.05$, ** $p < 0.01$, *** $p < 0.001$.

## 5.3. Iron metabolism in CSCs

### 5.3.1. MCF7 spheres show higher intracellular iron pool, iron uptake and sensitivity to iron withdrawal

Iron as well as CSCs has been shown to play an important role in cancer progression but the role of iron and iron metabolism in CSC maintenance has not been studied so far. To identify the significance of iron for the biology of CSCs, we have tested the level of LIP, iron uptake, intracellular iron localization and sensitivity to iron chelators in MCF7 spheres as model of CSCs. Using the calcein fluorescence-based method, we have found significantly higher LIP in MCF7 spheres than in normal adherent cells (Fig. 5.13. A). Furthermore, we have noticed significantly higher uptake of $^{55}Fe$ in these cells (Fig. 5.13. B), and intracellular distribution showed significantly higher $^{55}Fe$ level in mitochondria (Fig. 5.13. C). To test the importance of iron for CSCs viability, we used cell permeable iron chelator SIH. Application of SIH led to a reduction in viability of MCF7 spheres compared to adherent counterparts as measured by Cell Titer-Glow (Fig. 5.13. D) and Cell Titer-Fluor (Fig. 5.13. E) viability assays. Together, these data describe an important role of iron for survival of MCF7 spheres, connected with higher LIP, iron uptake and accumulation of iron inside mitochondria.

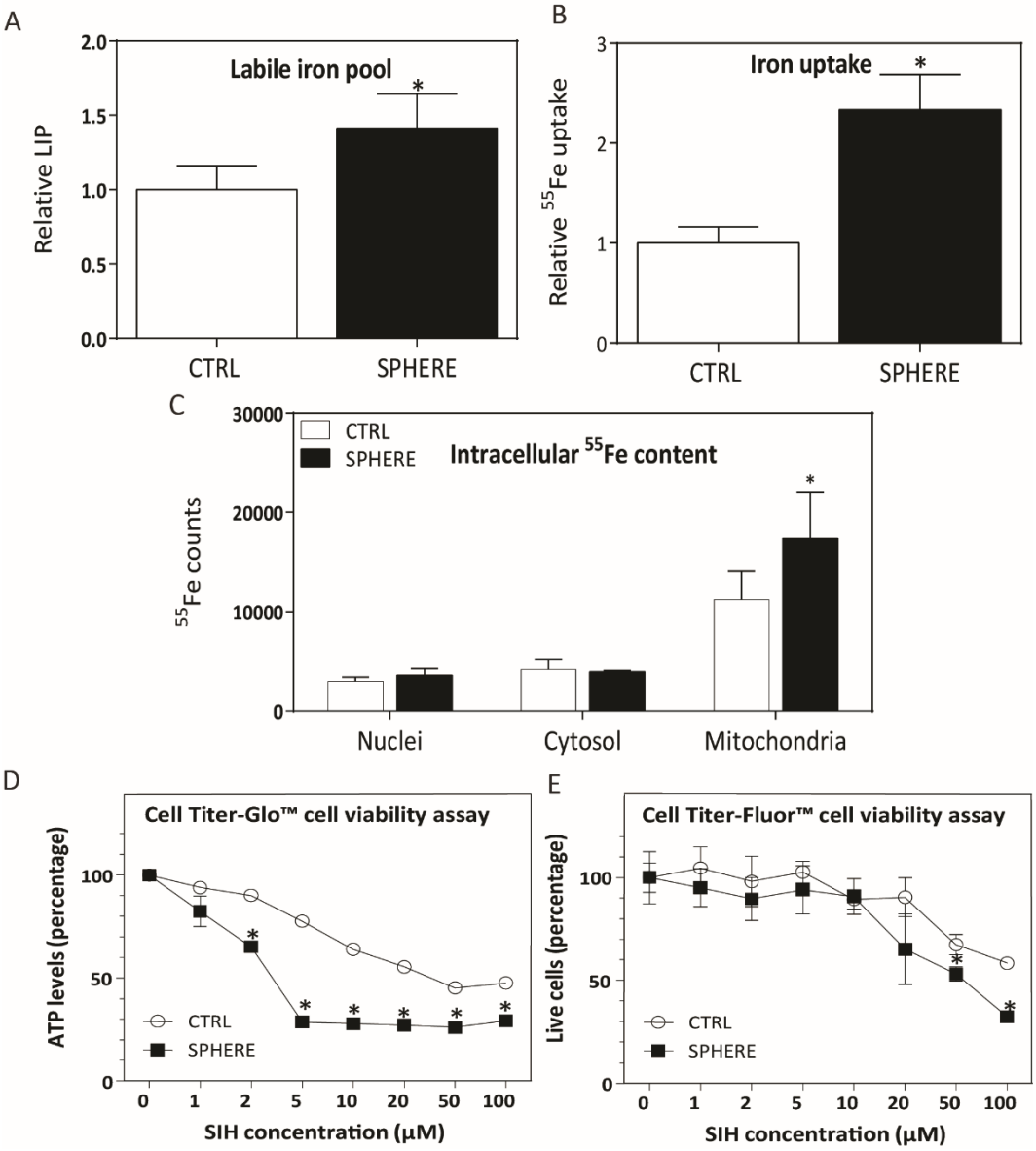


**Fig. 5.13. MCF7 spheres show higher intracellular iron pool, iron uptake and sensitivity to iron withdrawal.** Measurement of **A**, labile iron pool (LIP) detected by the calcein fluorescence method and **B**, $^{55}$Fe uptake in control and sphere MCF7 cells. **C**, Intracellular distribution of $^{55}$Fe in spheres and adherent MCF7 cells. Sphere and adherent MCF7 cells were exposed to increasing concentration of iron chelating agent salicyl isonicotinoyl hydrazone (SIH) and cell viability was measured by **D**, Cell Titer-Glow and **E**, Cell Titer-Fluor assays. Experiments were performed at least in triplicate, standard error is SEM. Statistical significance was calculated using the unpaired t-test, where the values obtained from spheres were compared to the control values; * $p < 0.05$. Panels **A**, **B**, **D** and **E** are not my own results and are adapted from (247).

### 5.3.2. CSCs derived from several cancer cell lines show alterations in expression of genes related to iron metabolism

To further explore the molecular mechanisms underlying our results, we performed expression profiling of genes that are related to metabolism of iron. We selected 39 genes coding for proteins involved in iron uptake, export, transport and storage of iron, ISC and haem biogenesis, and regulation of iron metabolism. Using fluidigm RT-qPCR from Biomark, we performed expression profiling of these genes in control adherent and sphere cells derived from various breast (MCF7, T47D, BT474, ZR-75-30) and prostate (DU-145, LNCaP) cancer cell lines and non-malignant (MCF10A) cell line of breast origin. We obtained expression profile of 34 genes that were detectable in our cell lines and showed appropriate qPCR standard curves (Table 5.2.). Next, we compared the mRNA expression profile between control and sphere cells and selected genes that showed altered expression (> 1,5 fold change) reproducibly at least in 60 % of tested cell lines. The result of this selection was a selection of 10 genes (*CYBRD1*, *TFRC*, *ACO1*, *IREB2*, *ABCB10*, *GLRX5, EPAS1*, *QSOX1*, *HEPH*, *HFE*) which we called as CSC iron metabolism-related gene signature.

In order to define, whether the expression of 10 selected genes related to iron metabolism is able to distinguish CSCs from non-CSCs, we performed principal component analysis (PCA) based on expression of the selected genes. Importantly, the PCA clusters control adherent cell samples separately from sphere cell samples in all tested cell lines (Fig. 5.14.). Thus, we identified iron metabolism-related gene expression profile, which is specific for our *in vitro* model of CSCs.

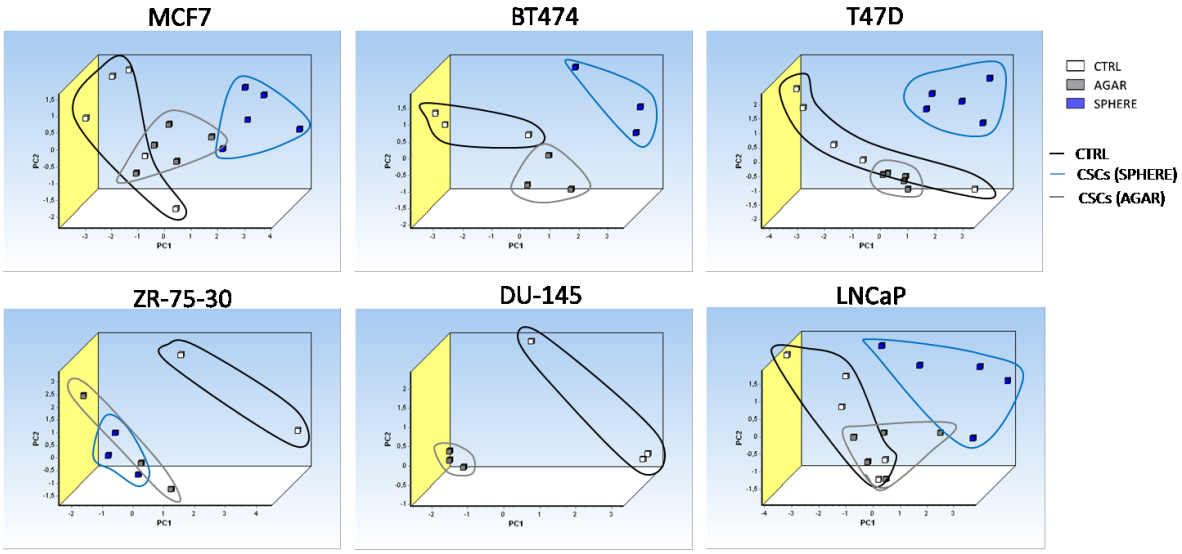


**Fig. 5.14. Principal component analysis (PCA) based on the expression of selected iron metabolism-related genes (*CYBRD1*, *TFRC*, *ACO1*, *IREB2*, *ABCB10*, *GLRX5*, *EPAS1*, *QSOX1*, *HEPH*, *HFE*) discriminates CSCs from control cancer cells.** PCA was run on malignant breast (MCF7, T47D, BT474, ZR-75-30) and prostate (DU-145, LNCaP) cell lines based on expression of selected genes in control and sphere cells by GenEx software.

**Table. 5.2. Expresion profile of iron metabolism-related genes in CSCs derived from breast and prostate cancer cell lines.**

| | | (MCF7 SPH) vs (MCF7 CTRL) | | (T47D SPH) vs (T47D CTRL) | | (BT474 SPH) vs (BT474 CTRL) | | (ZR-75-30 SPH) vs (ZR-75-30 | | (DU-145 AGAR) vs (DU-145 CTRL) | | (LNCaP SPH) vs (LNCaP CTRL) | |
|---|---|---|---|---|---|---|---|---|---|---|---|---|---|
| | **Iron related genes** | Fold change | *P-Value* | Fold change | *P-Value* | Fold change | *P-Value* | Fold change | *P-Value* | Fold change | *P-Value* | Fold change | *P-Value* |
| 1 | *ABCB10* | 1.93 | *0.0167* | 1.72 | *0.1498* | 1.71 | *0.1549* | 1.86 | *0.0290* | 2.40 | *0.0454* | 1.34 | *0.0851* |
| 2 | *ABCB6* | 1.86 | *0.0437* | 1.34 | ***0.0001*** | 1.45 | *0.0545* | 1.08 | *0.8031* | 1.82 | *0.0091* | 1.19 | *0.1194* |
| 3 | *ABCB7* | 1.36 | *0.0166* | 1.85 | *0.0255* | 1.52 | *0.0131* | 1.39 | *0.1430* | 2.05 | *0.0782* | 1.16 | *0.3627* |
| 4 | *ABCB8* | 1.39 | *0.1300* | 1.46 | *0.0760* | 1.31 | *0.0261* | 1.04 | *0.8613* | 1.94 | *0.0214* | 1.04 | *0.7424* |
| 5 | *ACO1* | **1.91** | ***0.0010*** | 1.59 | *0.1147* | 2.60 | *0.0424* | 2.19 | *0.0189* | 2.01 | *0.0335* | 1.44 | *0.0472* |
| 6 | *BMP6* | -1.11 | *0.7923* | | | -1.51 | *0.4697* | | | 4.10 | *0.0449* | 1.52 | *0.1418* |
| 7 | *CYBRD1* | 1.85 | *0.0940* | 1.43 | *0.0059* | 7.85 | *0.0014* | 1.60 | *0.6814* | 3.52 | *0.0035* | 3.12 | *0.1309* |
| 8 | *EPAS1 (HIF2a)* | 1.78 | *0.0836* | 1.39 | *0.2402* | 3.26 | *0.0867* | 1.51 | *0.4439* | 5.53 | *0.0178* | 1.78 | *0.3774* |
| 9 | *FTH1* | 1.31 | *0.3190* | 1.17 | *0.3845* | -1.03 | *0.9079* | -1.19 | *0.0306* | 1.20 | *0.3677* | 1.02 | *0.8960* |
| 10 | *FTL1* | 1.78 | *0.0242* | -1.22 | *0.2448* | 1.51 | *0.1079* | 1.11 | *0.3238* | 1.10 | *0.7044* | -1.10 | *0.4926* |
| 11 | *FXN* | -1.43 | *0.0388* | -2.53 | *0.0042* | -1.34 | *0.0390* | 1.02 | *0.9228* | -2.85 | *0.0495* | -1.13 | *0.4466* |
| 12 | *GLRX2* | -1.41 | *0.4361* | 1.69 | *0.3087* | | | | | | | -1.03 | *0.9492* |
| 13 | *GLRX5* | **-1.84** | ***0.0007*** | -3.67 | *0.0231* | -2.52 | *0.0834* | -1.24 | *0.5379* | -1.14 | *0.6391* | -1.49 | *0.2423* |
| 14 | *HAMP* | 1.37 | *0.4913* | | | 3.42 | *0.1412* | 1.93 | *0.7012* | -1.42 | *0.5643* | | |
| 15 | *HEPH* | 3.65 | *0.1227* | 3.66 | *0.0026* | **6.84** | ***0.0008*** | 1.12 | *0.9126* | | | 1.94 | *0.0610* |
| 16 | *HFE* | 1.65 | *0.0583* | 1.59 | *0.0167* | | | 1.01 | *0.9604* | 2.12 | *0.0204* | | |
| 17 | *HIF1* | -1.28 | *0.1434* | 1.21 | *0.4935* | -1.12 | *0.6406* | 1.82 | *0.0073* | 2.22 | *0.0696* | 1.68 | *0.1311* |
| 18 | *HMOX1* | 1.61 | *0.0436* | 1.82 | *0.0850* | 1.67 | *0.0198* | 1.08 | *0.5925* | 1.53 | *0.2438* | 1.29 | *0.1401* |
| 19 | *HMOX2* | 1.23 | *0.0807* | -1.13 | *0.4845* | 1.73 | *0.0041* | 1.13 | *0.5075* | -2.47 | *0.0226* | 1.33 | *0.0094* |
| 20 | *IREB2* | 1.63 | *0.0208* | 2.79 | *0.0136* | 1.96 | *0.0443* | 2.06 | *0.0014* | 4.20 | *0.0262* | 1.65 | *0.0458* |
| 21 | *ISCA1* | -1.05 | *0.7360* | 1.22 | *0.0810* | -1.04 | *0.8895* | -2.04 | *0.1140* | -1.01 | *0.9017* | -1.48 | *0.2392* |
| 22 | *ISCA2* | -1.17 | *0.3320* | -1.62 | *0.1246* | -1.06 | *0.7136* | -1.46 | *0.2241* | -1.78 | *0.1333* | -1.08 | *0.2160* |
| 23 | *ISCU* | 1.16 | *0.3817* | 1.18 | *0.0268* | 1.28 | *0.0820* | 1.09 | *0.4547* | 1.17 | *0.3265* | 1.18 | *0.1909* |
| 24 | *LYRM4 (ISD11)* | -1.10 | *0.1764* | -1.07 | *0.5439* | 1.01 | *0.9250* | -1.10 | *0.1621* | -1.38 | *0.2701* | 1.05 | *0.4894* |
| 25 | *QSOX1* | **2.84** | ***0.0009*** | **4.77** | ***0.0003*** | **2.85** | ***0.0001*** | 1.03 | *0.9050* | 1.30 | *0.4621* | 1.87 | *0.0021* |
| 26 | *SLC11A2v2 (NRAMP2, IRE)* | 1.31 | *0.4048* | 1.99 | *0.0451* | 1.32 | *0.2426* | 2.08 | *0.0649* | 39.37 | *0.0123* | -1.06 | *0.8948* |
| 27 | *SLC25A28 (MFRN2)* | -1.02 | *0.9334* | -1.03 | *0.8638* | -1.10 | *0.6242* | 1.12 | *0.0613* | 1.32 | *0.4156* | 1.10 | *0.6073* |
| 28 | *SLC25A37 (MFRN1)* | -1.29 | *0.1087* | -1.49 | *0.1463* | -1.38 | *0.2714* | -1.26 | *0.2743* | -2.42 | *0.1699* | -1.04 | *0.8360* |
| 29 | *SLC48A1 (HRG-1)* | 1.33 | *0.2906* | -1.22 | *0.5409* | 1.55 | *0.1263* | -1.87 | *0.5940* | 2.00 | *0.1705* | 2.35 | *0.1635* |
| 30 | *STEAP3* | 1.26 | *0.4476* | 1.21 | *0.6134* | -2.51 | *0.0448* | -1.19 | *0.7325* | 1.61 | *0.2908* | -1.53 | *0.4283* |
| 31 | *TFR2* | 2.55 | *0.0088* | 2.54 | *0.4361* | -2.42 | *0.4624* | -1.39 | *0.4275* | 1.37 | *0.5287* | -1.56 | *0.3756* |
| 32 | *TFRC* | 2.11 | *0.0041* | -1.08 | *0.8108* | 1.95 | *0.0865* | 2.46 | *0.0364* | 4.04 | *0.0553* | 3.07 | *0.0056* |
| 33 | *TMPRSS6* | 1.70 | *0.2885* | | | -1.85 | *0.3358* | | | | | **31.66** | ***0.0004*** |
| 34 | *VEGFA* | 1.43 | *0.4778* | 3.28 | *0.0035* | 1.28 | *0.3248* | -1.36 | *0.4863* | 1.99 | *0.0035* | -1.07 | *0.8677* |
| 35 | *SLC40A1* | 2.84 | *0.0090* | 5.50 | *0.0060* | 2.61 | *0.0067* | 2.19 | *0.0046* | 8.02 | *0.0007* | -7.07 | *0.2052* |
| 36 | *SLC39A14* | 1.84 | *0.0282* | 3.58 | *0.0075* | 2.74 | *0.0207* | 2.03 | *0.2367* | 4.25 | *0.0182* | -2.03 | *0.2767* |

Table shows fold changes in expression of given genes (downregulation is expressed as negative fold change, red field show fold change > 1.5, yellow field show fold change < -1.5), statistical significance was calculated by t-test, green field show $p < 0.05$. The analysis was performed by GenEx software. Genes *FTMT*, *HFE2*, *HIF3* were excluded from the analysis due to assay inefficiency or their low detection.

### 5.3.3. CSCs show increased expression of components involved in iron uptake machinery

Product of *CYBRD1* gene is a ferric reductase that is highly expressed on duodenal brush border, where it plays an important role in absorption of intestinal iron (170). We detected upregulation of *CYBRD1* mRNA in spheres derived from most cell lines tested (MCF7, LNCaP; significantly in BT474, T47D, DU-145,) with approximate 2-7 fold induction (Fig. 5.15. A, Table 5.2.). This has been replicated also on protein level in MCF7 sphere model where both detected isoforms of CYBRD1 protein were significantly upregulated (Fig. 5.15. B). *TFRC* gene codes for TfR1 and plays a crucial role in uptake of Tf bound iron (176). Expression of *TFRC* mRNA was also upregulated in spheres (DU-145, significantly in MCF7, BT474, ZR-75-30, LNCaP) (Fig. 5.15. C, Table 5.2.). On protein level, we detected increased level of TfR1 in MCF7 sphere cells which did not reach statistical significance (Fig. 5.15. D).

To further assess alternative mechanisms of the iron uptake, especially of the NTBI uptake, we also assessed the expression of the ZIP14 protein (coded by *SLC39A14* gene). Although we detected upregulation of *SLC39A14* mRNA in spheres derived from most cell lines tested (statistically significant in MCF7, BT474, T47D and DU-145), we did not detect any significant change on the protein level in MCF7 spheres (Fig. 5.15. E, F, Table 5.2.).

Together, our results suggest that ZIP14 is not involved in higher iron uptake in our model of CSCs, pointing to TfR1 and possibly CYBRD1 as the main mediators of higher iron import in these cells. Expression of *TFRC* mRNA is subjected to regulation by IRP/IRE system which is discussed in the next chapter.

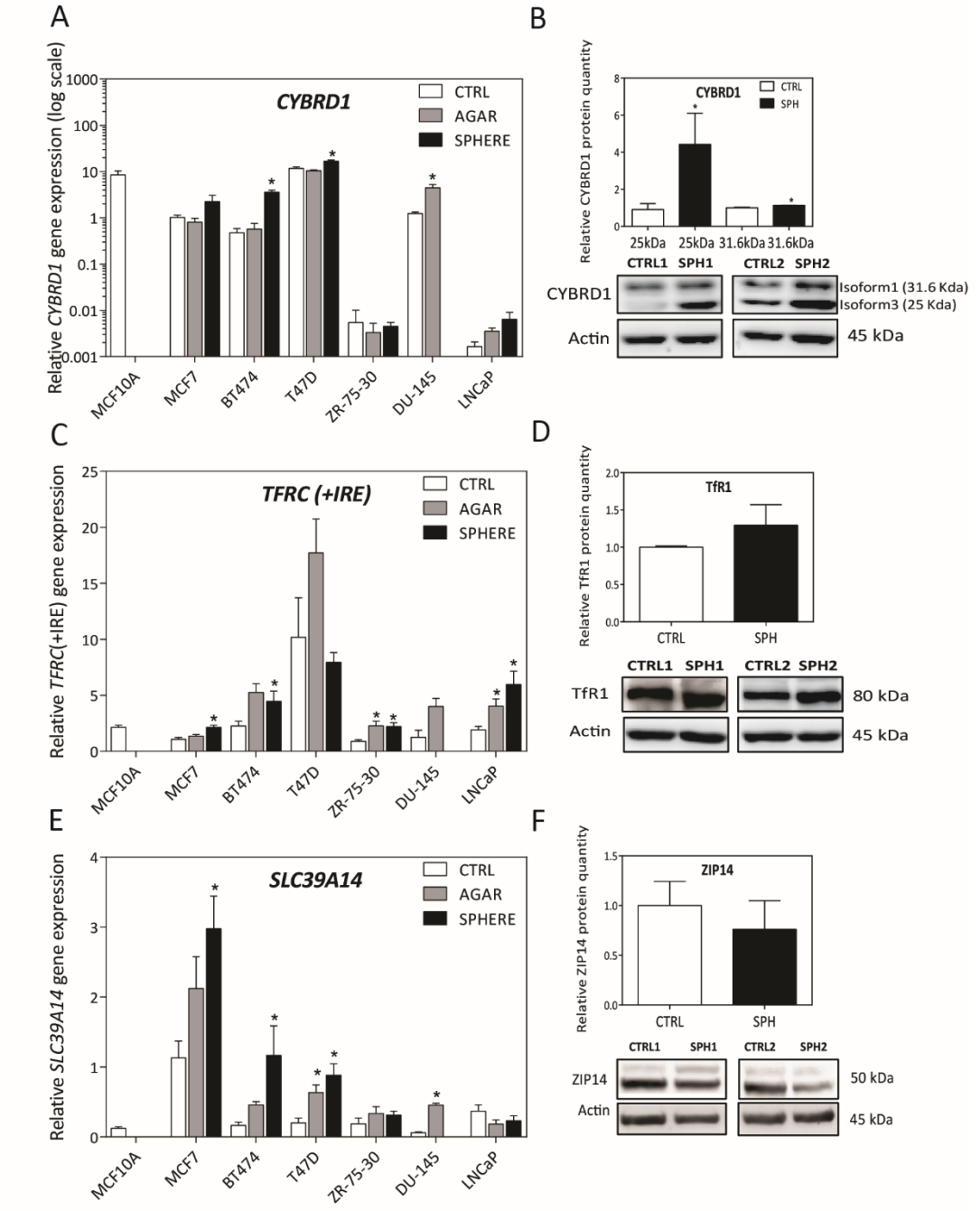


**Fig. 5.15. CSCs exhibit increased expression of components involved in iron uptake machinery. A**, **C**, **E**, RT-qPCR showing expression of *CYBRD1*, *TFRC* and *SLC39A14* mRNAs in control and sphere cells derived from breast (MCF7, T47D, BT474, ZR-75-30) and prostate (DU-145, LNCaP) cancer cell lines. **B**, **D**, **F**, Western blots showing expression of CYBRD1, TfR1 and ZIP14 proteins in control and sphere cells derived from MCF7 cell lines with densitometry evaluation performed by image J software in upper panels. Experiments were performed at least in triplicate, standard error is SEM. Statistical significance was calculated by GenEx software using the unpaired t-test; * $p < 0.05$. Panels **B**, **D** and **F** are not my own results and are adapted from (247).

### 5.3.4. CSCs exert activation of components of the IRP/IRE system

The main components of the IRP/IRE system are IRP1 (coded by *ACO1* gene) and IRP2 (coded by *IREB2* gene). In our experimental model, we saw significant upregulation of *ACO1* mRNA level in all tested cell lines except T47D cells, where the increase was not significant (Fig. 5.16. A, Table 5.2.). The significantly higher level of ACO1 protein level was also detected in MCF7 sphere model (Fig. 5.16. B). The *IREB2* mRNA expression was significantly elevated in all tested cell lines (Fig. 5.16. C, Table 5.2.), whereas on the protein level, we detected significant decrease in IREB2 expression in MCF7 sphere model (Fig. 5.16. D). This discrepancy between mRNA and protein level could be plausibly explained, taking into account our other results. Since IREB2 is targeted for proteasomal degradation upon high iron levels (267) and we detected higher LIP in MCF7 spheres, the lower level of IREB2 protein is the expected outcome.

ACO1 is an ISC containing enzyme, upon iron deprivation ISC is removed as a consequence of conformational change revealing IRP1 properties of ACO1, which binds to IRE in UTRs to enhance *TFRC* and *DMT1* genes mRNA expression and decrease *FTH*, *FTL* and *FPN* genes mRNA expression. Similar IRE-binding properties has IREB2 (202–206). For this reason we analysed the binding ability of IRP1 and IRP2 to IREs by a modified electrophoretic mobility shift assay (EMSA). We detected significantly higher binding activity of IRP1 to IRE sequence of human ferritin in MCF7 sphere model (Fig. 5.16. E). The activity of IRP2 was also higher in MCF7 spheres but not significantly (Fig. 5.16. E).

The conformational change in ACO1 enzyme leading to ISC removal is stimulated by insufficient/dysfunctional ISC biogenesis (218) or generation of ROS (219) as discussed further. Together, these results confirm activation of the IRP/IRE system in our CSC model *in vitro* and are in line with higher iron uptake by TfR1 whose mRNA is stabilised by an active IRE/IRP system.

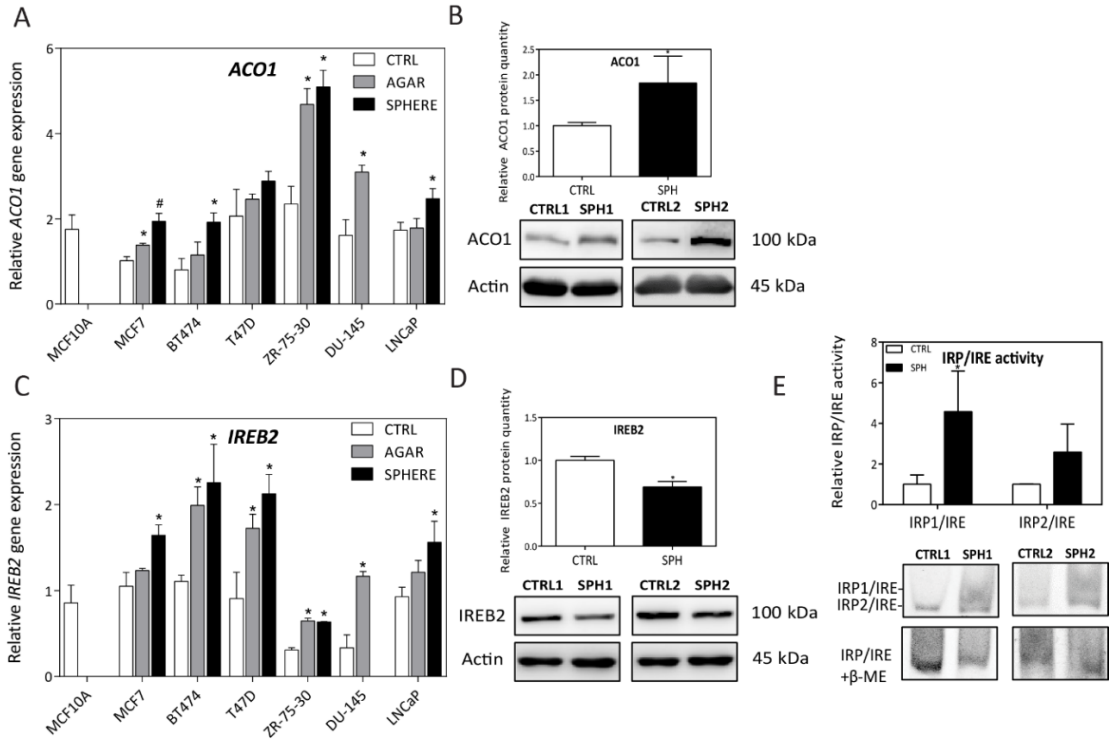


**Fig. 5.16. CSCs exert activation of components of IRP/IRE system. A**, **C**, RT-qPCR showing mRNA expression level of *ACO1* and *IREB2* genes in control and sphere cells derived from breast (MCF7, T47D, BT474, ZR-75-30) and prostate (DU-145, LNCaP) cancer cell lines. **B**, **D**, Western blots showing expression level of ACO1 and IREB2 proteins in control and sphere cells derived from MCF7 cell lines with densitometry evaluation performed by image J software in upper panels. **E**, Fluorescent EMSA showing activity of IRP/IRE system in control and sphere cells derived from MCF7 cell line with densitometry evaluation performed by image J software in upper panel. Experiments were performed at least in triplicate, standard error is SEM. Statistical significance was calculated by GenEx software using the unpaired t-test; * $p < 0.05$, # denotes statistical significance involving Dun-Bonferroni correction. Panels **B**,**D** and **E** are not my own results and are adapted from (247).

## 5.3.5. CSCs show deregulation of post-transcriptionally regulated proteins by IRP

We also probed other proteins related to iron uptake, storage and export, which are known to be regulated post-transcriptionally, and thus were not selected by expression profiling. Firstly, we checked for the expression of NRAMP2 (also known as DMT1), which is a known transporter of iron from gut lumen into enterocytes but also from acidic environment of lysosomes to cytoplasm (169,178). While we detected significant increase on mRNA level of *SLC11A2* gene (coding for NRAMP2 protein) in T47D and DU-145

sphere cells (Fig. 5.17. A, Table 5.2.), we measured significantly decreased NRAMP2 protein expression in MCF7 spheres (Fig. 5.17. B), suggesting decreased transport of iron from acidic endosomes to cytosol and its lysosomal compartmentalization. This result may explain the fact that while we detect higher LIP in CSCs, we have active IRPs showing that cells are short of the biologically active form of iron.

Next, we investigated the level of ferritin, which is the major iron storage protein, capable of binding an enormous amount of iron, store it and release it when needed. Ferritin is composed of two subunits coded by the *FTL1* and *FTH1* genes. FTL subunit plays a role in iron nucleation and protein stability, whereas FTH subunit carries the ferroxidase activity necessary for iron storage (189). We detected a significant increase in *FTL1* mRNA only in MCF7 cells and no difference was seen in *FTH1* mRNA level in tested cell lines (Fig. 5.17. C, D, Table 5.2.). However, we documented a significant decrease in ferritin protein level in MCF7 spheres (Fig. 5.17. E), which is in line with described increase in the IRP/IRE system activity. Finally, we also tested the expression level of the iron exporter ferroportin (coded by the *SLC40A1* gene). We measured significant upregulation of *SLC40A1* mRNA level in spheres from MCF7, BT474, T47D, ZR-75-30 and DU-145 cell lines (Fig. 5.17. F, Table 5.2.), while no significant change was seen on FPN protein level in MCF7 spheres (Fig. 5.17. G), leaving us with the idea that iron export is not involved in higher LIP in MCF7 spheres.

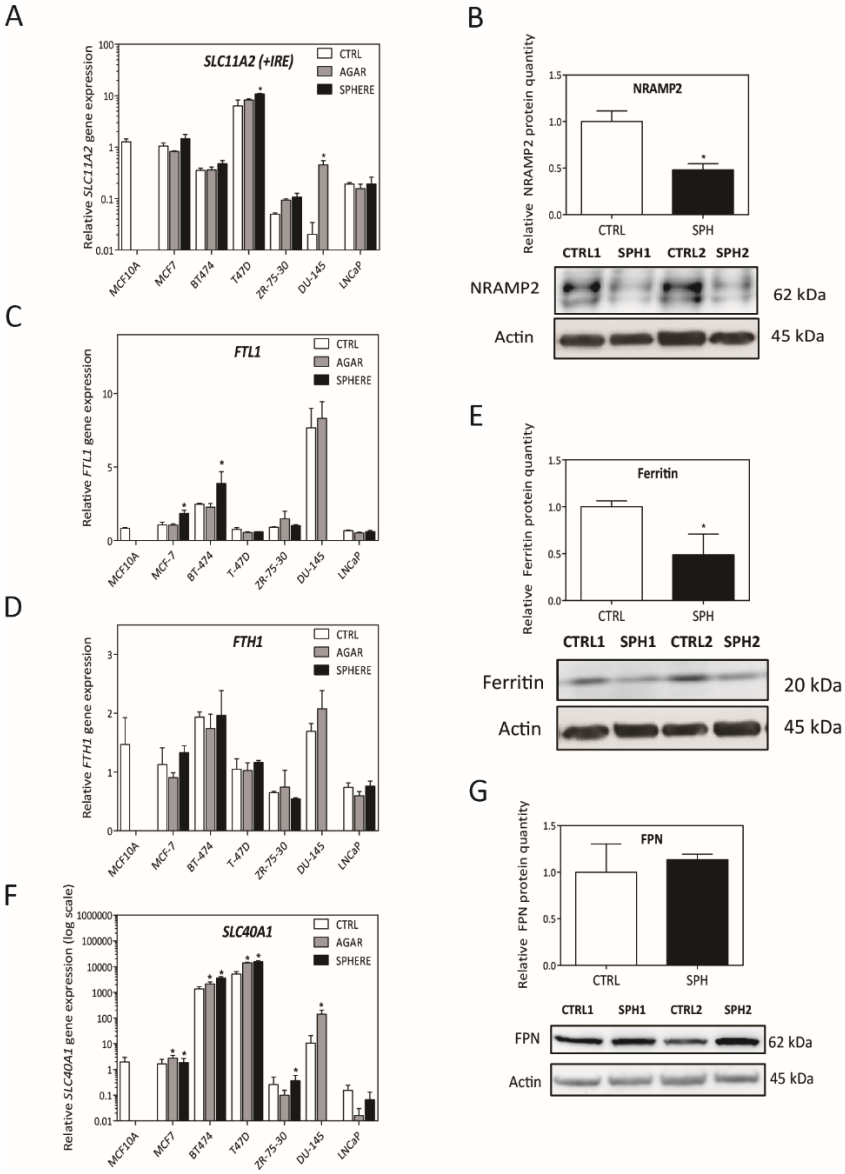


**Fig. 5.17. CSCs show deregulation of post-transcriptionally regulated proteins by IRPs.** **A**, **C**, **D**, **F**, RT-qPCR showing expression level of *SLC11A2*, *FTL1*, *FTH1* and *SLC40A1* genes in control and sphere cells derived from breast (MCF7, T47D, BT474, ZR-75-30) and prostate (DU-145, LNCaP) cancer cell lines. **B**, **E**, **G**, Western blots showing expression level of NRAMP2, Ferritin (light chain) and FPN proteins in control and sphere cells derived from MCF7 cell lines with densitometry evaluation performed by image J software in upper panels. Experiments were performed at least in triplicate, standard error is SEM. Statistical significance was calculated by GenEx software using the unpaired t-test; * $p < 0.05$. Panels **B**, **E**, **F** and **G** are not my own results and are adapted from (247).

### 5.3.6. CSCs show a decrease in expression of genes participating in haem and ISC biogenesis

ABCB10 is a transporter localised into inner mitochondrial membrane, where it forms complex with MFRN1 and ferrochelatase, participating in haem biosynthesis (268). The mRNA level of *ABCB10* gene was increased in spheres derived from all cell lines tested, reaching significance in MCF7, ZR-70-30 and DU-145 cells (Fig. 5.18. A, Table 5.2.), yet the level of protein was strongly decreased in MCF7 spheres (Fig. 5.18. B). This suggests that ABCB10 protein expression is regulated by some posttranscriptional mechanism. Lower level of ABCB10 protein in our model is in line with already published data about ABCB10 function. It was reported that ABCB10 is important for haematopoietic differentiation and its knockdown leads to iron accumulation within mitochondria (269). Since, we are studying CSCs, where we observed high mitochondrial iron accumulation, lower level of ABCB10 protein might give an explanation of the molecular mechanism underlying this finding.

GLRX5 is an important component of the ISC biogenesis machinery that facilitate insertion of nascent ISC into target apoproteins (235). We detected a decrease in mRNA expression of *GLRX5* gene in spheres obtained from all cell lines tested (statistically significant in spheres from MCF7 and T47D; Fig. 5.18. C, Table 5.2.). Furthermore, we also detected a significant reduction in GLRX5 protein level in MCF7 spheres (Fig. 5.18. D).

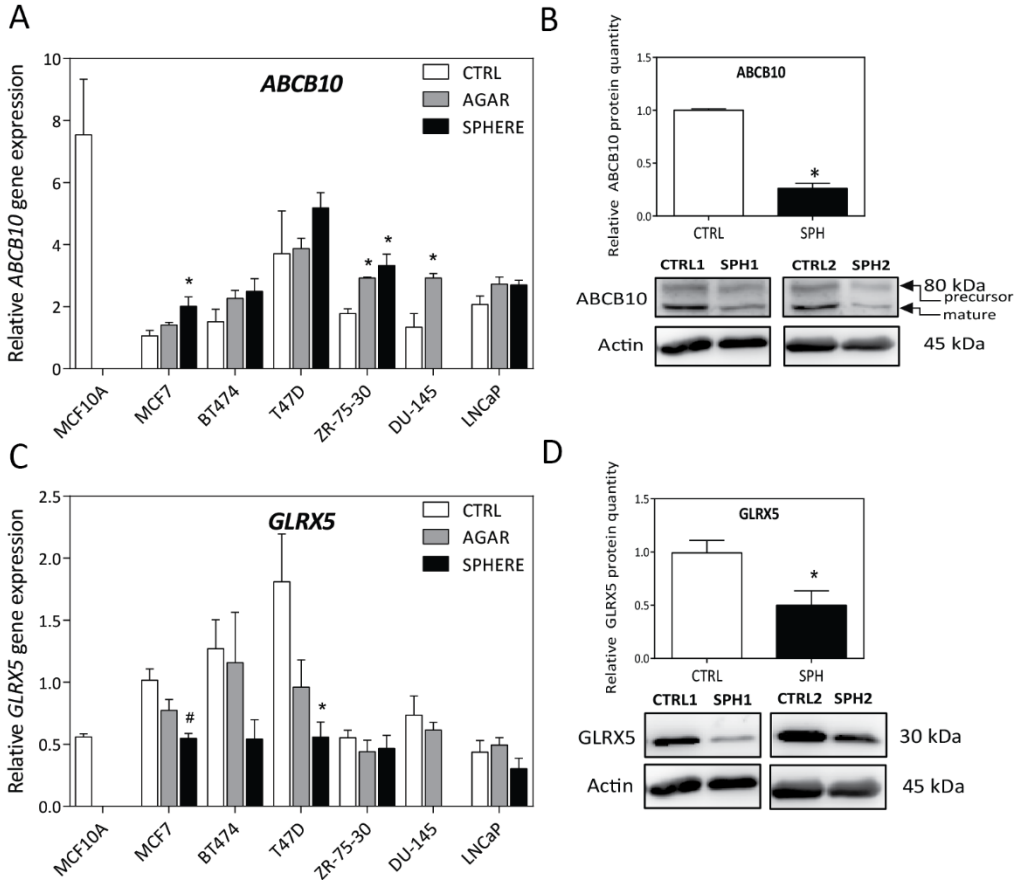


**Fig. 5.18. CSCs exhibit reduced expression of *ABCB10* and *GLRX5* mRNA and protein levels.** **A**, **C**, RT-qPCR showing mRNA expression level of *ABCB10* and *GLRX5* genes in control and sphere cells derived from breast (MCF7, T47D, BT474, ZR-75-30) and prostate (DU-145, LNCaP) cancer cell lines. **B**, **D**, Western blots showing expression level of ABCB10 and GLRX5 proteins in control and sphere cells derived from MCF7 cell lines with densitometry evaluation performed by image J software in upper panels. Experiments were performed at least in triplicate, standard error is SEM. Statistical significance was calculated by GenEx software using the unpaired t-test; * $p < 0.05$, # denotes statistical significance involving Dun-Bonferroni correction. Panels **B** and **D** are not my own results and are adapted from (247).

## 5.3.7. CSCs show altered function of the ISC containing enzymes and higher oxidative stress

The higher activity of IRP1/2 and decreased level of ABCB10 and GLRX5 proteins may be the cause or the consequence of improper function of ISC machinery and higher level of ROS. The properly assembled ISC is necessary for enzymatic function of ACO1 and mitochondrial CI. Therefore, we assessed their enzymatic activity and noticed decreased activity of both enzymes in MCF7 spheres, whereas only ACO1 (both the cytosolic and

mitochondrial form) activity was decreased significantly (Fig. 5.19. A, B). We also measured the level of ROS by a set of probes such as 2′,7′-dichlorofluorescein diacetate (DCF-DA, general reactive oxygen species probe), hydroxyphenylfluorescein (HPF, detecting hydroxyl radical), dihydroethidium (DHE, detect superoxide production) and mitochondrial superoxide indicator (mitoSOX). The level of ROS was significantly elevated in MCF7 spheres (Fig. 5.19. E) as well as the level of mitochondrial membrane potential ($\Delta\Psi m$) measured by tetramethylrhodamine, methyl ester probe (TMRM; Fig. 5.19. F). Glutathione plays an essential role in preventing oxidative stress by serving as an electron donor being simultaneously converted into its oxidised form GSSG (270). Consistently with higher level of ROS, we detected reduced level of GSH in MCF7 spheres and also lower ratio of GSH/GSSG, confirming higher oxidative stress in spheres (Fig. 5.19. C, D).

Together, these data document lower activity of ISC cluster containing enzymes ACO1 and CI and higher oxidative stress in CSCs, which may be caused by higher LIP in these cells.

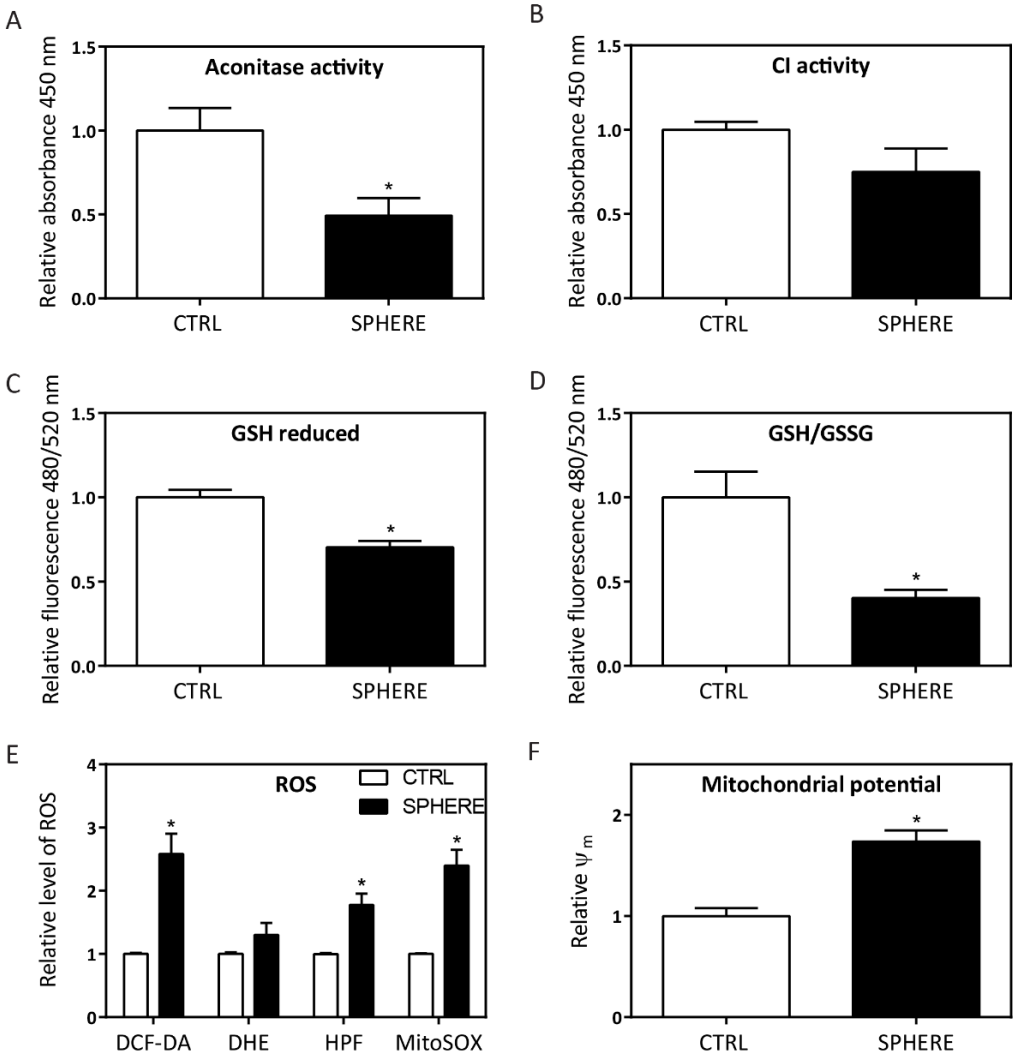


**Fig. 5.19. CSCs exhibit altered function of ISC containing enzymes (aconitase and mitochondrial complex I (CI)) and higher oxidative stress.** Control and sphere cells derived from MCF7 cell line were assessed for **A**, enzymatic activity of mitochondrial and cytosolic aconitase, **B**, enzymatic activity of mitochondrial CI, **C**, level of reduced glutathione (GSH), **D**, ratio of reduced and oxidised glutathione GSH/GSSG, **E**, level of reactive oxygen species (ROS) measured by using 2′,7′-dichlorofluorescein diacetate (DCF-DA), dihydroethidium (DHE), hydroxyphenylfluorescein (HPF) and mitochondrial superoxide indicator (mitoSOX) probes and **F**, mitochondrial potential measured by tetramethylrhodamine methylester probe. Experiments were performed at least in triplicate, standard error is SEM. Statistical significance was calculated by using the unpaired t-test; * $p < 0.05$. Panels **A**, **B**, **C** and **D** are not my own results and are adapted from (247).

### 5.3.8. CSCs activate hypoxia induced genes

Product of the *EPAS1* gene is the HIF-2α protein, which together with HIF-1α plays a central role in response of cells to hypoxia. HIF-2α was also shown to play an important role in iron metabolism. *EPAS1* mRNA is a target of IRP1 and HIF-2α as a transcription factor regulates expression of iron related genes (271). HIFs are targeted for proteasomal degradation under normal oxygen tension and stabilised under hypoxia, but can also be stabilised by increased ROS (272). *EPAS1* mRNA level was slightly elevated in spheres of tested cell lines (significantly only in DU-145) (Fig. 5.20. A, Table 5.2.), and protein level of HIF-2α was significantly increased in MCF7 spheres (Fig. 5.20. B).

Next, we detected significantly increased mRNA level of the HIF target gene *sulfhydryl oxidase 1* (*QSOX1*) in spheres derived from MCF7, BT474, T47D, LNCaP cell lines (Fig. 5.20. C, Table 5.2.). QSOX1 is an enzyme catalysing generation of disulphide bonds within proteins, accompanied by production of hydrogen peroxide as a side product of the reaction (273). This protein has two isoforms. The first isoform is inserted into membrane by its transmembrane domain. The second QSOX1 isoform emerges after proteolytic cleavage within the ectodomain of the protein, leaving transmembrane domain associated with the cell and excreting ectodomain into extracellular matrix (273). We found higher expression of the short QSOX1 protein isoform in MCF7 spheres (Fig. 5.20. D), which is in correlation with published literature associating QSOX1 with tumour progression and invasion (273).

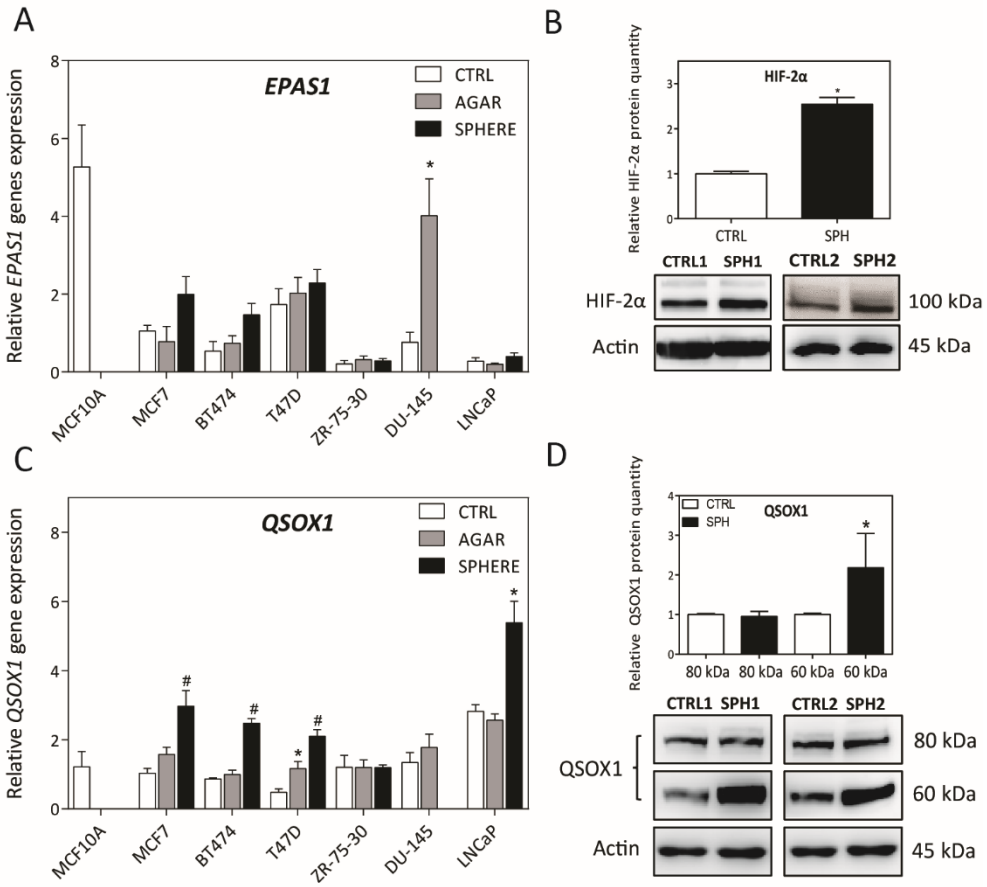


**Fig. 5.20. CSCs exhibit higher expression of *EPAS1* and *QSOX1* mRNA and protein level. A**, **C**, RT-qPCR showing mRNA expression level of *EPAS1* and *QSOX1* genes in control and sphere cells derived from breast (MCF7, T47D, BT474, ZR-75-30) and prostate (DU-145, LNCaP) cancer cell lines. **B**, **D**, Western blots showing expression level of HIF-2α and QSOX1 proteins in control and sphere cells derived from MCF7 cell lines with densitometry evaluation performed by image J software in upper panels. Experiments were performed at least in triplicate, standard error is SEM. Statistical significance was calculated by GenEx software using the unpaired t-test; * $p < 0.05$, # denotes statistical significance involving Dun-Bonferroni correction. Panels **B** and **D** are not my own results and are adapted from (247).

## 5.3.9. Deregulation of iron export related HEPH oxidase and HFE protein linked to iron overload in CSCs

We detected changes in the *HEPH* expression, whose protein product is a multi-copper oxidase anchored into basolateral membrane of enterocytes, helping FPN to export iron from these cells (FPN is discussed in the next chapter as an IRE/IRP responsive protein) (174). We detected increased expression of *HEPH* mRNA in spheres derived from all cell lines

tested (significantly in BT474 and T47D) (Fig. 5.21. A, Table 5.2.). We detected two isoforms of HEPH protein in MCF7 spheres, from which expression of canonical 130 kDa isoform was statistically increased and expression of the 100 kDa isoform was only slightly decreased (Fig. 5.21. B).

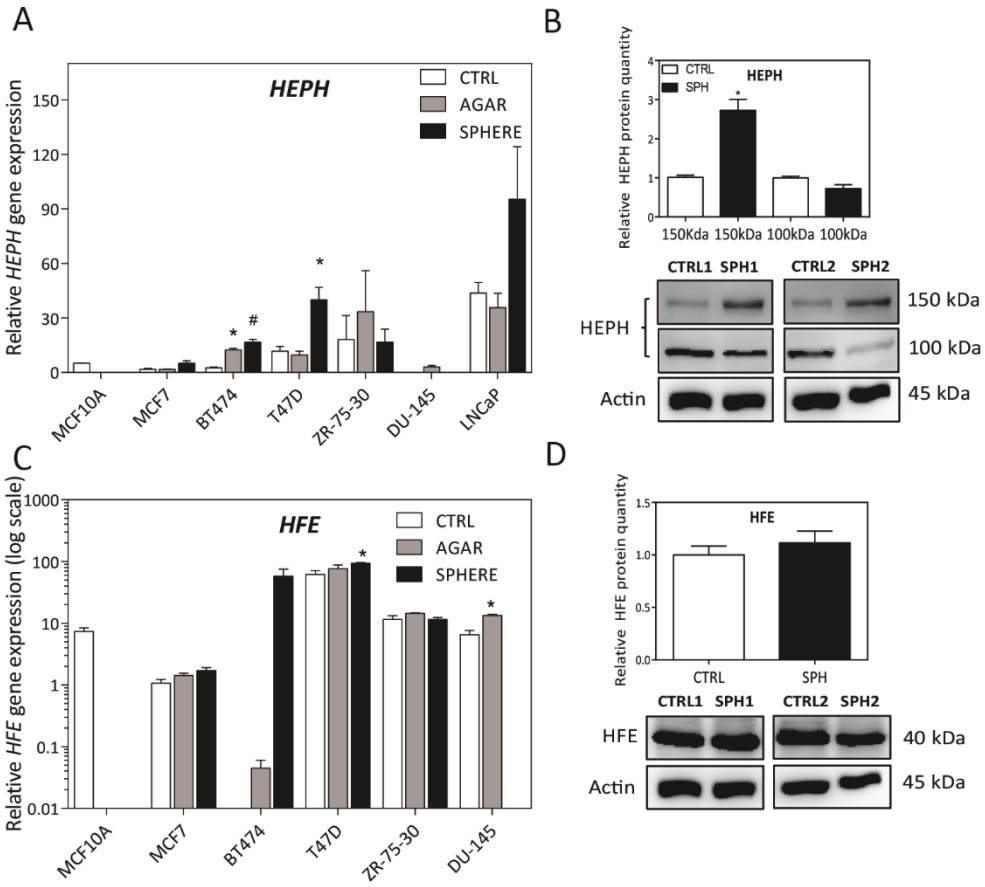


**Fig. 5.21. CSCs exhibit higher expression of *HEPH* mRNA and protein levels and higher *HFE* mRNA level.** **A**, **C**, RT-qPCR showing mRNA expression level of *HEPH* and *HFE* genes in control and sphere cells derived from breast (MCF7, T47D, BT474, ZR-75-30) and prostate (DU-145, LNCaP) cancer cell lines. **B**, **D**, Western blots showing expression level of HEPH and HFE proteins in control and sphere cells derived from MCF7 cell lines with densitometry evaluation performed by image J software in upper panels. Experiments were performed at least in triplicate, standard error is SEM. Statistical significance was calculated by GenEx software using the unpaired t-test; * $p < 0.05$, # denotes statistical significance involving Dun-Bonferroni correction. Panels **B** and **D** are not my own results and are adapted from (247).

The *HFE* gene codes for haemochromatosis protein, whose mutations leads to excessive iron overload in haemochromatosis patients and it is connected with cancer development (274). We detected upregulation of *HFE* mRNA in all spheres tested (significantly in T47D and

DU145; Fig. 5.21. C, Table 5.2.). Nevertheless, the level of HFE protein remained unchanged in MCF7 spheres (Fig. 5.21. D), suggesting that this protein is not linked to CSC phenotype.

# 6. DISCUSSION

## 6.1. Mechanisms of resistance in CSCs

CSCs are reported to play a major role in cancer resistance causing unresponsive reactions of tumours to treatment and relapse of the disease due to residual cancer cells in the organism (2). The mechanisms of resistance are highly complex, ranging from efflux of the drugs by ABC transporters to metabolic and epigenetic adaptations as well as to inhibition of apoptosis (10,11).

### 6.1.1. Expression profiling of ABC transporters in CSCs

The basic mechanism of protection of CSCs is through the expression of ABC transporters serving as guardians of stem cell population in the body (275). Unfortunately these ATP powered efflux pumps afford protection of CSCs in the tumours as well, shielding them from the adverse effect of chemotherapy (275). Although there is direct evidence for the role of ABCB1, ABCC1 and ABCG2 in multidrug resistance, the contribution of other family members is not so well explored (276). Moreover, the mechanism by which the ABC transporters are involved in the maintenance of the CSCs phenotype *via* their drug-efflux-independent function is even less understood (275). For these reasons we have decided to study the expression of all members of ABC transporters in our model of CSCs.

Since CSCs are known to be more resistant to cancer treatment due to overexpression of the ABC transporters (275), we have checked a response of our sphere model of CSCs to common chemotherapeutic drugs such as daunorubicin and doxorubicin. MCF7 spheres and T47D spheres were much less sensitive than their adherent counterparts. Daunorubicin and doxorubicin were reported as substrates of ABCB1, ABCC1, ABCG2, ABCC2 and ABCC3 transporters (162,163), therefore we applied ABCB1, ABCG2 and ABCC1 inhibitors in order to reverse the unresponsiveness of CSCs to daunorubicin and doxorubicin. Unexpectedly, we observed that these inhibitors alone had significant effect on viability of spheres. Even though the specificity of individual inhibitors is rather controversial and we were interested in all ABC transporters, we performed expression profiling analysis of 48

members of the human ABC transporter family in our model of CSCs. On the mRNA level, many of the ABC transporter genes were upregulated; the most significantly *ABCA1*, *ABCA3*, *ABCA5*, *ABCA12*, *ABCA13*, *ABCB7*, *ABCB9*, *ABCB10*, *ABCC1*, *ABCC2*, *ABCC3*, *ABCC5, ABCC8*, *ABCC10*, *ABCC11* and *ABCG2*, and these changes were observed in majority of the tested cell lines. This result correlates with the hypothesis that CSCs express higher level of these ATP-driven pumps (277). However, we realised that the protein levels of ABC transporters quite often do not correlate with the mRNA levels, which is not a surprise, as post-transcriptional and post-translational modifications of ABC transporters are ubiquitous and already described (278,279). Based on the protein level, we then selected transporters that were consistently upregulated (ABCB8, ABCC1, ABCC2, ABCC10 and ABCG2) or downregulated (ABCB10, ABCF2) in spheres derived from three breast cancer cell lines. The role of the individual transporters in CSC biology is currently being investigated by further experiments.

The protein data nicely explain the results obtained with the daunorubicin and doxorubicin as we observed increased expression of ABCC1, ABCC2, ABCG2 and ABCC3 (only in T47D cells) transporters, which pump these chemotherapeutics out of the cell. The results obtained with ABC transporter inhibitors also correlate with protein data. The decrease in sphere viability after using ABCG2 inhibitors is in line with published data that ABCG2 expression is conserved in stem cells, protecting them from cell death and preserving stem cell phenotype (152). It is also considered a CSC marker, thus further validating our sphere model (152). Another interesting response in cell viability was observed with an inhibitor of ABCC1, as our sphere cells were highly sensitive to inhibition of this transporter whose expression was highly upregulated. Apart from xenobiotics, ABCC1 transports proinflammatory cysteinyl leukotriene $C_4$ and glutathione and glucuronide conjugates (151). By transporting GSH and GSSG, ABCC1 is also involved in regulating responses during oxidative stress and was recently reported as an important mediator of oxidative stress in endothelial murine EOMA cells (126). Since we detected higher ROS in our sphere model, the ABCC1 transporter might have an important function in cellular detoxification and its inhibition thus may lead to further increase in intracellular ROS, which is deleterious for cells. This hypothesis still needs further experimental verification.

The inhibition of ABCB1 transporter by verapamil had significant impact on viability only in BT474 sphere cells while no difference was observed in other cell lines, yet the protein level of this well-known transporter was very low, rising the probability that the observed effect was likely non-specific. Interestingly, there is no change in protein level of ABCB1 transporter in our model of CSCs. The *ABCB1* mRNA expression was scarcely detectable in all prostate and breast cancer cell lines tested and ABCB1 protein level was very low in the tested breast cancer cell lines, both in the adherent and sphere cells. Since ABCB1 transporter is one of the most studied, characterised and main detoxifying representative of ABC transporters, increased expression was expected at least in some of the CSCs. Interestingly, ABCB1 expression was documented to be high in MCF7, T47D and BT474 cells resistant against certain chemotherapeutics, but this seems to be rather an adaptive response of the cells because normal levels of ABCB1 in these cell lines are low (280–284). However, this might be cell type specific as ABCB1 inhibition leads to a decrease in CSCs properties and seems to reverse resistance in non-small cell lung cancer and in renal cell carcinoma (154,155).

Apart from ABCC1 and ABCG2, protein profiling data also showed constistent changes in expression of ABCC2, ABCB8, ABCC10, ABCB10 and ABCF2 transporters. ABCC2 is expressed in the apical membranes of canalicular cells in the liver where it functions as the major exporter of organic anions from the liver into the bile. ABCC2 expression is associated with resistance to platinum containing drugs in various cancer types (285–288) and correlates with poorly differentiated state of the tumour. Reports associating ABCC2 expression with CSCs are scarce and further investigation is required to shed more light on its role in biology of CSCs. The same holds true for ABCC10, which also transports a broad range of xenobiotics but no report describes its function in CSCs (289). Interestingly, mitochondrial transporter ABCB8 is involved in doxorubicin resistance in melanoma cells, by protecting mitochondrial genome, but its role in other breast and ovarian cancer cell lines remains elusive (290) and its function in CSCs as well as its physiological functions are not well known.

Surprisingly, ABCB10 and ABCF2 transporters were highly downregulated on the protein level in our sphere model. Since ABCB10 is related to iron metabolism, it is discussed in the next section 6.2. and here we focus only on ABCF2. ABCF2 is reported as a prognostic

marker in ovarian cancer (291) where it contributes to cisplatin resistance (292). On the other hand, in breast cancer it is reported to play a suppressive role in metastatic sites and its expression in $ER^-/PR^-$ breast tumours is a good prognostic marker (293). Since ABCF2 have only NBDs and lacks the transmembrane domains, it has cellular function unrelated to transport and similarly to ABCF1, it plays a role in other cellular processes such as inflammation or translation initiation (140). Moreover, the expression of ABCF1, the transporter from the same group as ABCF2, was correlated with differentiated states (140) and it is possible that the same expression pattern applies for ABCF2, which correlates with obtained data. The exact molecular mechanism how ABCF2 contributes to the CSC phenotype remains to be determined.

Similarly, other transporters may play roles unrelated to drug transport and be involved in the maintenance of CSCs phenotype. The mentioned increase in mRNA level of *ABCA1*, *ABCA3*, *ABCA5*, *ABCA12*, *ABCA13*, *ABCB7*, *ABCB9*, *ABCC3*, *ABCC5, ABCC8* and *ABCC11* was not consistently replicated on protein level, therefore we are not discussing these transporters further. Transport of endogenous substrates by ABC transporters may act in an autocrine or paracrine way to influence cellular processes such as apoptosis, proliferation, differentiation, cell migration and metastasis (162). Recent reports also show multiple subcellular localization of ABC transporters, thus transporters thought to be only in the plasma membrane were also found in mitochondrial or nuclear membranes and therefore might be transporting molecules within the subcellular compartments (126,287,294). Besides, some transporters are localized in membranes of subcellular organelles as lysosomes (ABCA2, ABCA3, ABCA5, ABCB9, ABCD4) (132,134,295), peroxisomes (ABCD1, ABCD2, ABCD3) (138), mitochondria (ABCB6, ABCB7, ABCB8, ABCB10) (128) or endoplasmatic reticulum (ABCB2, ABCB3) (125), fullfiling important functions in protein, lipid and fatty acid metabolism as well as in immune response. Some ABC transporters were reported to act as transcription factors besides their function of transporting molecules (296). For these reasons it is appropriate to investigate whether the expression of ABC transporters has a fundamental role in the CSC phenotype, or occurs as a result of other genetic changes during tumorigenesis. However, due to the large number of known ABC transporters and their high expression levels in stem cells, it is likely that partial functional redundancy might mask their importance for stem cell maintenance or growth.

To further elucidate the function of those individual ABC transporters more precisely, we are currently working on a model of individual ABC overexpression or knockout by the CRISPR technology and we believe that this would give some important answers to the puzzle of the CSC biology.

### 6.1.2. Regulation of oestrogen receptor signalling by miR-301a-3p in ERα positive breast cancer

High level of miR-301a-3p correlates with metastatic potential and was shown to be a negative prognostic marker in many human cancers (122,297). However, the role of miR-301a-3p in progression of ER-positive breast cancer has not been elucidated yet. Breast cancer present the prevailing type of carcinoma in women worldwide. The majority of diagnosed breast cancer are classified as ER-positive subtypes, characterised by good prognosis for patient, who benefit from treatment with the anti-oestrogenic drug, tamoxifen. Although the drug is efficient and well tolerated, the reason for cancer relapse and metastasis formation is the loss of ERα, leading to non-responsiveness to endocrine therapy (298,299). Development of resistance connected with the transition from ER-positive to ER-negative breast cancer thus represents a very important clinical problem and finding markers predicting oestrogen independence is of high importance. Dysregulated miRNA expression may underline the abnormal function of cellular processes by regulating expression of drug targets and thus constitute a resistant phenotype (300).

*ESR1* gene coding for ERα mRNA has a long 3' UTR region of about 4.3 kbp bearing many evolutionarily conserved miRNA target sites. Several miRNAs such as miR-22 (301), -206 (302,303), -145 (304) have already been reported to regulate ERα protein expression. We analysed the *cis* regulatory sequences in the 3´ UTR of the *ESR1* gene mRNA and identified two seed sequences, which are able to bind miR-301a-3p. To validate our hypothesis, we have generated a reporter vector where *Cypridina* luciferase gene is coupled to the 3´ UTR of *ESR1* gene and demonstrated that deletion of these two sites results in higher luciferase expression. Thus, we confirmed the role of these two sites in the negative regulation of the ERα protein expression. Interestingly, the first site closer to the end of translation is a preferred binding site for miR-301a-3p as deletion of this site only resulted in phenotype

identical to the deletion of both binding sites. However, the deletion of the second site also led to an increase in reporter luciferase expression suggesting that this site can be utilised by miR-301a-3p as well albeit its miR-301a-3p binding is less profound.

Our results demonstrate that miR-301a-3p supresses *ESR1* mRNA and ERα protein expression and, more importantly, inhibits the canonical ER signalling pathway in ER positive MCF7, T47D and BT474 breast cancer cell lines. High miR-301a-3p expression leads to lower expression of genes positively regulated by ERα (*PGRA*, *GREB1*, *CXCL12*, *CSTD*) and to induction of genes negatively regulated by ERα (*BMP7*). Moreover, we showed that overexpression of miR-301a-3p caused inhibition of proliferation of oestrogen-dependent MCF7 cells *in vitro* and suppressed the growth of miR-301a-3p overexpressing tumours derived from MCF7 cells in nude mice. These results confirm that *ESR1* mRNA is a direct target of miR-301a-3p *in vitro* and *in vivo* and are consistent with already published results referring to other miRNAs targeting ERα (303,304). On the contrary, we did not detect any significant changes when using miR-301a-3p anti-miR with exception of BT474 cells. These cells express significantly higher level of miR-301a-3p compared to MCF7 and T47D cells, which is probably the reason why miR-301a-3p anti-miR had an impact only on these cells. *ESR1* mRNA and ERα protein is relatively abundant in MCF7 and T47D cells and thus further increase in ERα protein is probably not beneficial for cells. Alternative explanation is that *ESR1* mRNA contains long 3' UTR with many other regulatory miRNA sites (305) and the impact of miR-301a-3p anti-miR could be limited by low expression of miR-301a-3p in comparison with other abundant and non-inhibited regulatory miRNAs as suggested by Androsavich and Chau (306).

Interestingly, we detected higher expression of the *HER2* gene in miR-301a-3p overexpressing tumours. This observation is in line with reports showing that a decrease in ERα signalling leads to upregulation of *HER2* in order to sustain proliferation by activation of other signalling pathways. Moreover, HER2 signalling further inhibits ERα signalling (307). Increased *HER2* gene expression also increases invasiveness and expression of CSC genes in breast cancer (308). Consistently, we observed upregulation of other markers related to CSCs, EMT and metastatic phenotype such as *CD44*, *ALDH1*, *ABCG2*, *VIM*, *ZEB1*, *ZEB2* and *VEGFA* in tumours derived from MCF7 cell line overexpressing miR-301a-3p. The correlation of miR-301a-3p expression with CSC phenotype was further confirmed

by analysis of our model of CSCs, where we observed highly upregulated miR-301a-3p expression together with significantly decreased ERα protein level accompanied by inhibition of expression of ERα target proteins GREB1 and PR. Moreover, other ERα-regulating miRNAs such as miR-22, -145 and -206 were not significantly and consistently elevated in sphere samples (data not shown) suggesting that miRNA regulation of ERα expression in connection with CSC phenotype is specific for miR-301a-3p. Furthermore, recent reports show that miR-301a-3p renders breast cancer non-responsive to the anti-oestrogenic drug tamoxifen and also involvement of miR-301a-3p in regulation of other signalling pathways that are important in the progression of breast cancer such as PTEN/AKT, NF-κB or Wnt/β-catenin (116,122,123). MiR-301a-3p was also shown to promote EMT by inhibiting E-cadherin expression (263). Thus, we hypothesised that upregulation of miR-301a-3p may represent a feasible mechanism contributing to the phenotypical shift of primarily ERα dependent cells towards tumour cells relying on other proliferative signals. More importantly, since miR-301a-3p overexpressing cells acquire properties of CSCs, which are highly invasive and resistant to treatment (2,276,309), they might represent the subpopulation that survives endocrine therapy and gives rise to relapsing metastasis.

Next, the analysis of biopsies from human breast tumours revealed the significantly higher level of miR-301a-3p expression in tumours which were classified as ER/PR negative in comparison with tumours which were ER/PR positive. Similarly, we detected a significant negative correlation between *ESR1* and miR-301a-3p expression, suggesting that miR-301a-3p might serve as a biomarker of cancer progression, patient prognosis and also the response to endocrine treatment. These data are in accordance with report showing that expression of miR-301a-3p is significantly associated with larger tumour size and lymph node metastases in triple negative breast cancer (310).

In conclusion, our study provides functional evidence that miR-301a-3p regulates ER signalling in the ER positive breast cancer cells *in vitro* as well as *in vivo* by direct inhibition of *ESR1* mRNA translation. Thus, miR-301a-3p forces oestrogen dependent cancer cells to become oestrogen-independent with high selection pressure to activate alternative survival/pro-proliferative pathways in order to proliferate. The transition of oestrogen-dependent tumour to oestrogen-independent tumour is one of the crucial steps in progression

of breast cancer. Collectively, our data together with published papers showing effects of miR-301a-3p on cancer motility and metastasis (116), suggest that miR-301a-3p might be used as a marker of poor patient prognosis with higher chance to become hormone-insensitive and resistant to tamoxifen.

## 6.2. Metabolism of iron in CSCs

Due to the irreplaceable function of iron in cellular reactions and processes necessary for cell growth and replication, it is not surprising that iron plays an important function in cancer development. This notion was supported by multiple experimental studies associating altered expression of genes and proteins involved in iron metabolism and iron regulation with tumorigenesis (reviewed in (311)). Application of iron chelating drugs has been shown to inhibit tumour growth, confirming its role in tumour biology (240,242,246). Thus, defining how iron contributes to development of cancer is essential for developing novel therapeutic strategies. CSCs are considered to be one of the main reasons for cancer progression and metastasis. However, no studies have described the role of iron and its metabolism in the maintenance and biology of CSCs so far. For this reason, we decided to describe the iron metabolism in spheres, derived from several cancer cell lines, which we used as an *in vitro* model of CSCs.

We detected higher LIP and iron uptake with predominant iron accumulation within mitochondria in MCF7 spheres. We also demonstrated that MCF7 spheres are more prone to iron withdrawal than control adherent MCF7 cells, suggesting that iron is an important micronutrient necessary for survival of CSCs. In order to better understand iron metabolism in CSCs, we performed expression profiling of genes related to iron metabolism. The selected genes with altered mRNA expression (more than 1.5 fold change), which changed reproducibly among studied cell lines, gave us iron metabolism-related gene expression signature typical for our model of CSCs. Among differentially expressed genes are individual genes participating in iron uptake (*CYBRD1*, *TFRC*), iron sensing and iron regulation (*ACO1*, *IREB1*), mitochondrial haem and ISC synthesis (*ABCB10*, *GLRX5*), hypoxia response (*EPAS1*, *QSOX1*), iron export and iron overload regulation (*HEPH*, *HFE*). Association of the expression of these genes with CSC phenotype was confirmed also by

PCA based on expression of selected genes, showing clear differentiation between control and sphere samples in all cell lines.

Next, we investigated expression of individual genes on protein level in our model of CSCs derived from MCF7 cell line. We detected higher level of *CYBRD1* mRNA in spheres and its 25 kDa protein isoform in MCF7 spheres. Increased *CYBRD1* mRNA level in spheres is in line with the detected activation of HIF-2α, which is known to regulate its expression to enhance iron uptake (312). High expression of DCYTB protein has been recently reported in breast cancer cells where it inhibits adhesion of cells to fibronectin (313), suggesting that in our model this reductase may have function unrelated to iron metabolism and pointing to possible role of different DCYTB protein isoforms in CSCs. High expression of TfR1 has been already connected with cancer progression (7) and it is expected due to HIF (314) and IRP/IRE system activation (204). Recently published data in glioblastoma CSCs highlights the importance of TfR1 for maintenance of CSC phenotype (248), supporting our results. In order to further decipher other possible mechanisms of iron uptake, we also assessed other proteins involved in the NTBI uptake such as ZIP14 and a putative NTBI transporter DMT1 (315,316). DMT1 has maximal iron transport activity at pH 5-6 and it is known that tumours exhibit acidic microenvironment (315,317). However, published studies showed that DMT1 is dispensable for NTBI uptake at least in normal hepatocytes (318) and its role as an NTBI uptake pump is rather unclear. Using our CSCs model, we found decreased DMT1 protein level and thus we do not consider DMT1 a substantial contributor to higher LIP in our model of spheres. Because the amount of DMT1 was detected in whole cell lysates, we cannot rule out that the actual amount/proportion of DMT1 on the plasma membrane differs in CSCs. We found that iron importer ZIP14 (coded by *SLC39A14* gene) was increased on mRNA level and ZIP14 protein level was decreased, suggesting for post-transcriptional mechanism of regulation. ZIP14 is reported to be targeted for proteasomal degradation in response to iron deprivation in HEPG2 cells (319), which we think is actually also occurring in our model of CSCs despite our data show higher LIP pool (see below). Decreased ZIP14 protein level is also in line with newly published data in human prostate cancer where authors connect lower ZIP14 expression with more invasive phenotype (320). In hepatocellular carcinoma, lower ZIP14 expression was also noticed probably to protect cells from tumour suppressive effect of zinc, which is another ZIP14 substrate (321). From the expression of these two iron importing proteins, we assume that higher iron uptake in MCF7 spheres is

thus facilitated mostly by higher level of TfR1 or *via* DCYTB, although we cannot fully exclude the contribution of other proteins from the ZIP family (such as ZIP8) that we did not assess.

We also detected higher level of ACO1 and IREB2 mRNA in our sphere model. On the protein level, ACO1 level was increased whereas IREB2 level was decreased. Since, ACO1 and IREB2 stands for IRP1 and IRP2, we also checked for their activity and detected higher IRP/IRE binding activity in MCF7 sphere model. IRPs are activated in cells in response to iron deprivation and would explain higher iron uptake and lower iron storage in our model. Yet, paradoxically, we found higher LIP in our model of spheres but since LIP measures all "chelatable" iron within the cells it does not discriminate between iron that is biologically active or inactive and thus iron measured as total LIP can be biologically inactive or locked within subcellular structures or vesicles and thus be consistent with the IRP activation in the cytosol. Interestingly, we found lower level of IRP2, yet it was active in the IRE binding. Since IRP2 is targeted to proteasomal degradation in iron repleted cells (224), this might explain the lower level of IREB2 protein in sphere cells but the exact mechanism remains to be clarified.

ACO1 contains the ISC in its active site and the IRE binding activity is exerted after ISC is removed. The presence of ISC in ACO1 is dependent on iron level within the cells and especially on the proper function of all components important for ISC biogenesis (218). The impaired ISC biogenesis is indicated by the lower activity of ISC containing enzymes, and consistently mitochondrial CI and aconitase activity (cytosolic and mitochondrial) was decreased in our MCF7 sphere model. The impaired ISC biogenesis is also a possible reason for accumulation of iron within mitochondria (322), which we observed in our sphere model. GLRX5 is an important component of Fe-S cluster biogenesis and its deficiency causes sideroblastic anemia connected with impairment of the ISC biogenesis, IRP1 activation, mitochondrial CI and aconitase activity decrease and mitochondrial iron accumulation in human erythroblast (323). We detected reduction in *GLRX5* gene and protein expression in our model of sphere cells which might partly explain the observed phenomenon of lower activity of ISC containing enzymes due to insufficient ISC formation resulting in IRP1 activation and mitochondrial iron accumulation. The evidence about the role of GLRX5 in carcinogenesis is scarce but the inhibition of ISC biogenesis may provide an explanation of

the genomic instability of CSCs, as impairment of the function of ISC dependent enzymes results in reduced activity of enzymes, which maintain the integrity of the genome (324).

Destabilization of ISC and thus IRP1 activation is also promoted by generation of ROS (219). We detected higher oxidative environment within sphere cells than in normal adherent cells. The overall level of ROS is higher not only in cytosol but also in mitochondria and this is also reflected by lower level of reduced glutathione and lower GSH/GSSG ratio in sphere cells. Although CSCs were reported to have lower amount of ROS due to higher expression of free radical scavenging system (70), we detected the opposite. ROS are critical signalling molecules involved in each stage of cancer development including tumour initiation, development and progression, and are also reported to be involved in EMT process (325). Our method of generating spheres is based on cultivation of cells as floating spheres in media without FBS supplemented with EGF and FGF that enrich population of cells with increased EMT and CSC markers. EMT process is known to increase the CSC phenotype (56) and it is also reported to be regulated by ROS (326). Moreover, Zhang et al. (327) showed that EMT process contributes to ROS production by inhibition of ferritin levels in cytosol leading to further increase in LIP. We detected significantly lower levels of ferritin and higher levels of LIP in our sphere model, which is consistent with higher ROS production. It is also reported that EMT process is initiated by specific CSCs (58,59), thus we can only speculate that CSCs initiate EMT process through deregulation of iron metabolism to produce higher ROS and induce EMT. Moreover, sphere formation led to higher ROS generation in ovarian cancer cells where application of ROS scavenger decreased their sphere forming capacity (328). Reduced level of mitochondrial transporter ABCB10 might present another mechanism that increases ROS level as it is reported to play a protecting role against ROS (329). Although the data document rather small (2-fold), yet significant increase in mRNA level in all tested cell lines, substantially reduced ABCB10 protein level in all tested cell lines suggests for some post-transcriptional mechanism of regulation of ABCB10 protein. ABCB10 is localised within inner mitochondrial membrane where it stabilises MFRN1 and forms a complex with ferrochelatase, participating in haem synthesis (268,330). Reduced level of ABCB10 protein in our model corresponds with the observed iron accumulation in mitochondria and higher level of ROS, a situation which has been observed in embryos of mice with ABCB10 deletion (269). Low ABCB10 level in our model is also in line with the notion that ABCB10 expression is induced during erythroid

differentiation (331). On the contrary, Wang et al. (332) reported higher ABCB10 protein activity in lung CSCs mediated by activation of HIF-1α in these cells. Thus, the correlation of ABCB10 expression with cancer progression and CSC phenotype needs further investigation. The increase in mitochondrial membrane potential in our sphere model correlates with published data that CSCs possess higher mitochondrial potential than other cancer cells (333).

Another role for ROS in reprogramming cells into CSCs might be through HIF transcription factors. Under normoxic conditions, HIFs are targeted for proteasomal degradation by the function of PHDs (334). These hydroxylases also require iron as an essential cofactor, thus shortage of intracellular iron results in their low activity and stabilization of HIFs (314). High ROS level has been shown to activate HIF transcription factors through inhibition of function of PHDs (272,335). On the other hand, HIF-2α has been shown to be a direct target of IRP1 that limits its mRNA expression during iron deficiency. Interestingly, our data show higher level of HIF-2α and HIF regulated protein QSOX1 and already mentioned DCYTB. The effect of activated IRP1 on HIF-2α mRNA expression is thus probably not the decisive factor in our model. Due to low levels of HIF1α and lack of reliable antibody, we were not able to probe the protein level of HIF-1α, so it remains an open question for further determination. Activity of HIF transcription factors has been shown to promote the activation of developmental pathways such as Notch, Wnt/β-catenin and Hedgehog (80–82) often activated in CSCs as they are important for maintaining the CSC phenotype (75). Both HIF transcription factors have stage specific roles during reprogramming of human cells into pluripotent SCs (336). Moreover, HIF-2α has been shown to activate OCT-4 and C-MYC transcription factors (337). It is thus plausible that cells activate HIFs to maintain CSCs phenotype but whether the increased iron level followed by ROS generation is the cause of HIF activation needs further investigation. The increase in activity of HIF transcription factors is also supported by increased expression of HIF-regulated gene *QSOX1*. QSOX1 is a sulfhydryl oxidase with both disulfide-generating and disulfide transferring capabilities (273). QSOX1 contributes to ROS generation as a result of its enzymatic activity creating feedback loop where ROS induce QSOX1 expression through activation of HIFs. We detected higher expression of short variant of QSOX1 protein without transmembrane domain that is known to be overexpressed in tumour cells (273). QSOX1 is secreted into extracellular matrix where it is thought to play a role in tissue remodelling to

facilitate cell invasion and metastasis (273). This is in line with published data that QSOX1 protein level correlates with aggressive phenotype of breast cancer (338) and inhibitory QSOX1 antibody inhibits cell migration (339). Research connecting QSOX1 expression with CSC phenotype has not been published yet, but it is likely that QSOX1 expression is supporting EMT.

We further looked at the expression of other genes connected with the regulation of iron metabolism on cellular as well as organismal level such as HEPH, HFE and DMT1. The HEPH protein was reported to be decreased in colorectal and breast cancer (340,341) and in our model we see increased 150 kDa isoform while only a slight decrease in 100 kDa isoform of this protein. HEPH mediates iron export from enterocytes by oxidizing $Fe^{2+}$ to $Fe^{3+}$ but its role in breast tissue and its relation to CSC phenotype has not been elucidated yet and needs further investigation. HFE is involved in regulation of the level of hepcidin, thus affecting indirectly the iron export from cells through the hepcidin/ferroportin axis (198). Mutations in this gene are connected with excessive iron loading in haemochromatosis patients resulting in increased risk of cancer development (274,342). Although we have seen an increase in the *HFE* mRNA level, no change was observed on the level of protein assuming this protein is not linked to CSC phenotype.

FPN is the only known iron exporter. The downregulation of FPN expression is correlated with worse prognosis in colorectal, breast and prostate cancer (343–346). Since we detected no difference in FPN protein level, we assume that iron export is not changed in CSCs and higher LIP is maintained mainly by higher iron uptake in these cells. Given the IRP activation, we expected lower level of ferroportin, which was not observed. Nevertheless, FPN can be regulated independently of IRPs and these mechanisms might explain changes in FPN expression in our system (347–349).

Ferritin is the main iron storage protein in the cell and its differential expression has been associated with progression of Hodgkin's lymphoma, breast and pancreatic cancer and hepatocellular carcinoma (350). Intriguingly, in breast cancer, the increased ferritin level was associated more with tumour stroma than with cancer cells (351). According to Alkhateeb et al. (352), ferritin is localised within tumour associated macrophages (TAM), which secrete ferritin into tumour stroma where it exerts pro-proliferative effect on cancer

cells unrelated to iron. Moreover, TAM associated FTL expression was reported as negative prognostic marker (353) and expression of FTH in cancer cells was shown to be a good indicator in treatment of breast cancer (354). Consistently, our results show decreased level of ferritin protein in our model of MCF7 spheres which is also in line with activation of the IRP/IRE system. The role of low ferritin level in maintenance of stem cell phenotype was supported by Lobello et al. (250), who showed that FTH is a negative regulator of ovarian CSCs expansion and EMT. Furthermore, FTH silenced MCF7 cells show EMT phenotype accompanied by increased level of ROS (249) which is in agreement with data obtained in our model. On the other hand, work of Schonberg et al. (248) reports glioblastoma CSCs depending on ferritin expression to propagate and form tumour, pointing to tissue dependent role of ferritin in cancer progression.

Another protein regulated by IRP/IRE system is the DMT1 which is involved in iron transport from gut lumen into enterocytes but also from acidic environment of lysosomes to cytoplasm; and as discussed above, DMT1 has also been implicated in the uptake of NTBI (316). Reports about DMT1 in cancer are scare with few showing high DMT1 expression in oesophageal adenocarcinoma, hepatocellular carcinoma and colorectal cancer (355–357). Unexpectedly, while we detected upregulation of *DMT1* mRNA level, protein level was much lower in our sphere model of CSCs. Since the activity of IRP should stabilise *DMT1* mRNA level, there must be some other post-transcriptional mechanism repressing its translation into protein or some post-translational process leading to DMT1 protein degradation. In neurons, DMT1 protein is targeted for proteasomal degradation in response to high iron levels (358). Since we detected higher LIP, it is possible that similar phenomenon is occurring in our model. The higher iron uptake through TfR1 and lower DMT1 protein level in spheres suggest that iron might remain locked in endosomes after TfR1 endocytosis and it is unable to enter cytosol, which could explain the activation of IRP/IRE system together with simultaneous accumulation of iron within mitochondria. In developing erythroid cells and also in non-erythroid cells, iron is transferred directly from transferrin-containing endosomes to mitochondria by so called “kiss and run mechanism”, thus bypassing the oxygen-rich cytosol (179,359,360). It is possible that similar process is occurring also in our model of CSCs, explaining higher iron uptake, higher LIP locked in endosomes, activation of IRP/IRE system due to shortage of iron in cytosol and accumulation of iron within mitochondria.

Altogether, our work shows that CSCs represented by our sphere model exhibit massive changes related to iron metabolism, highlighting the importance of iron metabolism in context of tumour development and biology of CSCs. The main discoveries are summarised in Fig. 6.1., however the research covering the area of iron metabolism in cancer is still not fully elucidated due to the complexity of these mechanisms and requires further experimental work.

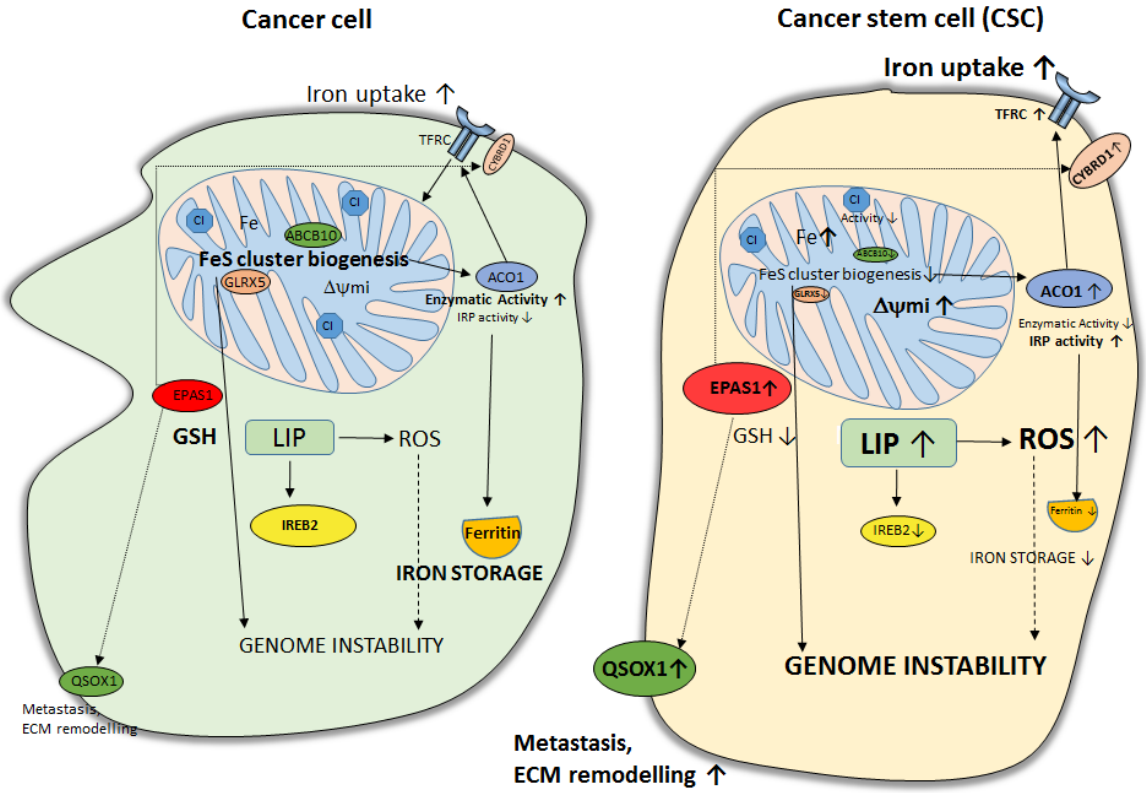


**Fig. 6.1. Scheme highlighting the changes in iron metabolism between cancer and cancer stem cells (CSC).** CSCs exhibit higher level of labile iron pool (LIP) and reactive oxygen species (ROS) together with lower reduced glutathione level (GSH). CSCs show defect in biogenesis of iron sulphur clusters (lower expression of ABCB10 and GLRX5) connected with mitochondrial iron accumulation and lower aconitase 1 (ACO1) and mitochondrial complex I (CI) activity, which may also affect genome stability and thus plasticity of CSCs. CSCs show activation of iron responsive element (IRP) connected with higher iron uptake by transferrin receptor (TfR1) and lower level of ferritin. CSCs exhibit also stabilization of hypoxia inducible factor-2α (HIF-2α, coded by *EPAS1* gene) followed by higher expression of HIF regulated gene QSOX1 involved in extracellular matrix (ECM) remodelling. CSCs have also higher level of CYBRD1 and lower level of IREB2 proteins. Figure adapted from (247).

# 7. SUMMARY

This work focus on the expression of ABC transporters in CSCs to reveal the most differentially expressed transporters for further study of their function in relation to the maintenance and biology of CSCs. Next, we focused on the regulation of ERα by miR-301a-3p in the context of CSCs and resistance. The last part of the thesis is then dedicated to the elucidation of iron metabolism in CSCs.

All specific aims presented in the chapter 3. have been achieved and conclusions derived from obtained data were published in two scientific papers (see List of publications), which form the basis of this work and where the author of this thesis is first author and shared first author. However this work also shows some data which have not been published yet, but indeed broadens our understanding of the biology of CSCs. The conclusions which reflect the specific aims asked in the chapter 3. are:

1) We document that both methods generates spheres whereas the expression of CSC and EMT markers such as *CD44*, *ABCG2*, *CXCR4*, *CDH2* and *SOX2* is more profound with the approach based on culturing cells in media without serum supplemented with proliferation supplement, EGF, FGF and heparin.

2) Elucidation of the mechanisms of resistance in CSCs

    a. Our sphere model of CSCs derived from T47D and MCF7 cells exhibit resistance to daunorubicin and doxorubicin and CSCs derived from MCF7, T47D and BT474 cells show a decrease in viability when exposed to ABCC1 and ABCG2 inhibitors.

    b. The most significantly upregulated ABC transporters on mRNA level in our model of prostate and breast CSCs are *ABCA1*, *ABCA3*, *ABCA5*, *ABCA12*, *ABCA13*, *ABCB7*, *ABCB9*, *ABCB10*, *ABCC1*, *ABCC2*, *ABCC3*, *ABCC5, ABCC8*, *ABCC10*, *ABCC11* and *ABCG2*.

    c. Our model of breast CSCs exhibit higher protein level of ABCB8, ABCC1, ABCC2, ABCC10 and ABCG2 transporters. On the other hand, we detected a decrease in protein level of ABCB10 and ABCF2 transporters.

d. MiR-301a-3p is highly expressed in our model of breast CSCs which exhibit inhibition of ER signalling.

e. MiR-301a-3p inhibits ER signalling by direct inhibition of *ESR1* mRNA translation in ER positive breast cancer cell lines and decreases sensitivity of oestrogen dependent MCF7 cell line to 17-β $E_2$.

f. Mir-301a-3p inhibits growth of the tumour derived from oestrogen dependent MCF7 cell line in nude mice, yet miR-301a-3p overexpressing tumours increase the expression of genes related to CSC and EMT phenotype. Moreover, miR-301a-3p expression negatively correlates with *ESR1* expression in biopsies from patient with breast cancer.

3) Elucidation of iron metabolism in CSCs

a. CSCs derived from MCF7 cell lines exhibit higher LIP, iron uptake with predominant iron accumulation in mitochondria and are more sensitive to iron chelation.

b. CSCs derived from prostate and breast cancer cell lines show deregulation of genes related to iron metabolism, the most upregulated genes being *CYBRD1*, *TFRC*, *ACO1*, *IREB2*, *ABCB10*, *EPAS1*, *QSOX1*, *HEPH*, *HFE* while *GLRX5* is downregulated. These genes constitute the so called iron metabolism-related CSC gene signature and PCA based on expression of this signature clearly distinguishes CSC population from non-CSC population *in vitro*.

c. MCF7 spheres show significant upregulation of CYBRD1, ACO1, EPAS1, QSOX1, HEPH protein level and a decrease in IREB2, ABCB10, GLRX5, NRAMP2 and FLH1 protein expression.

d. MCF7 spheres show activation of IRP/IRE system, higher oxidative environment reflected by increased ROS generation, lower GSH level and lower GSH/GSSG ratio, a decrease in aconitase and mitochondrial CI activity and higher mitochondrial potential.

Taken together, our research provides evidence that CSCs are very plastic cells with highly diverse characteristics encompassing changes in iron metabolism and in the expression of ABC transporters and miRNAs, distinguishing them from normal cancer cells. Due to this plasticity, CSCs have unique properties enabling them to resist the chemotherapy and metastasise to various parts of the body. It is then of high clinical importance to fully clarify the biology of CSCs maintenance and self-renewal in order to be able to effectively fight against cancer.

# 8. REFERENCES


1. Miller KD, Siegel RL, Lin CC, Mariotto AB, Kramer JL, Rowland JH, et al. Cancer treatment and survivorship statistics, 2016. CA Cancer J Clin. 2016 Jul;66(4):271–89.

2. Nassar D, Blanpain C. Cancer Stem Cells: Basic Concepts and Therapeutic Implications. Annu Rev Pathol Mech Dis. 2016 May 23;11(1):47–76.

3. Alferez DG, Simões BM, Howell SJ, Clarke RB. The Role of Steroid Hormones in Breast and Effects on Cancer Stem Cells. Curr Stem Cell Reports. 2018 Mar 13;4(1):81–94.

4. Guttilla IK, Adams BD, White BA. ERa, microRNAs, and the epithelial– mesenchymal transition in breast cancer. Trends Endocrinol Metab. 2011;23:73–82.

5. Abbaspour N, Hurrell R, Kelishadi R. Review on iron and its importance for human health. J Res Med Sci. Wolters Kluwer -- Medknow Publications; 2014 Feb;19(2):164–74.

6. Torti S V., Torti FM. Iron and cancer: more ore to be mined. Nat Rev Cancer. 2013 Apr 18;13(5):342–55.

7. Zhou L, Zhao B, Zhang L, Wang S, Dong D, Lv H, et al. Alterations in Cellular Iron Metabolism Provide More Therapeutic Opportunities for Cancer. Int J Mol Sci. 2018 May 22;19(5):1545.

8. Noulsri E, Richardson DR, Lerdwana S, Fucharoen S, Yamagishi T, Kalinowski DS, et al. Antitumor activity and mechanism of action of the iron chelator, Dp44mT, against leukemic cells. Am J Hematol. 2009 Mar;84(3):170–6.

9. Chitambar CR, Antholine WE. Iron-Targeting Antitumor Activity of Gallium Compounds and Novel Insights Into Triapine ® -Metal Complexes. Antioxid Redox Signal. 2013 Mar 10;18(8):956–72.

10. Mansoori B, Mohammadi A, Davudian S, Shirjang S, Baradaran B. The Different Mechanisms of Cancer Drug Resistance: A Brief Review. Adv Pharm Bull. 2017 Sep 25;7(3):339–48.

11. Pan S-T, Li Z-L, He Z-X, Qiu J-X, Zhou S-F. Molecular mechanisms for tumour resistance to chemotherapy. Clin Exp Pharmacol Physiol. 2016 Aug;43(8):723–37.

12. Balkwill FR, Capasso M, Hagemann T. The tumor microenvironment at a glance. J Cell Sci. 2012 Dec 1;125(Pt 23):5591–6.

13. Burrell RA, McGranahan N, Bartek J, Swanton C. The causes and consequences of genetic heterogeneity in cancer evolution. Nature. 2013 Sep 19;501(7467):338–45.

14. Bakhoum SF, Landau DA. Chromosomal Instability as a Driver of Tumor Heterogeneity and Evolution. Cold Spring Harb Perspect Med. 2017 Jun 1;7(6):a029611.

15. Gordon DJ, Resio B, Pellman D. Causes and consequences of aneuploidy in cancer. Nat Rev Genet. 2012 Mar 24;13(3):189–203.

16. Greaves M, Maley CC. Clonal evolution in cancer. Nature. 2012 Jan 19;481(7381):306–13.

17. Wang Y, Waters J, Leung ML, Unruh A, Roh W, Shi X, et al. Clonal evolution in breast cancer revealed by single nucleus genome sequencing. Nature. 2014 Aug 30;512(7513):155–60.

18. Ding L, Ley TJ, Larson DE, Miller CA, Koboldt DC, Welch JS, et al. Clonal evolution in relapsed acute myeloid leukaemia revealed by whole-genome sequencing. Nature. 2012 Jan 11;481(7382):506–10.

19. Wang J, Ma Y, Cooper MK. Cancer stem cells in glioma: challenges and opportunities. Transl Cancer Res. 2013 Oct 1;2(5):429–41.

20. Beck B, Blanpain C. Unravelling cancer stem cell potential. Nat Rev Cancer. 2013;13(10):727–38.

21. Meacham CE, Morrison SJ. Tumour heterogeneity and cancer cell plasticity. Nature. Howard Hughes Medical Institute; 2013 Sep 19;501(7467):328–37.

22. Siegel RL, Miller KD, Jemal A. Cancer statistics, 2017. CA Cancer J Clin. 2017 Jan 1;67(1):7–30.

23. Schnitt SJ. Classification and prognosis of invasive breast cancer: from morphology to molecular taxonomy. Mod Pathol. 2010 May 3;23(S2):S60–4.

24. Onitilo AA, Engel JM, Greenlee RT, Mukesh BN. Breast cancer subtypes based on ER/PR and Her2 expression: comparison of clinicopathologic features and survival. Clin Med Res. Marshfield Clinic; 2009 Jun 1;7(1–2):4–13.

25. Curtis C, Shah SP, Chin S-F, Turashvili G, Rueda OM, Dunning MJ, et al. The genomic and transcriptomic architecture of 2,000 breast tumours reveals novel subgroups. Nature. 2012 Apr 18;486(7403):346–52.

26. Kennecke H, Yerushalmi R, Woods R, Cheang MCU, Voduc D, Speers CH, et al. Metastatic behavior of breast cancer subtypes. J Clin Oncol. 2010;28(20):3271–7.

27. Nilsson S, Mäkelä S, Treuter E, Tujague M, Thomsen J, Andersson G, et al. Mechanisms of estrogen action. Physiol Rev. 2001 Oct;81(4):1535–65.

28. Stingl J. Estrogen and Progesterone in Normal Mammary Gland Development and in Cancer. Horm

Cancer. 2011 Apr 16;2(2):85–90.

29. Huang B, Omoto Y, Iwase H, Yamashita H, Toyama T, Coombes RC, et al. Differential expression of estrogen receptor α, β1, and β2 in lobular and ductal breast cancer. Proc Natl Acad Sci U S A. National Academy of Sciences; 2014 Feb 4;111(5):1933–8.

30. Wei X-L, Dou X-W, Bai J-W, Luo X-R, Qiu S-Q, Xi D-D, et al. ERα inhibits epithelial-mesenchymal transition by suppressing Bmi1 in breast cancer. Oncotarget. 2015 Aug 6;6(25):21704–17.

31. Ye Y, Xiao Y, Wang W, Yearsley K, Gao JX, Shetuni B, et al. ERα signaling through slug regulates E-cadherin and EMT. Oncogene. 2010 Mar 11;29(10):1451–62.

32. McDonnell DP, Wardell SE, Norris JD. Oral Selective Estrogen Receptor Downregulators (SERDs), a Breakthrough Endocrine Therapy for Breast Cancer. J Med Chem. 2015 Jun 25;58(12):4883–7.

33. Early Breast Cancer Trialists' Collaborative Group (EBCTCG). Effects of chemotherapy and hormonal therapy for early breast cancer on recurrence and 15-year survival: an overview of the randomised trials. Lancet. 2005 May;365(9472):1687–717.

34. Tamoxifen for early breast cancer: an overview of the randomised trials. Early Breast Cancer Trialists' Collaborative Group. Lancet. 1998 May 16;351(9114):1451–67.

35. Giacinti L, Claudio PP, Lopez M, Giordano A. Epigenetic Information and Estrogen Receptor Alpha Expression in Breast Cancer. Oncologist. 2006 Jan 1;11(1):1–8.

36. Tang Z, Treilleux I, Brown M. A transcriptional enhancer required for the differential expression of the human estrogen receptor in breast cancers. Mol Cell Biol. 1997 Mar 1;17(3):1274–80.

37. Karnik PS, Kulkarni S, Liu XP, Budd GT, Bukowski RM. Estrogen receptor mutations in tamoxifen-resistant breast cancer. Cancer Res. 1994 Jan 15;54(2):349–53.

38. Shi L, Dong B, Li Z, Lu Y, Ouyang T, Li J, et al. Expression of ER-α36, a Novel Variant of Estrogen Receptor α, and Resistance to Tamoxifen Treatment in Breast Cancer. J Clin Oncol. 2009 Jul 20;27(21):3423–9.

39. Le Romancer M, Poulard C, Cohen P, Sentis S, Renoir J-M, Corbo L. Cracking the estrogen receptor's posttranslational code in breast tumors. Endocr Rev. 2011 Oct;32(5):597–622.

40. Iorio M V, Ferracin M, Liu C-G, Veronese A, Spizzo R, Sabbioni S, et al. MicroRNA Gene Expression Deregulation in Human Breast Cancer. Cancer Res. 2005;65(16):7065–70.

41. Blanpain C, Fuchs E. Stem cell plasticity. Plasticity of epithelial stem cells in tissue regeneration. Science. 2014 Jun 13;344(6189):1242281.

42. Lapidot T, Sirard C, Vormoor J, Murdoch B, Hoang T, Caceres-Cortes J, et al. A cell initiating human acute myeloid leukaemia after transplantation into SCID mice. Nature. 1994 Feb 17;367(6464):645–8.

43. Bonnet D, Dick JE. Human acute myeloid leukemia is organized as a hierarchy that originates from a primitive hematopoietic cell. Nat Med. 1997 Jul;3(7):730–7.

44. Ishizawa K, Rasheed ZA, Karisch R, Wang Q, Kowalski J, Susky E, et al. Tumor-Initiating Cells Are Rare in Many Human Tumors. Cell Stem Cell. 2010 Sep 3;7(3):279–82.

45. Al-Hajj M, Wicha MS, Benito-Hernandez A, Morrison SJ, Clarke MF. Prospective identification of tumorigenic breast cancer cells. Proc Natl Acad Sci U S A. 2003 Apr 1;100(7):3983–8.

46. Ginestier C, Hur MH, Charafe-Jauffret E, Monville F, Dutcher J, Brown M, et al. ALDH1 is a marker of normal and malignant human mammary stem cells and a predictor of poor clinical outcome. Cell Stem Cell. 2007 Nov;1(5):555–67.

47. Li C, Heidt DG, Dalerba P, Burant CF, Zhang L, Adsay V, et al. Identification of Pancreatic Cancer Stem Cells. Cancer Res. 2007 Feb 1;67(3):1030–7.

48. Singh SK, Hawkins C, Clarke ID, Squire JA, Bayani J, Hide T, et al. Identification of human brain tumour initiating cells. Nature. 2004 Nov 18;432(7015):396–401.

49. O'Brien CA, Pollett A, Gallinger S, Dick JE. A human colon cancer cell capable of initiating tumour growth in immunodeficient mice. Nature. 2007 Jan 19;445(7123):106–10.

50. Collins AT, Berry PA, Hyde C, Stower MJ, Maitland NJ. Prospective identification of tumorigenic prostate cancer stem cells. Cancer Res. 2005 Dec 1;65(23):10946–51.

51. Boiko AD, Razorenova O V, van de Rijn M, Swetter SM, Johnson DL, Ly DP, et al. Human melanoma-initiating cells express neural crest nerve growth factor receptor CD271. Nature. 2010 Jul 1;466(7302):133–7.

52. Zhang S, Balch C, Chan MW, Lai H-C, Matei D, Schilder JM, et al. Identification and Characterization of Ovarian Cancer-Initiating Cells from Primary Human Tumors. Cancer Res. 2008 Jun 1;68(11):4311–20.

53. Clarke MF, Dick JE, Dirks PB, Eaves CJ, Jamieson CHM, Jones DL, et al. Cancer Stem Cells—Perspectives on Current Status and Future Directions: AACR Workshop on Cancer Stem Cells. Cancer Res. 2006 Oct 1;66(19):9339–44.

54. Polyak K, Weinberg RA. Transitions between epithelial and mesenchymal states: acquisition of

malignant and stem cell traits. Nat Rev Cancer. 2009 Apr 5;9(4):265–73.

55. Chaffer CL, Weinberg RA. A Perspective on Cancer Cell Metastasis. Science (80- ). 2011 Mar 25;331(6024):1559–64.

56. Mani SA, Guo W, Liao M-J, Eaton EN, Ayyanan A, Zhou AY, et al. The Epithelial-Mesenchymal Transition Generates Cells with Properties of Stem Cells. Cell. 2008 May 16;133(4):704–15.

57. Puisieux A, Brabletz T, Caramel J. Oncogenic roles of EMT-inducing transcription factors. Nat Cell Biol. 2014 Jun 1;16(6):488–94.

58. Dieter SM, Ball CR, Hoffmann CM, Nowrouzi A, Herbst F, Zavidij O, et al. Distinct types of tumor-initiating cells form human colon cancer tumors and metastases. Cell Stem Cell. 2011 Oct 4;9(4):357–65.

59. Lawson DA, Bhakta NR, Kessenbrock K, Prummel KD, Yu Y, Takai K, et al. Single-cell analysis reveals a stem-cell program in human metastatic breast cancer cells. Nature. 2015 Oct 1;526(7571):131–5.

60. Gundem G, Van Loo P, Kremeyer B, Alexandrov LB, Tubio JMC, Papaemmanuil E, et al. The evolutionary history of lethal metastatic prostate cancer. Nature. 2015 Apr 1;520(7547):353–7.

61. Celià-Terrassa T, Kang Y. Distinctive properties of metastasis-initiating cells. Genes Dev. Cold Spring Harbor Laboratory Press; 2016 Apr 15;30(8):892–908.

62. Abubaker K, Latifi A, Luwor R, Nazaretian S, Zhu H, Quinn MA, et al. Short-term single treatment of chemotherapy results in the enrichment of ovarian cancer stem cell-like cells leading to an increased tumor burden. Mol Cancer. 2013 Mar 27;12(1):24.

63. Bao S, Wu Q, McLendon RE, Hao Y, Shi Q, Hjelmeland AB, et al. Glioma stem cells promote radioresistance by preferential activation of the DNA damage response. Nature. 2006 Dec 7;444(7120):756–60.

64. Dylla SJ, Beviglia L, Park I-K, Chartier C, Raval J, Ngan L, et al. Colorectal cancer stem cells are enriched in xenogeneic tumors following chemotherapy. Gilliland DG, editor. PLoS One. 2008 Jun 18;3(6):e2428.

65. Dembinski JL, Krauss S. Characterization and functional analysis of a slow cycling stem cell-like subpopulation in pancreas adenocarcinoma. Clin Exp Metastasis. 2009 Oct 7;26(7):611–23.

66. Roesch A, Fukunaga-Kalabis M, Schmidt EC, Zabierowski SE, Brafford PA, Vultur A, et al. A temporarily distinct subpopulation of slow-cycling melanoma cells is required for continuous tumor

growth. Cell. 2010 May 14;141(4):583–94.

67. Gao M-Q, Choi Y-P, Kang S, Youn JH, Cho N-H. CD24+ cells from hierarchically organized ovarian cancer are enriched in cancer stem cells. Oncogene. 2010 May 6;29(18):2672–80.

68. Wang X, Ma Z, Xiao Z, Liu H, Dou Z, Feng X, et al. Chk1 knockdown confers radiosensitization in prostate cancer stem cells. Oncol Rep. 2012 Dec;28(6):2247–54.

69. Gallmeier E, Hermann PC, Mueller M-T, Machado JG, Ziesch A, De Toni EN, et al. Inhibition of ataxia telangiectasia- and Rad3-related function abrogates the in vitro and in vivo tumorigenicity of human colon cancer cells through depletion of the CD133(+) tumor-initiating cell fraction. Stem Cells. 2011 Mar;29(3):418–29.

70. Diehn M, Cho RW, Lobo NA, Kalisky T, Dorie MJ, Kulp AN, et al. Association of reactive oxygen species levels and radioresistance in cancer stem cells. Nature. NIH Public Access; 2009 Apr 9;458(7239):780–3.

71. Qi L, Bellail AC, Rossi MR, Zhang Z, Pang H, Hunter S, et al. Heterogeneity of primary glioblastoma cells in the expression of caspase-8 and the response to TRAIL-induced apoptosis. Apoptosis. 2011 Nov 30;16(11):1150–64.

72. Madjd Z, Mehrjerdi AZ, Sharifi AM, Molanaei S, Shahzadi SZ, Asadi-Lari M. CD44+ cancer cells express higher levels of the anti-apoptotic protein Bcl-2 in breast tumours. Cancer Immun. 2009 Apr 23;9:4.

73. Siebzehnrubl FA, Silver DJ, Tugertimur B, Deleyrolle LP, Siebzehnrubl D, Sarkisian MR, et al. The ZEB1 pathway links glioblastoma initiation, invasion and chemoresistance. EMBO Mol Med. 2013 Aug;5(8):1196–212.

74. Takebe N, Miele L, Harris PJ, Jeong W, Bando H, Kahn M, et al. Targeting Notch, Hedgehog and Wnt pathways in cancer stem cells: clinical update. Nat Rev Clin Oncol. 2015 Aug 7;12(8):445–64.

75. Karamboulas C, Ailles L. Developmental signaling pathways in cancer stem cells of solid tumors. Biochim Biophys Acta - Gen Subj. 2013 Feb;1830(2):2481–95.

76. Albini A, Bruno A, Gallo C, Pajardi G, Noonan DM, Dallaglio K. Cancer stem cells and the tumor microenvironment: interplay in tumor heterogeneity. Connect Tissue Res. 2015 Sep 3;56(5):414–25.

77. Korkaya H, Liu S, Wicha MS. Breast cancer stem cells, cytokine networks, and the tumor microenvironment. J Clin Invest. 2011 Oct 3;121(10):3804–9.

78. Samanta D, Gilkes DM, Chaturvedi P, Xiang L, Semenza GL. Hypoxia-inducible factors are required

for chemotherapy resistance of breast cancer stem cells. Proc Natl Acad Sci. 2014 Dec 16;111(50):E5429–38.

79. Marie-Egyptienne DT, Lohse I, Hill RP. Cancer stem cells, the epithelial to mesenchymal transition (EMT) and radioresistance: Potential role of hypoxia. Cancer Lett. 2013 Nov 28;341(1):63–72.

80. Hu Y-Y, Fu L-A, Li S-Z, Chen Y, Li J-C, Han J, et al. Hif-1α and Hif-2α differentially regulate Notch signaling through competitive interaction with the intracellular domain of Notch receptors in glioma stem cells. Cancer Lett. 2014 Jul 10;349(1):67–76.

81. LIU H-L, LIU D, DING G-R, LIAO P-F, ZHANG J-W. Hypoxia-inducible factor-1α and Wnt/β-catenin signaling pathways promote the invasion of hypoxic gastric cancer cells. Mol Med Rep. 2015 Sep;12(3):3365–73.

82. Bijlsma MF, Groot AP, Oduro JP, Franken RJ, Schoenmakers SHHF, Peppelenbosch MP, et al. Hypoxia induces a hedgehog response mediated by HIF-1α. J Cell Mol Med. 2009 Aug 2;13(8b):2053–60.

83. Dean M, Fojo T, Bates S. Tumour stem cells and drug resistance. Nat Rev Cancer. 2005 Apr;5(4):275–84.

84. Kim M, Turnquist H, Jackson J, Sgagias M, Yan Y, Gong M, et al. The multidrug resistance transporter ABCG2 (breast cancer resistance protein 1) effluxes Hoechst 33342 and is overexpressed in hematopoietic stem cells. Clin Cancer Res. 2002 Jan;8(1):22–8.

85. Bleau A-M, Hambardzumyan D, Ozawa T, Fomchenko EI, Huse JT, Brennan CW, et al. PTEN/PI3K/Akt pathway regulates the side population phenotype and ABCG2 activity in glioma tumor stem-like cells. Cell Stem Cell. 2009 Mar 6;4(3):226–35.

86. Ma I, Allan AL. The Role of Human Aldehyde Dehydrogenase in Normal and Cancer Stem Cells. Stem Cell Rev Reports. 2011 Jun 20;7(2):292–306.

87. Singh S, Brocker C, Koppaka V, Chen Y, Jackson BC, Matsumoto A, et al. Aldehyde dehydrogenases in cellular responses to oxidative/electrophilic stress. Free Radic Biol Med. 2013 Mar;56:89–101.

88. Cojoc M, Mäbert K, Muders MH, Dubrovska A. A role for cancer stem cells in therapy resistance: Cellular and molecular mechanisms. Semin Cancer Biol. 2015 Apr;31:16–27.

89. Bartel DP. MicroRNAs: genomics, biogenesis, mechanism, and function. Cell. 2004 Jan 23;116(2):281–97.

90. Lee Y, Kim M, Han J, Yeom K-H, Lee S, Baek SH, et al. MicroRNA genes are transcribed by RNA

polymerase II. EMBO J. 2004 Oct 13;23(20):4051–60.

91. Gregory RI, Yan K, Amuthan G, Chendrimada T, Doratotaj B, Cooch N, et al. The Microprocessor complex mediates the genesis of microRNAs. Nature. 2004 Nov 11;432(7014):235–40.

92. Lund E, Güttinger S, Calado A, Dahlberg JE, Kutay U. Nuclear Export of MicroRNA Precursors. Science (80- ). 2004 Jan 2;303(5654):95–8.

93. Hutvágner G, McLachlan J, Pasquinelli AE, Bálint E, Tuschl T, Zamore PD. A cellular function for the RNA-interference enzyme Dicer in the maturation of the let-7 small temporal RNA. Science. 2001 Aug 3;293(5531):834–8.

94. Gregory RI, Chendrimada TP, Cooch N, Shiekhattar R. Human RISC couples microRNA biogenesis and posttranscriptional gene silencing. Cell. 2005 Nov 18;123(4):631–40.

95. Xu W, Wang Z, Liu Y. The Characterization of microRNA-Mediated Gene Regulation as Impacted by Both Target Site Location and Seed Match Type. Preiss T, editor. PLoS One. Public Library of Science; 2014 Jan;9(9):e108260.

96. Hon LS, Zhang Z. The roles of binding site arrangement and combinatorial targeting in microRNA repression of gene expression. Genome Biol. 2007 Jan;8(8):R166.

97. Tsang J, Zhu J, van Oudenaarden A. MicroRNA-mediated feedback and feedforward loops are recurrent network motifs in mammals. Mol Cell. 2007 Jun 8;26(5):753–67.

98. Babashah S, Soleimani M. The oncogenic and tumour suppressive roles of microRNAs in cancer and apoptosis. Eur J Cancer. Pergamon; 2011 May 1;47(8):1127–37.

99. Iorio M V, Croce CM. microRNA involvement in human cancer. Carcinogenesis. 2012 Jun;33(6):1126–33.

100. Sun X, Jiao X, Pestell TG, Fan C, Qin S, Mirabelli E, et al. MicroRNAs and cancer stem cells: the sword and the shield. Oncogene. 2014 Oct 18;33(42):4967–77.

101. Liu Y, Li H, Feng J, Cui X, Huang W, Li Y, et al. Lin28 Induces Epithelial-to-Mesenchymal Transition and Stemness via Downregulation of Let-7a in Breast Cancer Cells. Sarkar FH, editor. PLoS One. 2013 Dec 11;8(12):e83083.

102. Yu F, Yao H, Zhu P, Zhang X, Pan Q, Gong C, et al. let-7 Regulates Self Renewal and Tumorigenicity of Breast Cancer Cells. Cell. 2007 Dec 14;131(6):1109–23.

103. Wang T, Wang G, Hao D, Liu X, Wang D, Ning N, et al. Aberrant regulation of the LIN28A/LIN28B and let-7 loop in human malignant tumors and its effects on the hallmarks of cancer. Mol Cancer. 2015

Dec 30;14(1):125.

104. Chien C-S, Wang M-L, Chu P-Y, Chang Y-L, Liu W-H, Yu C-C, et al. Lin28B/Let-7 Regulates Expression of Oct4 and Sox2 and Reprograms Oral Squamous Cell Carcinoma Cells to a Stem-like State. Cancer Res. 2015 Jun 15;75(12):2553–65.

105. Liu C, Kelnar K, Liu B, Chen X, Calhoun-Davis T, Li H, et al. The microRNA miR-34a inhibits prostate cancer stem cells and metastasis by directly repressing CD44. Nat Med. 2011 Feb 16;17(2):211–5.

106. Ji Q, Hao X, Zhang M, Tang W, Yang M, Li L, et al. MicroRNA miR-34 Inhibits Human Pancreatic Cancer Tumor-Initiating Cells. Bernhard EJ, editor. PLoS One. 2009 Aug 28;4(8):e6816.

107. Choi YJ, Lin C-P, Ho JJ, He X, Okada N, Bu P, et al. miR-34 miRNAs provide a barrier for somatic cell reprogramming. Nat Cell Biol. 2011 Oct 23;13(11):1353–60.

108. Korpal M, Lee ES, Hu G, Kang Y. The miR-200 Family Inhibits Epithelial-Mesenchymal Transition and Cancer Cell Migration by Direct Targeting of E-cadherin Transcriptional Repressors *ZEB1* and *ZEB2*. J Biol Chem. 2008 May 30;283(22):14910–4.

109. Shimono Y, Zabala M, Cho RW, Lobo N, Dalerba P, Qian D, et al. Downregulation of miRNA-200c links breast cancer stem cells with normal stem cells. Cell. 2009 Aug 7;138(3):592–603.

110. Bracken CP, Gregory PA, Kolesnikoff N, Bert AG, Wang J, Shannon MF, et al. A Double-Negative Feedback Loop between ZEB1-SIP1 and the microRNA-200 Family Regulates Epithelial-Mesenchymal Transition. Cancer Res. 2008 Oct 1;68(19):7846–54.

111. Garofalo M, Croce CM. MicroRNAs as therapeutic targets in chemoresistance. Drug Resist Updat. 2013 Jul;16(3–5):47–59.

112. Zhang P, Wang L, Rodriguez-Aguayo C, Yuan Y, Debeb BG, Chen D, et al. miR-205 acts as a tumour radiosensitizer by targeting ZEB1 and Ubc13. Nat Commun. 2014 Dec 5;5:5671.

113. Chang C-J, Chao C-H, Xia W, Yang J-Y, Xiong Y, Li C-W, et al. p53 regulates epithelial-mesenchymal transition and stem cell properties through modulating miRNAs. Nat Cell Biol. 2011 Mar 20;13(3):317–23.

114. Selcuklu SD, Donoghue MTA, Spillane C. *miR-21* as a key regulator of oncogenic processes. Biochem Soc Trans. 2009 Aug 1;37(4):918–25.

115. Chen Z, Chen L-Y, Dai H-Y, Wang P, Gao S, Wang K. miR-301a promotes pancreatic cancer cell proliferation by directly inhibiting Bim expression. J Cell Biochem. 2012 Oct 1;113(10):3229–35.

116. Shi W, Gerster K, Alajez NM, Tsang J, Waldron L, Pintilie M, et al. MicroRNA-301 mediates proliferation and invasion in human breast cancer. Cancer Res. 2011 Apr 15;71(8):2926–37.

117. Wang M, Li C, Yu B, Su L, Li J, Ju J, et al. Overexpressed miR-301a promotes cell proliferation and invasion by targeting RUNX3 in gastric cancer. J Gastroenterol. Springer Japan; 2013 Sep 1;48(9):1023–33.

118. Fang Y, Sun B, Xiang J, Chen Z. MiR-301a Promotes Colorectal Cancer Cell Growth and Invasion by Directly Targeting SOCS6. Cell Physiol Biochem. 2015 Jan;35(1):227–36.

119. Zhou P, Chang R, Jiang W, Wu L, Wu K, Wang Z. MiR-301a is a candidate oncogene that targets the homeobox gene gax in human hepatocellular carcinoma. Dig Dis Sci. 2012 May 29;57(5):1171–80.

120. Structural and functional organization of the Ska complex, a key component of the kinetochore-microtubule interface.pdf.crdownload.

121. Cao G, Huang B, Liu Z, Zhang J, Xu H, Xia W, et al. Intronic miR-301 feedback regulates its host gene, ska2, in A549 cells by targeting MEOX2 to affect ERK/CREB pathways. Biochem Biophys Res Commun. Elsevier Inc.; 2010 Jun 11;396(4):978–82.

122. Ma F, Zhang J, Zhong L, Wang L, Liu Y, Wang Y, et al. Upregulated microRNA-301a in breast cancer promotes tumor metastasis by targeting PTEN and activating Wnt/β-catenin signaling. Gene. 2014 Feb 10;535(2):191–7.

123. Lu Z, Li Y, Takwi A, Li B, Zhang J, Conklin DJ, et al. miR-301a as an NF-κB activator in pancreatic cancer cells. EMBO J. 2011 Jan 5;30(1):57–67.

124. Zhang Y-K, Wang Y-J, Gupta P, Chen Z-S. Multidrug Resistance Proteins (MRPs) and Cancer Therapy. AAPS J. 2015;17(4):802–12.

125. Perria CL, Rajamanickam V, Lapinski PE, Raghavan M. Catalytic Site Modifications of TAP1 and TAP2 and Their Functional Consequences. J Biol Chem. 2006 Dec 29;281(52):39839–51.

126. Gordillo GM, Biswas A, Khanna S, Spieldenner JM, Pan X, Sen CK. Multidrug Resistance-associated Protein-1 (MRP-1)-dependent Glutathione Disulfide (GSSG) Efflux as a Critical Survival Factor for Oxidant-enriched Tumorigenic Endothelial Cells. J Biol Chem. 2016 May 6;291(19):10089–103.

127. Tsuchida M, Emi Y, Kida Y, Sakaguchi M. Human ABC transporter isoform B6 (ABCB6) localizes primarily in the Golgi apparatus. Biochem Biophys Res Commun. 2008 May 2;369(2):369–75.

128. Schaedler TA, Faust B, Shintre CA, Carpenter EP, Srinivasan V, van Veen HW, et al. Structures and functions of mitochondrial ABC transporters. Biochem Soc Trans. 2015 Oct 1;43(5):943–51.

129. Chapuy B, Koch R, Radunski U, Corsham S, Cheong N, Inagaki N, et al. Intracellular ABC transporter A3 confers multidrug resistance in leukemia cells by lysosomal drug sequestration. Leukemia. 2008 Aug 8;22(8):1576–86.

130. Robey RW, Pluchino KM, Hall MD, Fojo AT, Bates SE, Gottesman MM. Revisiting the role of ABC transporters in multidrug-resistant cancer. Nat Rev Cancer. 2018 Apr 11;

131. Dean M, Rzhetsky A, Allikmets R. The human ATP-binding cassette (ABC) transporter superfamily. Genome Res. 2001 Jul;11(7):1156–66.

132. Albrecht C, Viturro E. The ABCA subfamily--gene and protein structures, functions and associated hereditary diseases. Pflugers Arch. 2007 Feb;453(5):581–9.

133. Zhou S-F. Structure, function and regulation of P-glycoprotein and its clinical relevance in drug disposition. Xenobiotica. 2008 Aug 22;38(7–8):802–32.

134. Zhao C, Haase W, Tampé R, Abele R. Peptide specificity and lipid activation of the lysosomal transport complex ABCB9 (TAPL). J Biol Chem. 2008 Jun 20;283(25):17083–91.

135. Dikkers A, Tietge U-J. Biliary cholesterol secretion: more than a simple ABC. World J Gastroenterol. 2010 Dec 21;16(47):5936–45.

136. Gadsby DC, Vergani P, Csanády L. The ABC protein turned chloride channel whose failure causes cystic fibrosis. Nature. NIH Public Access; 2006 Mar 23;440(7083):477–83.

137. Nichols CG. KATP channels as molecular sensors of cellular metabolism. Nature. 2006 Mar 23;440(7083):470–6.

138. Kawaguchi K, Morita M. ABC Transporter Subfamily D: Distinct Differences in Behavior between ABCD1–3 and ABCD4 in Subcellular Localization, Function, and Human Disease. Biomed Res Int. 2016;2016:1–11.

139. Barthelme D, Scheele U, Dinkelaker S, Janoschka A, Macmillan F, Albers S-V, et al. Structural organization of essential iron-sulfur clusters in the evolutionarily highly conserved ATP-binding cassette protein ABCE1. J Biol Chem. 2007 May 11;282(19):14598–607.

140. Wilcox SM, Arora H, Munro L, Xin J, Fenninger F, Johnson LA, et al. The role of the innate immune response regulatory gene ABCF1 in mammalian embryogenesis and development. Tian X, editor. PLoS One. 2017 May 19;12(5):e0175918.

141. Sag D, Cekic C, Wu R, Linden J, Hedrick CC. The cholesterol transporter ABCG1 links cholesterol homeostasis and tumour immunity. Nat Commun. 2015 Dec 27;6(1):6354.

142. Mo W, Zhang J-T. Human ABCG2: structure, function, and its role in multidrug resistance. Int J Biochem Mol Biol. 2012;3(1):1–27.

143. Patel SB, Graf G, Temel R. ABCG5 and ABCG8: More than a defense against xenosterols. J Lipid Res. 2018 May 4;jlr.R084244.

144. Szakács G, Annereau J-P, Lababidi S, Shankavaram U, Arciello A, Bussey KJ, et al. Predicting drug sensitivity and resistance: profiling ABC transporter genes in cancer cells. Cancer Cell. 2004 Aug;6(2):129–37.

145. Fletcher JI, Williams RT, Henderson MJ, Norris MD, Haber M. ABC transporters as mediators of drug resistance and contributors to cancer cell biology. Drug Resist Updat. 2016 May;26:1–9.

146. Marzac C, Garrido E, Tang R, Fava F, Hirsch P, De Benedictis C, et al. ATP Binding Cassette transporters associated with chemoresistance: transcriptional profiling in extreme cohorts and their prognostic impact in a cohort of 281 acute myeloid leukemia patients. Haematologica. 2011 Sep 1;96(9):1293–301.

147. Ueda K, Cornwell MM, Gottesman MM, Pastan I, Roninson IB, Ling V, et al. The mdr1 gene, responsible for multidrug-resistance, codes for P-glycoprotein. Biochem Biophys Res Commun. 1986 Dec 30;141(3):956–62.

148. Trock BJ, Leonessa F, Clarke R. Multidrug resistance in breast cancer: a meta-analysis of MDR1/gp170 expression and its possible functional significance. J Natl Cancer Inst. 1997 Jul 2;89(13):917–31.

149. Doyle LA, Yang W, Abruzzo L V, Krogmann T, Gao Y, Rishi AK, et al. A multidrug resistance transporter from human MCF-7 breast cancer cells. Proc Natl Acad Sci U S A. 1998;95(26):15665–70.

150. Cole SP, Bhardwaj G, Gerlach JH, Mackie JE, Grant CE, Almquist KC, et al. Overexpression of a transporter gene in a multidrug-resistant human lung cancer cell line. Science. 1992 Dec 4;258(5088):1650–4.

151. Cole SPC, Deeley RG. Transport of glutathione and glutathione conjugates by MRP1. Trends Pharmacol Sci. 2006 Aug;27(8):438–46.

152. Ding X, Wu J, Jiang C. ABCG2: A potential marker of stem cells and novel target in stem cell and cancer therapy. Life Sci. 2010 Apr 24;86(17–18):631–7.

153. Yoh K, Ishii G, Yokose T, Minegishi Y, Tsuta K, Goto K, et al. Breast cancer resistance protein impacts clinical outcome in platinum-based chemotherapy for advanced non-small cell lung cancer. Clin

Cancer Res. 2004 Mar 1;10(5):1691–7.

154. Sugano T, Seike M, Noro R, Soeno C, Chiba M, Zou F, et al. Inhibition of ABCB1 Overcomes Cancer Stem Cell-like Properties and Acquired Resistance to MET Inhibitors in Non-Small Cell Lung Cancer. Mol Cancer Ther. 2015 Nov 1;14(11):2433–40.

155. Huang B, Fu SJ, Fan WZ, Wang ZH, Chen Z Bin, Guo SJ, et al. PKCε inhibits isolation and stemness of side population cells via the suppression of ABCB1 transporter and PI3K/Akt, MAPK/ERK signaling in renal cell carcinoma cell line 769P. Cancer Lett. 2016 Jun 28;376(1):148–54.

156. Schatton T, Murphy GF, Frank NY, Yamaura K, Waaga-Gasser AM, Gasser M, et al. Identification of cells initiating human melanomas. Nature. 2008 Jan 17;451(7176):345–9.

157. Sims-Mourtada J, Izzo JG, Ajani J, Chao KSC. Sonic Hedgehog promotes multiple drug resistance by regulation of drug transport. Oncogene. 2007 Aug 16;26(38):5674–9.

158. Bhattacharya S, Das A, Mallya K, Ahmad I. Maintenance of retinal stem cells by Abcg2 is regulated by notch signaling. J Cell Sci. 2007 Aug 1;120(Pt 15):2652–62.

159. Oliveira BR, Figueiredo MA, Trindade GS, Marins LF. OCT4 mutations in human erythroleukemic cells: implications for multiple drug resistance (MDR) phenotype. Mol Cell Biochem. 2015 Feb;400(1–2):41–50.

160. Haber M, Smith J, Bordow SB, Flemming C, Cohn SL, London WB, et al. Association of high-level MRP1 expression with poor clinical outcome in a large prospective study of primary neuroblastoma. J Clin Oncol. 2006 Apr 1;24(10):1546–53.

161. Porro A, Haber M, Diolaiti D, Iraci N, Henderson M, Gherardi S, et al. Direct and coordinate regulation of ATP-binding cassette transporter genes by Myc factors generates specific transcription signatures that significantly affect the chemoresistance phenotype of cancer cells. J Biol Chem. 2010 Jun 18;285(25):19532–43.

162. Fletcher JI, Haber M, Henderson MJ, Norris MD. ABC transporters in cancer: more than just drug efflux pumps. Nat Rev Cancer. 2010 Feb 15;10(2):147–56.

163. van de Ven R, Oerlemans R, van der Heijden JW, Scheffer GL, de Gruijl TD, Jansen G, et al. ABC drug transporters and immunity: novel therapeutic targets in autoimmunity and cancer. J Leukoc Biol. 2009 Nov;86(5):1075–87.

164. Palmeira A, Sousa E, Vasconcelos MH, Pinto MM. Three decades of P-gp inhibitors: skimming through several generations and scaffolds. Curr Med Chem. 2012;19(13):1946–2025.

165. Jaramillo AC, Al Saig F, Cloos J, Jansen G, Peters GJ. Review Open Access Cancer Drug Resistance How to overcome ATP-binding cassette drug efflux transporter-mediated drug resistance? Cancer Drug Resist. 2018;1:6–29.

166. Bystrom LM, Guzman ML, Rivella S. Iron and Reactive Oxygen Species: Friends or Foes of Cancer Cells? Antioxid Redox Signal. 2014 Apr 20;20(12):1917–24.

167. Minotti G, Aust SD. The role of iron in oxygen radical mediated lipid peroxidation. Chem Biol Interact. 1989;71(1):1–19.

168. Puig S, Ramos-Alonso L, Romero AM, Martínez-Pastor MT. The elemental role of iron in DNA synthesis and repair. Metallomics. 2017 Sep 7;

169. Gunshin H, Mackenzie B, Berger U V., Gunshin Y, Romero MF, Boron WF, et al. Cloning and characterization of a mammalian proton-coupled metal-ion transporter. Nature. 1997 Jul 31;388(6641):482–8.

170. McKie AT, Barrow D, Latunde-Dada GO, Rolfs A, Sager G, Mudaly E, et al. An Iron-Regulated Ferric Reductase Associated with the Absorption of Dietary Iron. Science (80- ). 2001 Mar 2;291(5509):1755–9.

171. Raffin SB, Woo CH, Roost KT, Price DC, Schmid R. Intestinal Absorption of Hemoglobin Iron-Heme Cleavage by Mucosal Heme Oxygenase. J Clin Invest. 1974 Dec 1;54(6):1344–52.

172. Ma Y, Yeh M, Yeh K-Y, Glass J. Iron Imports. V. Transport of iron through the intestinal epithelium. Am J Physiol Gastrointest Liver Physiol. 2006 Mar;290(3):G417-22.

173. Donovan A, Lima CA, Pinkus JL, Pinkus GS, Zon LI, Robine S, et al. The iron exporter ferroportin/Slc40a1 is essential for iron homeostasis. Cell Metab. 2005 Mar;1(3):191–200.

174. Vashchenko G, MacGillivray R. Multi-Copper Oxidases and Human Iron Metabolism. Nutrients. 2013 Jun 27;5(7):2289–313.

175. Brissot P, Ropert M, Le Lan C, Loréal O. Non-transferrin bound iron: A key role in iron overload and iron toxicity. Biochim Biophys Acta - Gen Subj. 2012 Mar;1820(3):403–10.

176. Harding C, Heuser J, Stahl P. Receptor-mediated endocytosis of transferrin and recycling of the transferrin receptor in rat reticulocytes. J Cell Biol. 1983 Aug;97(2):329–39.

177. Ohgami RS, Campagna DR, Greer EL, Antiochos B, McDonald A, Chen J, et al. Identification of a ferrireductase required for efficient transferrin-dependent iron uptake in erythroid cells. Nat Genet. 2005 Nov 16;37(11):1264–9.

178. Fleming MD, Romano MA, Su MA, Garrick LM, Garrick MD, Andrews NC. Nramp2 is mutated in the anemic Belgrade (b) rat: evidence of a role for Nramp2 in endosomal iron transport. Proc Natl Acad Sci U S A. 1998 Feb 3;95(3):1148–53.

179. Hamdi A, Roshan TM, Kahawita TM, Mason AB, Sheftel AD, Ponka P. Erythroid cell mitochondria receive endosomal iron by a "kiss-and-run" mechanism. Biochim Biophys Acta - Mol Cell Res. 2016 Dec;1863(12):2859–67.

180. Mühlenhoff U, Hoffmann B, Richter N, Rietzschel N, Spantgar F, Stehling O, et al. Compartmentalization of iron between mitochondria and the cytosol and its regulation. Eur J Cell Biol. 2015 Jul;94(7–9):292–308.

181. Simcox JA, McClain DA. Iron and Diabetes Risk. Cell Metab. 2013 Mar 5;17(3):329–41.

182. Dautry-Varsat A, Ciechanover A, Lodish HF. pH and the recycling of transferrin during receptor-mediated endocytosis. Proc Natl Acad Sci U S A. 1983 Apr;80(8):2258–62.

183. Trinder D, Baker E. Transferrin receptor 2: a new molecule in iron metabolism. Int J Biochem Cell Biol. 2003 Mar;35(3):292–6.

184. Sheokand N, Kumar S, Malhotra H, Tillu V, Raje CI, Raje M. Secreted glyceraldehye-3-phosphate dehydrogenase is a multifunctional autocrine transferrin receptor for cellular iron acquisition. Biochim Biophys Acta - Gen Subj. 2013 Jun;1830(6):3816–27.

185. Jenkitkasemwong S, Wang C-Y, Coffey R, Zhang W, Chan A, Biel T, et al. SLC39A14 Is Required for the Development of Hepatocellular Iron Overload in Murine Models of Hereditary Hemochromatosis. Cell Metab. 2015 Jul 7;22(1):138–50.

186. Leidgens S, Bullough KZ, Shi H, Li F, Shakoury-Elizeh M, Yabe T, et al. Each member of the poly-r(C)-binding protein 1 (PCBP) family exhibits iron chaperone activity toward ferritin. J Biol Chem. 2013 Jun 14;288(24):17791–802.

187. Yanatori I, Richardson DR, Imada K, Kishi F. Iron Export through the Transporter Ferroportin 1 Is Modulated by the Iron Chaperone PCBP2. J Biol Chem. 2016 Aug 12;291(33):17303–18.

188. Nandal A, Ruiz JC, Subramanian P, Ghimire-Rijal S, Sinnamon RA, Stemmler TL, et al. Activation of the HIF prolyl hydroxylase by the iron chaperones PCBP1 and PCBP2. Cell Metab. 2011 Nov 2;14(5):647–57.

189. Arosio P, Carmona F, Gozzelino R, Maccarinelli F, Poli M. The importance of eukaryotic ferritins in iron handling and cytoprotection. Biochem J. 2015 Nov 15;472(1):1–15.

190. Theil EC. Ferritin: the protein nanocage and iron biomineral in health and in disease. Inorg Chem. 2013 Nov 4;52(21):12223–33.

191. Nemeth E, Tuttle MS, Powelson J, Vaughn MB, Donovan A, Ward DM, et al. Hepcidin Regulates Cellular Iron Efflux by Binding to Ferroportin and Inducing Its Internalization. Science (80- ). 2004 Dec 17;306(5704):2090–3.

192. Singh B, Arora S, Agrawal P, Gupta SK. Hepcidin: A novel peptide hormone regulating iron metabolism. Clin Chim Acta. 2011 May 12;412(11–12):823–30.

193. Wang R-H, Li C, Xu X, Zheng Y, Xiao C, Zerfas P, et al. A role of SMAD4 in iron metabolism through the positive regulation of hepcidin expression. Cell Metab. 2005 Dec;2(6):399–409.

194. Andriopoulos Jr B, Corradini E, Xia Y, Faasse SA, Chen S, Grgurevic L, et al. BMP6 is a key endogenous regulator of hepcidin expression and iron metabolism. Nat Genet. 2009 Apr 1;41(4):482–7.

195. Corradini E, Meynard D, Wu Q, Chen S, Ventura P, Pietrangelo A, et al. Serum and liver iron differently regulate the bone morphogenetic protein 6 (BMP6)-SMAD signaling pathway in mice. Hepatology. 2011 Jul;54(1):273–84.

196. Babitt JL, Huang FW, Wrighting DM, Xia Y, Sidis Y, Samad TA, et al. Bone morphogenetic protein signaling by hemojuvelin regulates hepcidin expression. Nat Genet. 2006 May 9;38(5):531–9.

197. Silvestri L, Pagani A, Nai A, De Domenico I, Kaplan J, Camaschella C. The serine protease matriptase-2 (TMPRSS6) inhibits hepcidin activation by cleaving membrane hemojuvelin. Cell Metab. 2008 Dec;8(6):502–11.

198. McDonald CJ, Wallace DF, Ostini L, Subramaniam VN. Parenteral vs. oral iron: influence on hepcidin signaling pathways through analysis of Hfe/Tfr2-null mice. Am J Physiol Gastrointest Liver Physiol. 2014 Jan 15;306(2):G132-9.

199. Crownover BK, Covey CJ. Hereditary hemochromatosis. Am Fam Physician. 2013 Feb 1;87(3):183–90.

200. Goswami T, Andrews NC. Hereditary hemochromatosis protein, HFE, interaction with transferrin receptor 2 suggests a molecular mechanism for mammalian iron sensing. J Biol Chem. 2006 Sep 29;281(39):28494–8.

201. Theil EC. The IRE (iron regulatory element) family: structures which regulate mRNA translation or stability. Biofactors. 1993 May;4(2):87–93.

202. Aziz N, Munro HN. Iron regulates ferritin mRNA translation through a segment of its 5' untranslated region. Proc Natl Acad Sci U S A. 1987 Dec;84(23):8478–82.

203. Zoller H, Theurl I, Koch R, Kaser A, Weiss G. Mechanisms of iron mediated regulation of the duodenal iron transporters divalent metal transporter 1 and ferroportin 1. Blood Cells Mol Dis. 29(3):488–97.

204. Müllner EW, Kühn LC. A stem-loop in the 3' untranslated region mediates iron-dependent regulation of transferrin receptor mRNA stability in the cytoplasm. Cell. 1988 Jun 3;53(5):815–25.

205. Role of the Ferroportin Iron-Responsive Element in Iron and Nitric Oxide Dependent Gene Regulation. Blood Cells, Mol Dis. Academic Press; 2002 Nov 1;29(3):315–26.

206. Harford JB, Klausner RD. Coordinate post-transcriptional regulation of ferritin and transferrin receptor expression: the role of regulated RNA-protein interaction. Enzyme. 1990;44(1–4):28–41.

207. Bhasker CR, Burgiel G, Neupert B, Emery-Goodman A, Kühn LC, May BK. The putative iron-responsive element in the human erythroid 5-aminolevulinate synthase mRNA mediates translational control. J Biol Chem. 1993 Jun 15;268(17):12699–705.

208. Sanchez M, Galy B, Muckenthaler MU, Hentze MW. Iron-regulatory proteins limit hypoxia-inducible factor-2alpha expression in iron deficiency. Nat Struct Mol Biol. 2007 May 8;14(5):420–6.

209. Zheng L, Kennedy MC, Blondin GA, Beinert H, Zalkin H. Binding of cytosolic aconitase to the iron responsive element of porcine mitochondrial aconitase mRNA. Arch Biochem Biophys. 1992 Dec;299(2):356–60.

210. Rogers JT, Randall JD, Cahill CM, Eder PS, Huang X, Gunshin H, et al. An iron-responsive element type II in the 5'-untranslated region of the Alzheimer's amyloid precursor protein transcript. J Biol Chem. American Society for Biochemistry and Molecular Biology; 2002 Nov 22;277(47):45518–28.

211. Cmejla R, Petrak J, Cmejlova J. A novel iron responsive element in the 3'UTR of human MRCKalpha. Biochem Biophys Res Commun. 2006 Mar 3;341(1):158–66.

212. Sanchez M, Galy B, Dandekar T, Bengert P, Vainshtein Y, Stolte J, et al. Iron regulation and the cell cycle: identification of an iron-responsive element in the 3'-untranslated region of human cell division cycle 14A mRNA by a refined microarray-based screening strategy. J Biol Chem. 2006 Aug 11;281(32):22865–74.

213. Sanchez M, Galy B, Schwanhaeusser B, Blake J, Bähr-Ivacevic T, Benes V, et al. Iron regulatory protein-1 and -2: transcriptome-wide definition of binding mRNAs and shaping of the cellular proteome by iron regulatory proteins. Blood. 2011 Nov 24;118(22):e168-79.

214. Gruer MJ, Artymiuk PJ, Guest JR. The aconitase family: three structural variations on a common theme. Trends Biochem Sci. 1997 Jan;22(1):3–6.

215. Voet D, Voet JG. Biochemistry. 3rd ed. Harris D, Fitzgerald P, editors. New York: Wiley; 2004.

216. Brazzolotto X, Timmins P, Dupont Y, Moulis J-M. Structural Changes Associated with Switching Activities of Human Iron Regulatory Protein 1. J Biol Chem. 2002 Apr 5;277(14):11995–2000.

217. Guo B, Yu Y, Leibold EA. Iron regulates cytoplasmic levels of a novel iron-responsive element-binding protein without aconitase activity. J Biol Chem. 1994 Sep 30;269(39):24252–60.

218. Anderson CP, Shen M, Eisenstein RS, Leibold EA. Mammalian iron metabolism and its control by iron regulatory proteins. Biochim Biophys Acta - Mol Cell Res. 2012 Sep;1823(9):1468–83.

219. Pantopoulos K. Iron metabolism and the IRE/IRP regulatory system: an update. Ann N Y Acad Sci. 2004 Mar;1012:1–13.

220. Bouton C, Drapier J-C. Iron regulatory proteins as NO signal transducers. Sci STKE. 2003 May 13;2003(182):pe17.

221. Clarke SL, Vasanthakumar A, Anderson SA, Pondarré C, Koh CM, Deck KM, et al. Iron-responsive degradation of iron-regulatory protein 1 does not require the Fe–S cluster. EMBO J. 2006 Feb 8;25(3):544–53.

222. Deck KM, Vasanthakumar A, Anderson SA, Goforth JB, Kennedy MC, Antholine WE, et al. Evidence That Phosphorylation of Iron Regulatory Protein 1 at Serine 138 Destabilizes the [4Fe-4S] Cluster in Cytosolic Aconitase by Enhancing 4Fe-3Fe Cycling. J Biol Chem. 2009 May 8;284(19):12701–9.

223. Fillebeen C, Caltagirone A, Martelli A, Moulis J-M, Pantopoulos K. IRP1 Ser-711 is a phosphorylation site, critical for regulation of RNA-binding and aconitase activities. Biochem J. 2005 May 15;388(Pt 1):143–50.

224. Vashisht AA, Zumbrennen KB, Huang X, Powers DN, Durazo A, Sun D, et al. Control of iron homeostasis by an iron-regulated ubiquitin ligase. Science. 2009 Oct 30;326(5953):718–21.

225. Salahudeen AA, Thompson JW, Ruiz JC, Ma H-W, Kinch LN, Li Q, et al. An E3 ligase possessing an iron-responsive hemerythrin domain is a regulator of iron homeostasis. Science. 2009 Oct 30;326(5953):722–6.

226. Beinert H, Holm RH, Münck E. Iron-sulfur clusters: nature's modular, multipurpose structures. Science. 1997 Aug 1;277(5326):653–9.

227. Mühlenhoff U, Balk J, Richhardt N, Kaiser JT, Sipos K, Kispal G, et al. Functional Characterization

of the Eukaryotic Cysteine Desulfurase Nfs1p from *Saccharomyces cerevisiae*. J Biol Chem. 2004 Aug 27;279(35):36906–15.

228. Mueller EG. Trafficking in persulfides: delivering sulfur in biosynthetic pathways. Nat Chem Biol. 2006 Apr;2(4):185–94.

229. Teralı K, Beavil RL, Pickersgill RW, van der Giezen M. The effect of the adaptor protein Isd11 on the quaternary structure of the eukaryotic cysteine desulphurase Nfs1. Biochem Biophys Res Commun. 2013 Oct 18;440(2):235–40.

230. Webert H, Freibert S-A, Gallo A, Heidenreich T, Linne U, Amlacher S, et al. Functional reconstitution of mitochondrial Fe/S cluster synthesis on Isu1 reveals the involvement of ferredoxin. Nat Commun. 2014 Oct 31;5:5013.

231. Parent A, Elduque X, Cornu D, Belot L, Le Caer J-P, Grandas A, et al. Mammalian frataxin directly enhances sulfur transfer of NFS1 persulfide to both ISCU and free thiols. Nat Commun. 2015 Jan 19;6:5686.

232. Stemmler TL, Lesuisse E, Pain D, Dancis A. Frataxin and Mitochondrial FeS Cluster Biogenesis. J Biol Chem. 2010 Aug 27;285(35):26737–43.

233. Rouault TA. Mammalian iron–sulphur proteins: novel insights into biogenesis and function. Nat Rev Mol Cell Biol. 2014 Nov 26;16(1):45–55.

234. Maio N, Kim KS, Singh A, Rouault TA. A Single Adaptable Cochaperone-Scaffold Complex Delivers Nascent Iron-Sulfur Clusters to Mammalian Respiratory Chain Complexes I–III. Cell Metab. 2017 Apr 4;25(4):945–953.e6.

235. Uzarska MA, Dutkiewicz R, Freibert S-A, Lill R, Mühlenhoff U. The mitochondrial Hsp70 chaperone Ssq1 facilitates Fe/S cluster transfer from Isu1 to Grx5 by complex formation. Mol Biol Cell. 2013 Jun 15;24(12):1830–41.

236. Sheftel AD, Wilbrecht C, Stehling O, Niggemeyer B, Elsasser H-P, Muhlenhoff U, et al. The human mitochondrial ISCA1, ISCA2, and IBA57 proteins are required for [4Fe-4S] protein maturation. Mol Biol Cell. 2012 Apr 1;23(7):1157–66.

237. Cai K, Liu G, Frederick RO, Xiao R, Montelione GT, Markley JL. Structural/Functional Properties of Human NFU1, an Intermediate [4Fe-4S] Carrier in Human Mitochondrial Iron-Sulfur Cluster Biogenesis. Structure. 2016 Dec 6;24(12):2080–91.

238. Lill R, Dutkiewicz R, Freibert SA, Heidenreich T, Mascarenhas J, Netz DJ, et al. The role of mitochondria and the CIA machinery in the maturation of cytosolic and nuclear iron–sulfur proteins.

Eur J Cell Biol. 2015;94(7–9):280–91.

239. Sharma AK, Pallesen LJ, Spang RJ, Walden WE. Cytosolic Iron-Sulfur Cluster Assembly (CIA) System: Factors, Mechanism, and Relevance to Cellular Iron Regulation. J Biol Chem. 2010 Aug 27;285(35):26745–51.

240. Lee J-C, Chiang K-C, Feng T-H, Chen Y-J, Chuang S-T, Tsui K-H, et al. The Iron Chelator, Dp44mT, Effectively Inhibits Human Oral Squamous Cell Carcinoma Cell Growth in Vitro and in Vivo. Int J Mol Sci. 2016 Aug 31;17(9):1435.

241. Jansson PJ, Hawkins CL, Lovejoy DB, Richardson DR. The iron complex of Dp44mT is redox-active and induces hydroxyl radical formation: an EPR study. J Inorg Biochem. 2010 Nov;104(11):1224–8.

242. Becton DL, Bryles P. Deferoxamine inhibition of human neuroblastoma viability and proliferation. Cancer Res. 1988 Dec 15;48(24 Pt 1):7189–92.

243. Yamasaki T, Saeki I, Sakaida I. Efficacy of iron chelator deferoxamine for hepatic arterial infusion chemotherapy in advanced hepatocellular carcinoma patients refractory to current treatments. Hepatol Int. 2014 Sep 29;8(S2):492–8.

244. Daniels TR, Bernabeu E, Rodríguez JA, Patel S, Kozman M, Chiappetta DA, et al. The transferrin receptor and the targeted delivery of therapeutic agents against cancer. Biochim Biophys Acta - Gen Subj. 2012 Mar;1820(3):291–317.

245. Louandre C, Ezzoukhry Z, Godin C, Barbare J-C, Mazière J-C, Chauffert B, et al. Iron-dependent cell death of hepatocellular carcinoma cells exposed to sorafenib. Int J Cancer. 2013 Oct 1;133(7):1732–42.

246. Kovar J, Naumann PW, Stewart BC, Kemp JD. Differing Sensitivity of Non-Hematopoietic Human Tumors to Synergistic Anti-Transferrin Receptor Monoclonal Antibodies and Deferoxamine in vitro. Pathobiology. 1995;63(2):65–70.

247. Rychtarcikova Z, Lettlova S, Tomkova V, Korenkova V, Langerova L, Simonova E, et al. Tumor-initiating cells of breast and prostate origin show alterations in the expression of genes related to iron metabolism. Oncotarget. 2017;8(4).

248. Schonberg DL, Miller TE, Wu Q, Flavahan WA, Das NK, Hale JS, et al. Preferential Iron Trafficking Characterizes Glioblastoma Stem-like Cells. Cancer Cell. 2015;28(4):441–55.

249. Aversa I, Zolea F, Ieranò C, Bulotta S, Trotta AM, Faniello MC, et al. Epithelial-to-mesenchymal transition in FHC-silenced cells: the role of CXCR4/CXCL12 axis. J Exp Clin Cancer Res. 2017 Dec 3;36(1):104.

250. Lobello N, Biamonte F, Pisanu ME, Faniello MC, Jakopin Ž, Chiarella E, et al. Ferritin heavy chain is a negative regulator of ovarian cancer stem cell expansion and epithelial to mesenchymal transition. Oncotarget. 2016 Sep 20;7(38):62019–33.

251. Chanvorachote P, Luanpitpong S. Iron induces cancer stem cells and aggressive phenotypes in human lung cancer cells. Am J Physiol Physiol. 2016 May 1;310(9):C728–39.

252. Guo W, Zhang S, Chen Y, Zhang D, Yuan L, Cong H, et al. An important role of the hepcidin-ferroportin signaling in affecting tumor growth and metastasis. Acta Biochim Biophys Sin (Shanghai). 2015 Sep;47(9):703–15.

253. Epsztejn S, Kakhlon O, Glickstein H, Breuer W, Cabantchik I. Fluorescence analysis of the labile iron pool of mammalian cells. Anal Biochem. 1997 May 15;248(1):31–40.

254. Schmitt S, Saathoff F, Meissner L, Schropp E-M, Lichtmannegger J, Schulz S, et al. A semi-automated method for isolating functionally intact mitochondria from cultured cells and tissue biopsies. Anal Biochem. 2013 Dec 1;443(1):66–74.

255. Oliveira L, Drapier J-C. Down-regulation of iron regulatory protein 1 gene expression by nitric oxide. Proc Natl Acad Sci. 2000 Jun 6;97(12):6550–5.

256. Christova T, Templeton DM. Effect of hypoxia on the binding and subcellular distribution of iron regulatory proteins. Mol Cell Biochem. 2007 Jul 4;301(1–2):21–32.

257. Brynychová V, Hlaváč V, Ehrlichová M, Václavíková R, Pecha V, Trnková M, et al. Importance of transcript levels of caspase-2 isoforms S and L for breast carcinoma progression. Future Oncol. 2013 Mar;9(3):427–38.

258. Tavassoli FA, Devilee P. Pathology and genetics: tumours of the breast and female genital organs. 4th ed. Lyon: IARC Press; 2003.

259. Chen S-F, Chang Y-C, Nieh S, Liu C-L, Yang C-Y, Lin Y-S. Nonadhesive culture system as a model of rapid sphere formation with cancer stem cell properties. Singh SR, editor. PLoS One. 2012 Feb 16;7(2):e31864.

260. Stapelberg M, Zobalova R, Nguyen MN, Walker T, Stantic M, Goodwin J, et al. Indoleamine-2,3-dioxygenase elevated in tumor-initiating cells is suppressed by mitocans. Free Radic Biol Med. 2014 Feb;67:41–50.

261. Borgna S, Armellin M, di Gennaro A, Maestro R, Santarosa M. Mesenchymal traits are selected along with stem features in breast cancer cells grown as mammospheres. Cell Cycle. 2014 Nov 3;11(22):4242–51.

262. Xu X-D, He X-J, Tao H-Q, Zhang W, Wang Y-Y, Ye Z-Y, et al. Abnormal expression of miR-301a in gastric cancer associated with progression and poor prognosis. J Surg Oncol. 2013 Sep 1;108(3):197–202.

263. Nam RK, Benatar T, Wallis CJD, Amemiya Y, Yang W, Garbens A, et al. MiR-301a regulates E-cadherin expression and is predictive of prostate cancer recurrence. Prostate. 2016;76(10):869–84.

264. Dontu G, El-Ashry D, Wicha MS. Breast cancer, stem/progenitor cells and the estrogen receptor. Trends Endocrinol Metab. 2004 Jul;15(5):193–7.

265. Lin C-Y, Ström A, Vega VB, Kong SL, Yeo AL, Thomsen JS, et al. Discovery of estrogen receptor alpha target genes and response elements in breast tumor cells. Genome Biol. 2004 Jan;5(9):R66.

266. Feoktistova M, Geserick P, Leverkus M. Crystal Violet Assay for Determining Viability of Cultured Cells. Cold Spring Harb Protoc. 2016 Apr 1;2016(4):pdb.prot087379.

267. Vashisht AA, Zumbrennen KB, Huang X, Powers DN, Durazo A, Sun D, et al. Control of Iron Homeostasis by an Iron-Regulated Ubiquitin Ligase. Science (80- ). 2009 Oct 30;326(5953):718–21.

268. Chen W, Dailey HA, Paw BH, Ajioka R, Phillips J, Kushner J, et al. Ferrochelatase forms an oligomeric complex with mitoferrin-1 and Abcb10 for erythroid heme biosynthesis. Blood. American Society of Hematology; 2010 Jul 29;116(4):628–30.

269. Yamamoto M, Arimura H, Fukushige T, Minami K, Nishizawa Y, Tanimoto A, et al. Abcb10 Role in Heme Biosynthesis In Vivo: Abcb10 Knockout in Mice Causes Anemia with Protoporphyrin IX and Iron Accumulation. Mol Cell Biol. American Society for Microbiology; 2014 Mar 15;34(6):1077–84.

270. Presnell CE, Bhatti G, Numan LS, Lerche M, Alkhateeb SK, Ghalib M, et al. Computational insights into the role of glutathione in oxidative stress. Curr Neurovasc Res. 2013 May;10(2):185–94.

271. Anderson SA, Nizzi CP, Chang Y-I, Deck KM, Schmidt PJ, Galy B, et al. The IRP1-HIF-2α Axis Coordinates Iron and Oxygen Sensing with Erythropoiesis and Iron Absorption. Cell Metab. 2013 Feb 5;17(2):282–90.

272. Mansfield KD, Guzy RD, Pan Y, Young RM, Cash TP, Schumacker PT, et al. Mitochondrial dysfunction resulting from loss of cytochrome c impairs cellular oxygen sensing and hypoxic HIF-α activation. Cell Metab. 2005 Jun;1(6):393–9.

273. Lake DF, Faigel DO. The Emerging Role of QSOX1 in Cancer. Antioxid Redox Signal. 2014;21(3):485–96.

274. Agudo A, Bonet C, Sala N, Muñoz X, Aranda N, Fonseca-Nunes A, et al. Hemochromatosis (HFE)

gene mutations and risk of gastric cancer in the European Prospective Investigation into Cancer and Nutrition (EPIC) study. Carcinogenesis. 2013 Jun 1;34(6):1244–50.

275. Begicevic R-R, Falasca M. ABC Transporters in Cancer Stem Cells: Beyond Chemoresistance. Int J Mol Sci. 2017 Nov 8;18(11):2362.

276. Dean M. ABC Transporters, Drug Resistance, and Cancer Stem Cells. J Mammary Gland Biol Neoplasia. 2009 Mar 18;14(1):3–9.

277. Colak S, Medema JP. Cancer stem cells - important players in tumor therapy resistance. FEBS J. 2014 Nov;281(21):4779–91.

278. Stolarczyk EI, Reiling CJ, Paumi CM. Regulation of ABC transporter function via phosphorylation by protein kinases. Curr Pharm Biotechnol. NIH Public Access; 2011 Apr;12(4):621–35.

279. Haenisch S, Nina Werk A, Cascorbi I. MicroRNAs and their relevance to ABC transporters. 2013;

280. Mutoh K, Tsukahara S, Mitsuhashi J, Katayama K, Sugimoto Y. Estrogen-mediated post transcriptional down-regulation of P-glycoprotein in MDR1-transduced human breast cancer cells. Cancer Sci. 2006 Nov;97(11):1198–204.

281. Hansen SN, Westergaard D, Thomsen MBH, Vistesen M, Do KN, Fogh L, et al. Acquisition of docetaxel resistance in breast cancer cells reveals upregulation of ABCB1 expression as a key mediator of resistance accompanied by discrete upregulation of other specific genes and pathways. Tumor Biol. 2015 Jun 18;36(6):4327–38.

282. Li W, Zhai B, Zhi H, Li Y, Jia L, Ding C, et al. Association of ABCB1, β tubulin I, and III with multidrug resistance of MCF7/DOC subline from breast cancer cell line MCF7. Tumor Biol. 2014 Sep 4;35(9):8883–91.

283. Vaidyanathan A, Sawers L, Gannon A-L, Chakravarty P, Scott AL, Bray SE, et al. ABCB1 (MDR1) induction defines a common resistance mechanism in paclitaxel- and olaparib-resistant ovarian cancer cells. Br J Cancer. 2016 Aug 14;115(4):431–41.

284. Zhang Y-K, Zhang G-N, Wang Y-J, Patel BA, Talele TT, Yang D-H, et al. Bafetinib (INNO-406) reverses multidrug resistance by inhibiting the efflux function of ABCB1 and ABCG2 transporters. Sci Rep. 2016 Sep 9;6(1):25694.

285. Taniguchi K, Wada M, Kohno K, Nakamura T, Kawabe T, Kawakami M, et al. A human canalicular multispecific organic anion transporter (cMOAT) gene is overexpressed in cisplatin-resistant human cancer cell lines with decreased drug accumulation. Cancer Res. 1996 Sep 15;56(18):4124–9.

286. Surowiak P, Materna V, Kaplenko I, Spaczynski M, Dolinska-Krajewska B, Gebarowska E, et al. ABCC2 (MRP2, cMOAT) Can Be Localized in the Nuclear Membrane of Ovarian Carcinomas and Correlates with Resistance to Cisplatin and Clinical Outcome. Clin Cancer Res. 2006 Dec 1;12(23):7149–58.

287. Maciejczyk A, Jagoda E, Wysocka T, Matkowski R, Györffy B, Lage H, et al. ABCC2 (MRP2, cMOAT) Localized in the Nuclear Envelope of Breast Carcinoma Cells Correlates with Poor Clinical Outcome. Pathol Oncol Res. 2012 Apr 11;18(2):331–42.

288. Sandusky GE, Mintze KS, Pratt SE, Dantzig AH. Expression of multidrug resistance-associated protein 2 (MRP2) in normal human tissues and carcinomas using tissue microarrays. Histopathology. 2002 Jul;41(1):65–74.

289. Kathawala RJ, Wang Y-J, Ashby Jr CR, Chen Z-S. Recent advances regarding the role of ABC subfamily C member 10 (ABCC10) in the efflux of antitumor drugs. Chin J Cancer. 2014 May 5;33(5):223–30.

290. Elliott AM, Al-Hajj MA. ABCB8 Mediates Doxorubicin Resistance in Melanoma Cells by Protecting the Mitochondrial Genome. Mol Cancer Res. 2009 Jan 1;7(1):79–87.

291. Tsuda H, Ito YM, Ohashi Y, Wong K-K, Hashiguchi Y, Welch WR, et al. Identification of Overexpression and Amplification of ABCF2 in Clear Cell Ovarian Adenocarcinomas by cDNA Microarray Analyses. Clin Cancer Res. 2005 Oct 1;11(19):6880–8.

292. Bao L, Wu J, Dodson M, Rojo de la Vega EM, Ning Y, Zhang Z, et al. *ABCF2* , an Nrf2 target gene, contributes to cisplatin resistance in ovarian cancer cells. Mol Carcinog. 2017 Jun;56(6):1543–53.

293. Ogawa Y, Tsuda H, Hai E, Tsuji N, Yamagata S, Tokunaga S, et al. Clinical role of ABCF2 expression in breast cancer. Anticancer Res. 26(3A):1809–14.

294. Roundhill E, Turnbull D, Burchill S. Localization of MRP-1 to the outer mitochondrial membrane by the chaperone protein HSP90. FASEB J. Federation of American Societies for Experimental Biology; 2016 May 1;30(5):1712–23.

295. Baker A, Carrier DJ, Schaedler T, Waterham HR, van Roermund CW, Theodoulou FL. Peroxisomal ABC transporters: functions and mechanism. Biochem Soc Trans. 2015 Oct 1;43(5):959–65.

296. Liang S-C, Yang C-Y, Tseng J-Y, Wang H-L, Tung C-Y, Liu H-W, et al. ABCG2 localizes to the nucleus and modulates CDH1 expression in lung cancer cells. Neoplasia. Neoplasia Press; 2015 Mar;17(3):265–78.

297. Cui L, Li Y, Lv X, Li J, Wang X, Lei Z, et al. Expression of MicroRNA-301a and its Functional Roles

in Malignant Melanoma. Cell Physiol Biochem. 2016;40(1–2):230–44.

298. Kuukasjärvi T, Kononen J, Helin H, Holli K, Isola J. Loss of estrogen receptor in recurrent breast cancer is associated with poor response to endocrine therapy. J Clin Oncol. 1996 Sep;14(9):2584–9.

299. Holdaway IM, Bowditch J V. Variation in receptor status between primary and metastatic breast cancer. Cancer. 1983 Aug 1;52(3):479–85.

300. Pogribny IP, Filkowski JN, Tryndyak VP, Golubov A, Shpyleva SI, Kovalchuk O. Alterations of microRNAs and their targets are associated with acquired resistance of MCF-7 breast cancer cells to cisplatin. Int J cancer. 2010 Oct 15;127(8):1785–94.

301. Pandey D, Picard D. miR-22 Inhibits Estrogen Signaling by Directly Targeting the Estrogen Receptor α mRNA. Mol Cell Biol. 2009;29(13):3783–90.

302. Adams BD, Furneaux H, White BA. The Micro-Ribonucleic Acid (miRNA) miR-206 Targets the Human Estrogen Receptor-α (ERα) and Represses ERα Messenger RNA and Protein Expression in Breast Cancer Cell Lines. Mol Endocrinol. 2007 May;21(5):1132–47.

303. Kondo N, Toyama T, Sugiura H, Fujii Y, Yamashita H. miR-206 Expression Is Down-regulated in Estrogen Receptor α–Positive Human Breast Cancer. Cancer Res. 2008;68(13):5004–8.

304. Spizzo R, Nicoloso MS, Lupini L, Lu Y, Fogarty J, Rossi S, et al. miR-145 participates with TP53 in a death-promoting regulatory loop and targets estrogen receptor-α in human breast cancer cells. Cell Death Differ. 2010 Feb 4;17(2):246–54.

305. Leivonen S-K, Mäkelä R, Östling P, Kohonen P, Haapa-Paananen S, Kleivi K, et al. Protein lysate microarray analysis to identify microRNAs regulating estrogen receptor signaling in breast cancer cell lines. Oncogene. 2009 Nov 5;28(44):3926–36.

306. Androsavich JR, Chau BN. Non-inhibited miRNAs shape the cellular response to anti-miR. Nucleic Acids Res. 2014 Jun 17;42(11):6945–55.

307. Gee JM, Robertson JF, Gutteridge E, Ellis IO, Pinder SE, Rubini M, et al. Epidermal growth factor receptor/HER2/insulin-like growth factor receptor signalling and oestrogen receptor activity in clinical breast cancer. Endocr Relat Cancer. 2005 Jul 1;12 Suppl 1(Supplement_1):S99–111.

308. Korkaya H, Paulson A, Iovino F, Wicha MS. HER2 regulates the mammary stem/progenitor cell population driving tumorigenesis and invasion. Oncogene. 2008 Oct 16;27(47):6120–30.

309. Liu S, Cong Y, Wang D, Sun Y, Deng L, Liu Y, et al. Breast Cancer Stem Cells Transition between Epithelial and Mesenchymal States Reflective of their Normal Counterparts. Stem Cell Reports.

2014;2(1):78–91.

310. Yu H, Li H, Qian H, Jiao X, Zhu X, Jiang X, et al. Upregulation of miR-301a correlates with poor prognosis in triple-negative breast cancer. Med Oncol. 2014 Nov;31(11):283.

311. Manz DH, Blanchette NL, Paul BT, Torti FM, Torti S V. Iron and cancer: recent insights. Ann N Y Acad Sci. NIH Public Access; 2016;1368(1):149–61.

312. Luo X, Hill M, Johnson A, Latunde-Dada GO. Modulation of Dcytb (Cybrd 1) expression and function by iron, dehydroascorbate and Hif-2α in cultured cells. Biochim Biophys Acta - Gen Subj. 2014 Jan;1840(1):106–12.

313. Lemler DJ, Lynch ML, Tesfay L, Deng Z, Paul BT, Wang X, et al. DCYTB is a predictor of outcome in breast cancer that functions via iron-independent mechanisms. Breast Cancer Res. 2017 Dec 7;19(1):25.

314. Peyssonnaux C, Nizet V, Johnson RS. Role of the hypoxia inducible factors HIF in iron metabolism. Cell Cycle. 2008 Jan 28;7(1):28–32.

315. Yanatori I, Kishi F. DMT1 and iron transport. Free Radic Biol Med. Pergamon; 2018 Jul 25;

316. Zhang A-S, Canonne-Hergaux F, Gruenheid S, Gros P, Ponka P. Use of Nramp2-transfected Chinese hamster ovary cells and reticulocytes from mk/mk mice to study iron transport mechanisms. Exp Hematol. Elsevier; 2008 Oct 1;36(10):1227–35.

317. Song J, Ge Z, Yang X, Luo Q, Wang C, You H, et al. Hepatic stellate cells activated by acidic tumor microenvironment promote the metastasis of hepatocellular carcinoma via osteopontin. Cancer Lett. 2015 Jan 28;356(2):713–20.

318. Wang C-Y, Knutson MD. Hepatocyte divalent metal-ion transporter-1 is dispensable for hepatic iron accumulation and non-transferrin-bound iron uptake in mice. Hepatology. 2013 Aug;58(2):788–98.

319. Zhao N, Zhang A-S, Worthen C, Knutson MD, Enns CA. An iron-regulated and glycosylation-dependent proteasomal degradation pathway for the plasma membrane metal transporter ZIP14. Proc Natl Acad Sci U S A. 2014 Jun 24;111(25):9175–80.

320. Liao Q-D, Wang C-G, Zhu Y-D, Chen W-H, Shao S-L, Jiang F-N, et al. Decreased expression of SLC39A14 is associated with tumor aggressiveness and biochemical recurrence of human prostate cancer. Onco Targets Ther. 2016;Volume 9:4197–205.

321. Franklin RB, Levy BA, Zou J, Hanna N, Desouki MM, Bagasra O, et al. ZIP14 zinc transporter downregulation and zinc depletion in the development and progression of hepatocellular cancer. J

Gastrointest Cancer. 2012 Jun 5;43(2):249–57.

322. Rouault TA. Mitochondrial iron overload: causes and consequences. Curr Opin Genet Dev. 2016 Jun;38:31–7.

323. Ye H, Jeong SY, Ghosh MC, Kovtunovych G, Silvestri L, Ortillo D, et al. Glutaredoxin 5 deficiency causes sideroblastic anemia by specifically impairing heme biosynthesis and depleting cytosolic iron in human erythroblasts. J Clin Invest. 2010 May 3;120(5):1749–61.

324. Paul VD, Lill R. Biogenesis of cytosolic and nuclear iron–sulfur proteins and their role in genome stability. Biochim Biophys Acta - Mol Cell Res. 2015 Jun;1853(6):1528–39.

325. Bao B, Azmi AS, Li Y, Ahmad A, Ali S, Banerjee S, et al. Targeting CSCs in tumor microenvironment: the potential role of ROS-associated miRNAs in tumor aggressiveness. Curr Stem Cell Res Ther. 2014 Jan;9(1):22–35.

326. Rhyu DY, Yang Y, Ha H, Lee GT, Song JS, Uh S, et al. Role of Reactive Oxygen Species in TGF- 1-Induced Mitogen-Activated Protein Kinase Activation and Epithelial-Mesenchymal Transition in Renal Tubular Epithelial Cells. J Am Soc Nephrol. 2005 Feb 9;16(3):667–75.

327. Zhang K-H, Tian H-Y, Gao X, Lei W-W, Hu Y, Wang D-M, et al. Ferritin heavy chain-mediated iron homeostasis and subsequent increased reactive oxygen species production are essential for epithelial-mesenchymal transition. Cancer Res. 2009;69(13):5340–8.

328. Kim B, Jung JW, Jung J, Han Y, Suh DH, Kim HS, et al. PGC1α induced by reactive oxygen species contributes to chemoresistance of ovarian cancer cells. Oncotarget. 2017 Sep 1;8(36):60299–311.

329. Liesa M, Qiu W, Shirihai OS. Mitochondrial ABC transporters function: The role of ABCB10 (ABC-me) as a novel player in cellular handling of reactive oxygen species. Biochim Biophys Acta - Mol Cell Res. 2012;1823(10):1945–57.

330. Chen W, Paradkar PN, Li L, Pierce EL, Langer NB, Takahashi-Makise N, et al. Abcb10 physically interacts with mitoferrin-1 (Slc25a37) to enhance its stability and function in the erythroid mitochondria. Proc Natl Acad Sci. National Academy of Sciences; 2009 Sep 22;106(38):16263–8.

331. Shirihai OS, Gregory T, Yu C, Orkin SH, Weiss MJ. ABC-me: a novel mitochondrial transporter induced by GATA-1 during erythroid differentiation. EMBO J. European Molecular Biology Organization; 2000 Jun 1;19(11):2492–502.

332. Wang Y, Liao X, Sun J, Yi B, Luo S, Liu T, et al. Characterization of HIF-1α/Glycolysis Hyperactive Cell Population via Small-Molecule-Based Imaging of Mitochondrial Transporter Activity. Adv Sci (Weinheim, Baden-Wurttemberg, Ger. Wiley-Blackwell; 2018;5(3):1700392.

333. Zhang B-B, Wang D-G, Guo F-F, Xuan C. Mitochondrial membrane potential and reactive oxygen species in cancer stem cells. Fam Cancer. Springer Netherlands; 2014 Sep 30;1–5.

334. Pouysségur J, Dayan F, Mazure NM. Hypoxia signalling in cancer and approaches to enforce tumour regression. Nature. 2006 May 25;441(7092):437–43.

335. Movafagh S, Crook S, Vo K. Regulation of Hypoxia-Inducible Factor-1a by Reactive Oxygen Species : New Developments in an Old Debate. J Cell Biochem. 2015 May;116(5):696–703.

336. Mathieu J, Zhou W, Xing Y, Sperber H, Ferreccio A, Agoston Z, et al. Hypoxia-inducible factors have distinct and stage-specific roles during reprogramming of human cells to pluripotency. Cell Stem Cell. 2014 May 1;14(5):592–605.

337. Gordan JD, Bertout JA, Hu C-J, Diehl JA, Simon MC. HIF-2alpha promotes hypoxic cell proliferation by enhancing c-myc transcriptional activity. Cancer Cell. Howard Hughes Medical Institute; 2007 Apr;11(4):335–47.

338. Knutsvik G, Collett K, Arnes J, Akslen LA, Stefansson IM. QSOX1 expression is associated with aggressive tumor features and reduced survival in breast carcinomas. Mod Pathol. 2016 Dec 26;29(12):1485–91.

339. Ilani T, Alon A, Grossman I, Horowitz B, Kartvelishvily E, Cohen SR, et al. A Secreted Disulfide Catalyst Controls Extracellular Matrix Composition and Function. Science (80- ). 2013 Jul 5;341(6141):74–6.

340. Brookes MJ, Hughes S, Turner FE, Reynolds G, Sharma N, Ismail T, et al. Modulation of iron transport proteins in human colorectal carcinogenesis. Gut. 2006 Oct 1;55(10):1449–60.

341. Wang Y-F, Zhang J, Su Y, Shen Y-Y, Jiang D-X, Hou Y-Y, et al. G9a regulates breast cancer growth by modulating iron homeostasis through the repression of ferroxidase hephaestin. Nat Commun. 2017 Aug 17;8(1):274.

342. Kallianpur AR, Hall LD, Yadav M, Christman BW, Dittus RS, Haines JL, et al. Increased prevalence of the HFE C282Y hemochromatosis allele in women with breast cancer. Cancer Epidemiol Biomarkers Prev. 2004 Feb;13(2):205–12.

343. Hamara K, Bielecka-Kowalska A, Przybylowska-Sygut K, Sygut A, Dziki A, Szemraj J. Alterations in expression profile of iron-related genes in colorectal cancer. Mol Biol Rep. 2013 Oct 28;40(10):5573–85.

344. XUE D, ZHOU C-X, SHI Y-B, LU H, HE X-Z. Decreased expression of ferroportin in prostate cancer. Oncol Lett. 2015 Aug;10(2):913–6.

345. Pinnix ZK, Miller LD, Wang W, D'Agostino R, Kute T, Willingham MC, et al. Ferroportin and Iron Regulation in Breast Cancer Progression and Prognosis. Sci Transl Med. 2010 Aug 4;2(43):43ra56-43ra56.

346. Deng Z, Manz DH, Torti S, Torti FM. Effects of ferroportin-mediated iron depletion in cells representative of different histological subtypes of prostate cancer. Antioxid Redox Signal. 2017 Oct 23;ars.2017.7023.

347. Zhang D-L, Hughes RM, Ollivierre-Wilson H, Ghosh MC, Rouault TA. A Ferroportin Transcript that Lacks an Iron-Responsive Element Enables Duodenal and Erythroid Precursor Cells to Evade Translational Repression. Cell Metab. 2009 May;9(5):461–73.

348. Troadec M-B, Ward DM, Lo E, Kaplan J, De Domenico I. Induction of FPN1 transcription by MTF-1 reveals a role for ferroportin in transition metal efflux. Blood. 2010 Nov 25;116(22):4657–64.

349. Taylor M, Qu A, Anderson ER, Matsubara T, Martin A, Gonzalez FJ, et al. Hypoxia-inducible factor-2α mediates the adaptive increase of intestinal ferroportin during iron deficiency in mice. Gastroenterology. 2011 Jun;140(7):2044–55.

350. Alkhateeb AA, Connor JR. The significance of ferritin in cancer: Anti-oxidation, inflammation and tumorigenesis. Biochim Biophys Acta - Rev Cancer. 2013 Dec;1836(2):245–54.

351. Rossiello R, Carriero M V, Giordano GG. Distribution of ferritin, transferrin and lactoferrin in breast carcinoma tissue. J Clin Pathol. 1984 Jan;37(1):51–5.

352. Alkhateeb AA, Han B, Connor JR. Ferritin stimulates breast cancer cells through an iron-independent mechanism and is localized within tumor-associated macrophages. Breast Cancer Res Treat. 2013 Feb 11;137(3):733–44.

353. Jézéquel P, Campion L, Spyratos F, Loussouarn D, Campone M, Guérin-Charbonnel C, et al. Validation of tumor-associated macrophage ferritin light chain as a prognostic biomarker in node-negative breast cancer tumors: A multicentric 2004 national PHRC study. Int J Cancer. 2012 Jul 15;131(2):426–37.

354. Liu NQ, De Marchi T, Timmermans AM, Beekhof R, Trapman-Jansen AMAC, Foekens R, et al. Ferritin Heavy Chain in Triple Negative Breast Cancer: A Favorable Prognostic Marker that Relates to a Cluster of Differentiation 8 Positive (CD8+) Effector T-cell Response. Mol Cell Proteomics. 2014 Jul;13(7):1814–27.

355. Xue X, Ramakrishnan SK, Weisz K, Triner D, Xie L, Attili D, et al. Iron Uptake via DMT1 Integrates Cell Cycle with JAK-STAT3 Signaling to Promote Colorectal Tumorigenesis. Cell Metab. 2016 Sep 13;24(3):447–61.

356. Tan MGK, Kumarasinghe MP, Wang SM, Ooi LLPJ, Aw SE, Hui KM. Modulation of iron-regulatory genes in human hepatocellular carcinoma and its physiological consequences. Exp Biol Med (Maywood). 2009 Jun;234(6):693–702.

357. Boult J, Roberts K, Brookes MJ, Hughes S, Bury JP, Cross SS, et al. Overexpression of cellular iron import proteins is associated with malignant progression of esophageal adenocarcinoma. Clin Cancer Res. 2008 Jan 15;14(2):379–87.

358. Howitt J, Putz U, Lackovic J, Doan A, Dorstyn L, Cheng H, et al. Divalent metal transporter 1 (DMT1) regulation by Ndfip1 prevents metal toxicity in human neurons. Proc Natl Acad Sci U S A. 2009 Sep 8;106(36):15489–94.

359. Sheftel AD, Zhang A-S, Brown C, Shirihai OS, Ponka P. Direct interorganellar transfer of iron from endosome to mitochondrion. Blood. 2007 Jul 1;110(1):125–32.

360. Das A, Nag S, Mason AB, Barroso MM. Endosome–mitochondria interactions are modulated by iron release from transferrin. J Cell Biol. 2016 Sep 26;214(7):831–45.

# Supplementary material

## Supplementary table 1. List of used primers

| Fluidigm RT-qPCR | | |
|---|---|---|
| Gene | | Primer sequence |
| *ABCA1* | Forward 5' | AGCCTGGAACTTCAGCCCTGGATGTACA |
| *ABCA1* | Reverse 5' | GCCAGGGTCTTTGGTGAGGGCGTTTAA |
| *ABCA2* | Forward 5' | ATCATGGTGAACGGTCGCCTG |
| *ABCA2* | Reverse 5' | GGTCCGCACCGTGATCATGTAG |
| *ABCA3* | Forward 5' | ACCTACATCCCCTGATGGCGGAGAAC |
| *ABCA3* | Reverse 5' | TACTCCATGATGGCCCGGTCCACA |
| *ABCA4* | Forward 5' | ACAGCAGACTGAAAGTCATGACCTCC |
| *ABCA4* | Reverse 5' | GTTCCTTTCTGGCTGCAGGAACG |
| *ABCA5* | Forward 5' | TTATCATGCTCACACTTAATAGTA |
| *ABCA5* | Reverse 5' | ATAAAGATGATCTCCGTAAGC |
| *ABCA6* | Forward 5' | CTATAAGCTGCCCGTGGCAGAC |
| *ABCA6* | Reverse 5' | GTGCACTGAGAAAGGCTGTATTCTTCC |
| *ABCA7* | Forward 5' | CTGTATGGCTGGTCGATCACAC |
| *ABCA7* | Reverse 5' | TTTATGCAGGTGAGCACCACATAG |
| *ABCA8* | Forward 5' | TCTTCGGGATTCAGCGTTCT |
| *ABCA8* | Reverse 5' | AACAAGTGCCAAGAAAAGGGC |
| *ABCA9* | Forward 5' | TGCCCTCAGGAGAATGCGCTGT |
| *ABCA9* | Reverse 5' | TAACCGTGTGATGGCGATCATTGCGTC |
| *ABCA10* | Forward 5' | ATGTCCACCCTCTATCTCGGGC |
| *ABCA10* | Reverse 5' | CTGCTCCAAGGTAGCCTGAGAGA |
| *ABCA12* | Forward 5' | ATGGTATGATCCAGAAGGCTATCACTCC |
| *ABCA12* | Reverse 5' | TACATGATGATGCCATGTCGGGC |
| *ABCA13* | Forward 5' | CAATAATGAAGGAGGTTCGGGAA |
| *ABCA13* | Reverse 5' | CATTTGAAGCTGCCGTTAACC |
| *ABCB1* | Forward 5' | AAAGCGACTGAATGTTCAGTGGCTCCGAG |
| *ABCB1* | Reverse 5' | ACCCGGCTGTTGTCTCCATAGGCAA |
| *ABCB2 (TAP1)* | Forward 5' | ATCCTGGATGATGCCACCAGT |
| *ABCB2 (TAP1)* | Reverse 5' | GAGAAGCACTGAGCGGGAGTA |
| *ABCB3 (TAP2)* | Forward 5' | CCTCAGCGCTGAAGCAGAAGTC |
| *ABCB3 (TAP2)* | Reverse 5' | ACAGTAAAGCCGCGTCCACCA |
| *ABCB4* | Forward 5' | AGGCGGCAAAGAACGGAACAG |
| *ABCB4* | Reverse 5' | AATACTCCAATCATTTTCACTGTCTTCGT |
| *ABCB5* | Forward 5' | GCAAGGGAAGCAAATGCGTA |
| *ABCB5* | Reverse 5' | TGCGATCCTCTGTTTCTGCC |
| *ABCB6* | Forward 5' | GCTCTGGCTGCATCCGAATA |
| *ABCB6* | Reverse 5' | TTGGGGCACAACTCCAATGT |
| *ABCB7* | Forward 5' | ATCCGGCCTTTAGTCTCTGTTAGCGG |

| | | |
|---|---|---|
| *ABCB7* | Reverse 5' | CTCTGGAATCTGCTGGTAGGCTCGAG |
| *ABCB8* | Forward 5' | GTGCATTTATTTCGGGTCGGG |
| *ABCB8* | Reverse 5' | CTGCGGTAGCCATCAGAGTA |
| *ABCB9* | Forward 5' | GCCTCCTTCTTCCTCATCGTG |
| *ABCB9* | Reverse 5' | TTTCTGGATGACGATGCCATCAA |
| *ABCB10* | Forward 5' | ATCATTGCTGTAATTTATGGGCG |
| *ABCB10* | Reverse 5' | ATTTCCAATACGTTCCTCAGCTA |
| *ABCB11* | Forward 5' | GCTACCAGGATAGTTTAAGGGCTTC |
| *ABCB11* | Reverse 5' | GATCTACAACAGCTAATGGAGGTTCG |
| *ABCC1* | Forward 5' | TCTCAGATCGCTCACCCCTGTTCTCG |
| *ABCC1* | Reverse 5' | CTGTGATCCACCAGAAGGTGATCCTCGAC |
| *ABCC2* | Forward 5' | TTGTGAACAGGTTTGCCGGCGATA |
| *ABCC2* | Reverse 5' | TGGCCATGCAGATCATGACAAGGG |
| *ABCC3* | Forward 5' | GGAGAAGGACCTCTGGTCCCTAAAGGAA |
| *ABCC3* | Reverse 5' | CCTTGTGTCGTGCCGTCTGCTTTTC |
| *ABCC4* | Forward 5' | CAAGATGCTGCCCGTGTACCA |
| *ABCC4* | Reverse 5' | AATTTTAAACAAGGGATTGAGCCACCAGA |
| *ABCC5* | Forward 5' | ATCATCCCCAGTCCTGGGTATAG |
| *ABCC5* | Reverse 5' | CAAGGCATCTTGGCATTCCAAC |
| *ABCC6* | Forward 5' | ACAAGTGTGCTGACCGAGGCGA |
| *ABCC6* | Reverse 5' | ATGAGGATCTGGGTCTTCCGGAGAAGG |
| *ABCC7 (CFTR)* | Forward 5' | ACTGGTGCATACTCTAATCACAG |
| *ABCC7 (CFTR)* | Reverse 5' | TATTAAGAATCCCACCTGCTTTCA |
| *ABCC8* | Forward 5' | TTCATCCAGAAGTACTTCCGGG |
| *ABCC8* | Reverse 5' | TGAGTCCTTCTACGGTTTCGG |
| *ABCC9* | Forward 5' | ATGATTGTGGGCCAAGTAGGA |
| *ABCC9* | Reverse 5' | TTACATTGCTCCAGTGAACTTTTCC |
| *ABCC10* | Forward 5' | GGGAGAAGGGTGTCACCCTTAG |
| *ABCC10* | Reverse 5' | CCAGAGGGTCATCGAGGAGATAGA |
| *ABCC11* | Forward 5' | TGGATCGTCAGCGGGAACATC |
| *ABCC11* | Reverse 5' | CAGAAGTTCCAGGTCCCGATTCAG |
| *ABCC12* | Forward 5' | TCCTTTGCAGAAAGATATGACCC |
| *ABCC12* | Reverse 5' | GAAAATGTGGCGAAGGAGAGTA |
| *ABCC13* | Forward 5' | ATCAAGAAACCATCTCTACTCTATGC |
| *ABCC13* | Reverse 5' | CTTCATTATGAGTGGGCTAGTGAA |
| *ABCD1* | Forward 5' | CCAGCGCATGTTCTACATCCCGCAGAG |
| *ABCD1* | Reverse 5' | CTTTGCATGTCCTCCACTGAGTCCGGGTA |
| *ABCD2* | Forward 5' | AAATGTTCCCATAATTACACCAGCAGG |
| *ABCD2* | Reverse 5' | AAGAGAGAACTTTTCCCACAACCATTG |
| *ABCD3* | Forward 5' | CTTCAGCAAGTACTTGACGGCGCGAAAC |
| *ABCD3* | Reverse 5' | GGTTTTCCACTTTTCTTACCGTGCAGGCC |
| *ABCD4* | Forward 5' | GAAGTCACAGGACTGCGAGA |
| *ABCD4* | Reverse 5' | GAGATGGAGACCCGCTCAAG |

| | | |
|---|---|---|
| *ABCE1* | Forward 5' | TAGGACCACGCTCGACGTCGGAGAAAAG |
| *ABCE1* | Reverse 5' | TTGTTCAACGCCGTTGGCGAAGCC |
| *ABCF1* | Forward 5' | AATGCAGACCTGTACATTGTAGCCGGCCG |
| *ABCF1* | Reverse 5' | GATGCTCAGGGCTCGGTTGGCAATGTG |
| *ABCF2* | Forward 5' | AATTGACCTTGACACACGAGTGGCTC |
| *ABCF2* | Reverse 5' | TTTCGGATCATGCCATCTGTGGGTAGTA |
| *ABCF3* | Forward 5' | TTCGCTACAATGCCAACAGG |
| *ABCF3* | Reverse 5' | TTCCTTGTCCACAGGCTTCAG |
| *ABCG1* | Forward 5' | GAAGGTGTCCTGCTACATCATGC |
| *ABCG1* | Reverse 5' | AAGCTTCAGATGTGCCGACAC |
| *ABCG2* | Forward 5' | TCGTTATTAGATGTCTTAGCTGCAA |
| *ABCG2* | Reverse 5' | TTGTACCACGTAACCTGAATTACA |
| *ABCG4* | Forward 5' | CTGGTACAGCCTCAAAGCGT |
| *ABCG4* | Reverse 5' | GCCCGTCATCCAGTACACAA |
| *ABCG5* | Forward 5' | TGCTTCTCCTACGTCCTGCAGA |
| *ABCG5* | Reverse 5' | CTTCTGGAAGGAGCCGGGATTG |
| *ABCG8* | Forward 5' | AGAGGAGAGAGGGCTGCCGAAA |
| *ABCG8* | Reverse 5' | AGGTGAAGTACAGGCTGTTGTCACTTTCA |
| *ACO1* | Forward 5' | TGCCATTACTAGCTGCACAAACA |
| *ACO1* | Reverse 5' | GACAGGCTAGTTTTGATGTAAGGCA |
| *BMP6* | Forward 5' | AACGACGCGGACATGGTCA |
| *BMP6* | Reverse 5' | ACTCTTTGTGGTGTCGCTGA |
| *CD44* | Forward 5' | GCTGACCTCTGCAAGGCTTTCAATAG |
| *CD44* | Reverse 5' | CTTCTTCGACTGTTGACTGCAATGCA |
| *CXCR4* | Forward 5' | TTGATGTGTGTCTAGGCAGGA |
| *CXCR4* | Reverse 5' | GATTCACTACACGCTCTGGAATG |
| *CYBRD1* | Forward 5' | AGTGATTGCAACAGCACTTATGGG |
| *CYBRD1* | Reverse 5' | AGGATCAGAAGGCCAAGCGTA |
| *EPAS1* | Forward 5' | CGCCATCATCTCTCTGGATTTCGGGAATC |
| *EPAS1* | Reverse 5' | TCTGGGTGCTGTGGCTCCTCAA |
| *FTH1* | Forward 5' | CTGATGAAGCTGCAGAACCAAC |
| *FTH1* | Reverse 5' | AATGTAATGCACACTCCATTGCATT |
| *FTL1* | Forward 5' | TTGTACCTGCAGGCCTCCTACACCTAC |
| *FTL1* | Reverse 5' | TCCTCGGCCAATTCGCGGAAGAA |
| *FTMT* | Forward 5' | AGGCTGCCATCAACCGCCAGATCA |
| *FTMT* | Reverse 5' | AGTTGTTCAAGGCCACGTCATCCCGG |
| *FXN* | Forward 5' | ACCGACATCGATGCGACCTGCA |
| *FXN* | Reverse 5' | CCTCAAATTCATCAAATAGACACTCTGCT |
| *GAPDH* | Forward 5' | GGGAAGGTGAAGGTCGGAGTCA |
| *GAPDH* | Reverse 5' | TTGATGGCAACAATATCCACTTTACCAGA |
| *GLRX2* | Forward 5' | AGCAAGTGAGCCGCTTCTCCCCTCTAAA |
| *GLRX2* | Reverse 5' | ATTGCTCTCCATCCTCCTCGCAGCTGA |
| *GLRX5* | Forward 5' | AAGAAGGACAAGGTGGTGGTCTTCCTCAA |

| | | |
|---|---|---|
| *GLRX5* | Reverse 5' | TTGTAGGCCGCGTAATCGCGGA |
| *HAMP* | Forward 5' | ACAGACGGCACGATGGCACTGA |
| *HAMP* | Reverse 5' | CAAGTTGTCCCGTCTGTTGTGGGAAAACA |
| *HEPH* | Forward 5' | GTGCATGCTCATGGAGTGCTA |
| *HEPH* | Reverse 5' | CCAGACCTCTCTGGGATGTTC |
| *HFE* | Forward 5' | AAGGAAGAGGCAGGGTTCAAGA |
| *HFE* | Reverse 5' | TTTGTCTCCTTCCCACAGTGAGT |
| *HFE2* | Forward 5' | GGAGCTGACCCACAGAGTAG |
| *HFE2* | Reverse 5' | CCGGAAGCCCTGTAAGTGA |
| *HIF1A* | Forward 5' | AAGACATCGCGGGGACCGATTCA |
| *HIF1A* | Reverse 5' | TTACTTCGCCGAGATCTGGCTGCATC |
| *HIF3A* | Forward 5' | TGAAGAGTACACTCACCAGCCGCG |
| *HIF3A* | Reverse 5' | GCAGGTGGCTTGTAGGCCCTCATA |
| *HMBS* | Forward 5' | CGAGACTCTGCTTCGCTGCATCGCTGAAA |
| *HMBS* | Reverse 5' | TGCCCATCCTTCATAGCTGTATGCACGGC |
| *HMOX1* | Forward 5' | CAACCCGACAGCATGCCCCAGGATTTG |
| *HMOX1* | Reverse 5' | GGGTCACCTGGCCCTTCTGAAAGTTCCTC |
| *HMOX2* | Forward 5' | TGAGAATGGCTGACCTCTCGGA |
| *HMOX2* | Reverse 5' | ATGTTGCCTTTCAAGAAGTCCTTGACAA |
| *HPRT1* | Forward 5' | GACACTGGCAAAACAATGCAGA |
| *HPRT1* | Reverse 5' | CGTGGGGTCCTTTTCACCAG |
| *IREB2* | Forward 5' | AAATGACAGTTCACATAAGAAGTTCTTCG |
| *IREB2* | Reverse 5' | AGCTTCCAACAAGACCCGTAT |
| *ISCA1* | Forward 5' | AGATGTCGGCTTCCTTAGTCCGGG |
| *ISCA1* | Reverse 5' | TGTTTACTGCTGAAGGTGTCAGGGTGAG |
| *ISCA2* | Forward 5' | GATCCGCCTCACAGACAGTTG |
| *ISCA2* | Reverse 5' | TGAAAATTTGTATTGGAATCCGGAGCA |
| *ISCU* | Forward 5' | TGAAATTACAGATTCAAGTGGATGA |
| *ISCU* | Reverse 5' | CTTTCCTTTCACCCATTCAGT |
| *LYRM4 (ISD11)* | Forward 5' | AACATATGCTGTCAGGAGGATAAG |
| *LYRM4 (ISD11)* | Reverse 5' | TGTCGACGAATTACTCCAAGG |
| *CDH2* | Forward 5' | GCGGAGATCCTACTGGACGGTT |
| *CDH2* | Reverse 5' | TTTCAAAGTCGATTGGTTTGACCACGG |
| *POLR2A* | Forward 5' | TGCTCCGTATTCGCATCATGAACA |
| *POLR2A* | Reverse 5' | ATCTGTCAGCATGTTGGACTCGATG |
| *PPIA* | Forward 5' | AACGTGGTATAAAAGGGGCGGG |
| *PPIA* | Reverse 5' | GTCGAAGAACACGGTGGGGTT |
| *QSOX1* | Forward 5' | AGTCCCATCATGACACGTGGC |
| *QSOX1* | Reverse 5' | GCCAGGTACTCTTCGTTATTTCTCGC |
| *RPLP0* | Forward 5' | ATCACAGAGGAAACTCTGCATTCTCG |
| *RPLP0* | Reverse 5' | GATAGAATGGGGTACTGATGCAACAGTT |
| *SLC11A2 (NRAMP2, IRE)* | Forward 5' | TGCACCATGAGGAAGAAGCA |
| *SLC11A2 (NRAMP2, IRE)* | Reverse 5' | GGTGGATACCTGAGTGGCTG |

| | | |
|---|---|---|
| *SLC25A28 (MFRN2)* | Forward 5' | AGGGATCCTGGAGCACTGCGTGATGTAC |
| *SLC25A28 (MFRN2)* | Reverse 5' | GAGGGCCTCCAACACATTGCGATAGCG |
| *SLC25A37 (MFRN1)* | Forward 5' | CCGTGTCCACCCACATGA |
| *SLC25A37 (MFRN1)* | Reverse 5' | TGGGCTTTGGGATCTGGACT |
| *SLC40A1 (FPN1)* | Forward 5' | CTACTGCAATCACAATCCAAAGGGA |
| *SLC40A1 (FPN1)* | Reverse 5' | GGCTAAGATGTTGGTTAACTGGTCAA |
| *SLC48A1* | Forward 5' | CTCGTCTGGACGGTGGTCTA |
| *SLC48A1* | Reverse 5' | TTGCATGTACATCACGTGCG |
| *SOX2* | Forward 5' | CAGAGAAGAGAGTGTTTGCAAAAGGGG |
| *SOX2* | Reverse 5' | GGCTTAAGCCTGGGGCTCAAA |
| *STEAP3* | Forward 5' | TAACAGGCAGGTGCCCATCTGC |
| *STEAP3* | Reverse 5' | GATCCCATGTCCACGGGCATGAAG |
| *TBP* | Forward 5' | TGTATCCACAGTGAATCTTGGTTGTAAA |
| *TBP* | Reverse 5' | CGTGGCTCTCTTATCCTCATGATTAC |
| *TFR2* | Forward 5' | TGGCTTCCCTTCCTTCAATCAAACC |
| *TFR2* | Reverse 5' | TTTGAGCTTCCTCAGCAGGCG |
| *TFRCv1* | Forward 5' | GACGCGCTAGTGTTCTTCTGTGTGGC |
| *TFRCv1* | Reverse 5' | CGAGCCAGGCTGAACCGGGTATATGA |
| *TFRCv2 (IRE)* | Forward 5' | GGCTGCAGGTTCTTCTGTGTGGCAGTT |
| *TFRCv2 (IRE)* | Reverse 5' | CGAGCCAGGCTGAACCGGGTATATGACA |
| *TMPRSS6* | Forward 5' | CTTGTACAACCAGTCGGACCCCTG |
| *TMPRSS6* | Reverse 5' | TTTCTCTCATCCAGGCCGTTGGG |
| *VEGFA* | Forward 5' | AGGGCAGAATCATCACGAAGTG |
| *VEGFA* | Reverse 5' | ATGTACTCGATCTCATCAGGGTACTC |
| RT-qPCR mouse genes | | |
| Gene | | Primer sequence |
| *mPolr2a* | Forward 5' | TGGTCCTTCGAATCCGCATC |
| *mPolr2a* | Reverse 5' | GGACTCAATGCATCGCAGGA |
| *mActin* | Forward 5' | CGAGTCGCGTCCACCC |
| *mActin* | Reverse 5' | ACCCATTCCCACCATCACAC |
| *mGapdh* | Forward 5' | GTGCAGTGCCAGCCTCGTCC |
| *mGapdh* | Reverse 5' | GCCACTGCAAATGGCAGCCC |
| *mAbcb10* | Forward 5' | CACATCCCCTGTTCGCCA |
| *mAbcb10* | Reverse 5' | GATGACACTGGACACAGCCA |
| *mAco1* | Forward 5' | AACACCAGCAATCCATCCGT |
| *mAco1* | Reverse 5' | GGTGACCACTCCACTTCCAG |
| *mCybrd* | Forward 5' | GTGACCGGCTTCGTCTTCA |
| *mCybrd* | Reverse 5' | TTAACCCGGCATGGATGGAT |
| *mCd34* | Forward 5' | ATCCGAGAAGTGAGGTTGGC |
| *mCd34* | Reverse 5' | GGAGCAGACACTAGCACCAG |
| *mEpas1* | Forward 5' | GGGGTTAAGGAACCCAGGTG |
| *mEpas1* | Reverse 5' | GGCATCACGGGATTTCTCCT |
| *mGlrx5* | Forward 5' | CCTACAACGTGCTGGACGAC |

| | | |
|---|---|---|
| *mGlrx5* | Reverse 5' | CTCGCCGTTGAGGTACACTT |
| *mHeph* | Forward 5' | CGAGCCGACCTTACACCATT |
| *mHeph* | Reverse 5' | TCAGTGGGGGCATGACTTTC |
| *mHfe* | Forward 5' | CCTCCACGTTTCCAGATCCT |
| *mHfe* | Reverse 5' | CTCTGAGGCACCCATGAAGAG |
| *mIreb2* | Forward 5' | TACCTGCATGACATTTGGCCT |
| *mIreb2* | Reverse 5' | CATCCCATGGAAACAGCACG |
| *mQsox1* | Forward 5' | CTGGACTAGCCACAACAGGG |
| *mQsox1* | Reverse 5' | AAAGTTGAGGGTGGCACCAA |
| *mTfrc* | Forward 5' | GAGGCGCTTCCTAGTACTCC |
| *mTfrc* | Reverse 5' | ACTTGCCGAGCAAGGCTAAA |
| *mKit* | Forward 5' | TGACGGTACATGGCTGCATT |
| *mKit* | Reverse 5' | ACCACCGTAAATGTGTCCCC |
| *mLtf* | Forward 5' | CCTGCTTGCTAACCAGACCA |
| *mLtf* | Reverse 5' | CTTTGCTGTTGGGAGCACAC |
| RT-qPCR human genes | | |
| Gene | | Primer sequence |
| *ESR1* | Forward 5' | CCGGCTCCGCAAATGCTACGA |
| *ESR1* | Reverse 5' | AGCGGGCTTGGCCAAAGGTT |
| *GREB1* | Forward 5' | GGACCAGCTTCAGTCACCTT |
| *GREB1* | Reverse 5' | CCAAGGGCTACCATTTGGGT |
| *PGRA* | Forward 5' | TGGTGTCCTTACCTGTGGGA |
| *PGRA* | Reverse 5' | CCAGCCTGACAGCACTTTCT |
| *BMP7* | Forward 5' | ACAAGGCCGTCTTCAGTACC |
| *BMP7* | Reverse 5' | GGTAGCGTGGGTGGAAGAAT |
| *CSTD* | Forward 5' | CTGGACATCGCTTGCTGGAT |
| *CSTD* | Reverse 5' | TGCCTCTCCACTTTGACACC |
| *CXCL12* | Forward 5' | GTGCCCTTCAGATTGTAGCCC |
| *CXCL12* | Reverse 5' | GCCCTTCCCTAACACTGGTT |
| *HER2* | Forward 5' | CACCCAAGTGTGCACCGGCA |
| *HER2* | Reverse 5' | GCACGTAGCCCTGCACCTCC |
| *CD44* | Forward 5' | GCTGACCTCTGCAAGGCTTTCAATAG |
| *CD44* | Reverse 5' | CTTCTTCGACTGTTGACTGCAATGCA |
| *ABCG2* | Forward 5' | TCGTTATTAGATGTCTTAGCTGCAA |
| *ABCG2* | Reverse 5' | TTGTACCACGTAACCTGAATTACA |
| *ALDH1* | Forward 5' | ATGCTTCCGAGAGGGGGCGA |
| *ALDH1* | Reverse 5' | CCCAACCTGCACAGTAGCGCA |
| *VIMENTIN* | Forward 5' | GCGACAACCTGGCCGAGGAC |
| *VIMENTIN* | Reverse 5' | GGTCAAGACGTGCCAGAGACGC |
| *VEGFA* | Forward 5' | AGGGCAGAATCATCACGAAGTG |
| *VEGFA* | Reverse 5' | ATGTACTCGATCTCATCAGGGTACTC |
| *POLR2A* | Forward 5' | TGCTCCGTATTCGCATCATGAACA |
| *POLR2A* | Reverse 5' | ATCTGTCAGCATGTTGGACTCGATG |

| | | |
|---|---|---|
| *TBP* | Forward 5' | TGTATCCACAGTGAATCTTGGTTGTAAA |
| *TBP* | Reverse 5' | CGTGGCTCTCTTATCCTCATGATTAC |
| *P0* | Forward 5' | ATCACAGAGGAAACTCTGCATTCTCG |
| *P0* | Reverse 5' | GATAGAATGGGGTACTGATGCAACAGTT |
| *ZEB1* | Forward 5' | AACCCAACTTGAACGTCACA |
| *ZEB1* | Reverse 5' | ATTACACCCAGACTGCGTCA |
| *ZEB2* | Forward 5' | TGCCCAACCATGAGTCCTCCCC |
| *ZEB2* | Reverse 5' | CGGTCTGGATCGTGGCTTCTGG |